BWRVIP-114NP-A: BWR Vessel and Internals Project

RAMA Fluence Methodology Theory Manual

1019049

Final Report, June 2009

EPRI Project Manager
R. Carter

ELECTRIC POWER RESEARCH INSTITUTE
3420 Hillview Avenue, Palo Alto, California 94304-1338 • PO Box 10412, Palo Alto, California 94303-0813 • USA
800.313.3774 • 650.855.2121 • askepri@epri.com • www.epri.com

BWRVIP-114NP-A: BWR Vessel and Internals Project

RAMA Fluence Methodology Theory Manual

1019049

Final Report, June 2009

EPRI Project Manager
R. Carter

ELECTRIC POWER RESEARCH INSTITUTE
3420 Hillview Avenue, Palo Alto, California 94304-1338 • PO Box 10412, Palo Alto, California 94303-0813 • USA
800.313.3774 • 650.855.2121 • askepri@epri.com • www.epri.com

DISCLAIMER OF WARRANTIES AND LIMITATION OF LIABILITIES

THIS DOCUMENT WAS PREPARED BY THE ORGANIZATION(S) NAMED BELOW AS AN ACCOUNT OF WORK SPONSORED OR COSPONSORED BY THE ELECTRIC POWER RESEARCH INSTITUTE, INC. (EPRI). NEITHER EPRI, ANY MEMBER OF EPRI, ANY COSPONSOR, THE ORGANIZATION(S) BELOW, NOR ANY PERSON ACTING ON BEHALF OF ANY OF THEM:

(A) MAKES ANY WARRANTY OR REPRESENTATION WHATSOEVER, EXPRESS OR IMPLIED, (I) WITH RESPECT TO THE USE OF ANY INFORMATION, APPARATUS, METHOD, PROCESS, OR SIMILAR ITEM DISCLOSED IN THIS DOCUMENT, INCLUDING MERCHANTABILITY AND FITNESS FOR A PARTICULAR PURPOSE, OR (II) THAT SUCH USE DOES NOT INFRINGE ON OR INTERFERE WITH PRIVATELY OWNED RIGHTS, INCLUDING ANY PARTY'S INTELLECTUAL PROPERTY, OR (III) THAT THIS DOCUMENT IS SUITABLE TO ANY PARTICULAR USER'S CIRCUMSTANCE; OR

(B) ASSUMES RESPONSIBILITY FOR ANY DAMAGES OR OTHER LIABILITY WHATSOEVER (INCLUDING ANY CONSEQUENTIAL DAMAGES, EVEN IF EPRI OR ANY EPRI REPRESENTATIVE HAS BEEN ADVISED OF THE POSSIBILITY OF SUCH DAMAGES) RESULTING FROM YOUR SELECTION OR USE OF THIS DOCUMENT OR ANY INFORMATION, APPARATUS, METHOD, PROCESS, OR SIMILAR ITEM DISCLOSED IN THIS DOCUMENT.

ORGANIZATION(S) THAT PREPARED THIS DOCUMENT

Electric Power Research Institute (EPRI)

TransWare Enterprises Inc.

NOTICE: THIS REPORT CONTAINS PROPRIETARY INFORMATION THAT IS THE INTELLECTUAL PROPERTY OF EPRI. ACCORDINGLY, IT IS AVAILABLE ONLY UNDER LICENSE FROM EPRI AND MAY NOT BE REPRODUCED OR DISCLOSED, WHOLLY OR IN PART, BY ANY LICENSEE TO ANY OTHER PERSON OR ORGANIZATION.

THE WORK DESCRIBED IN THIS REPORT WAS PROCURED, REVIEWED, ACCEPTED, AND ISSUED ACCORDING TO EPRI'S QUALITY ASSURANCE PROGRAM AND PREPARED UNDER TRANSWARE NUCLEAR QUALITY ASSURANCE PROGRAM, BOTH OF WHICH COMPLY WITH THE REQUIREMENTS OF TITLE 10 OF THE CODE OF FEDERAL REGULATIONS, PART 50, APPENDIX B.

NOTE

For further information about EPRI, call the EPRI Customer Assistance Center at 800.313.3774 or e-mail askepri@epri.com.

Electric Power Research Institute, EPRI, and TOGETHER...SHAPING THE FUTURE OF ELECTRICITY are registered service marks of the Electric Power Research Institute, Inc.

Copyright © 2009 Electric Power Research Institute, Inc. All rights reserved.

NRC SAFETY EVALUATION

In accordance with an NRC request, the NRC Safety Evaluation immediately follows this page. Other NRC and BWRVIP correspondence on this subject are included in appendices.

Note: The changes proposed by the NRC in this Safety Evaluation as well those proposed by the BWRVIP in response to NRC Requests for Information have been incorporated into the current version of the report (BWRVIP-114-A).

UNITED STATES
NUCLEAR REGULATORY COMMISSION
WASHINGTON, D.C. 20555-0001

May 13, 2005

Bill Eaton, BWRVIP Chairman
Entergy Operations, Inc.
Echelon One
1340 Echelon Parkway
Jackson, MS 39213-8202

SUBJECT: SAFETY EVALUATION OF PROPRIETARY EPRI REPORTS, "BWR VESSEL AND INTERNALS PROJECT, RAMA FLUENCE METHODOLOGY MANUAL (BWRVIP-114)," "RAMA FLUENCE METHODOLOGY BENCHMARK MANUAL-EVALUATION OF REGULATORY GUIDE 1.190 BENCHMARK PROBLEMS (BWRVIP-115)," "RAMA FLUENCE METHODOLOGY-SUSQUEHANNA UNIT 2 SURVEILLANCE CAPSULE FLUENCE EVALUATION FOR CYCLES 1-5 (BWRVIP-117)," AND "RAMA FLUENCE METHODOLOGY PROCEDURES MANUAL (BWRVIP-121)," AND "HOPE CREEK FLUX WIRE DOSIMETER ACTIVATION EVALUATION FOR CYCLE 1 (TWE-PSE-001-R-001)" (TAC NO. MB9765)

Dear Mr. Eaton:

By letters dated June 11, 2003, June 26, 2003, August 5, 2003, October 29, 2003, and March 24, 2004, respectively, the Boiling Water Reactor Vessel and Internals Project (BWRVIP) submitted the following Electric Power Research Institute (EPRI) proprietary reports for staff review and approval, "BWR Vessel and Internals Project, RAMA Fluence Methodology Manual (BWRVIP-114)," "RAMA Fluence Methodology Benchmark Manual-Evaluation of Regulatory Guide 1.190 Benchmark Problems (BWRVIP-115)," "RAMA Fluence Methodology-Susquehanna Unit 2 Surveillance Capsule Fluence Evaluation for Cycles 1-5 (BWRVIP-117)," "RAMA Fluence Methodology Procedures Manual (BWRVIP-121)," and "Hope Creek Flux Wire Dosimeter Activation Evaluation for Cycle 1 (TWE-PSE-001-R-001)."

The reports listed above provide and support a methodology which is a new approach to neutron transport that has been developed by the BWRVIP for determining neutron fluence to the reactor pressure vessel (RPV) and internal components of BWR plants. The Radiation Analysis Modeling Application (RAMA) code will be applied in the reactor beltline region defined by the top and bottom planes of the active fuel and the inner wall of the biological shield. The methodology employs the RAMA computer code for evaluating the neutron flux from the core through the downcomer, vessel internals, and through the RPV wall.

The staff has completed its review of the proposed methodology and finds that the methodology performs as described; however, the BWRVIP did not quantify the bias and uncertainty required for the qualification of the methodology, as stated in RG 1.190, "Radiation Embrittlement of Reactor Vessel Materials." Therefore, the staff's approval is conditional based on the following criteria: (1) for plants that are similar in core, shroud and downcomer-vessel geometry to that of the Susquehanna and Hope Creek plants, the RAMA methodology can be applied without a bias for the calculation of vessel neutron fluence, (2) for plants (or plant groups) with a different geometry than that of the Susquehanna or Hope Creek plants, a plant-specific application for RPV neutron fluence is required to establish the value of a bias, and (3) relevant benchmarking will be required for shroud and reactor internals applications.

The staff evaluation of the proposed RAMA methodology is attached. Please contact Meena Khanna of my staff at 301-415-2150 if you have any further questions regarding this subject.

Sincerely,

Matthew A. Mitchell for

William H. Bateman, Chief
Materials and Chemical Engineering Branch
Division of Engineering
Office of Nuclear Reactor Regulation

Enclosure: As stated

cc: BWRVIP Service List

U.S. NUCLEAR REGULATORY COMMISSION OFFICE OF NUCLEAR REACTOR REGULATION SAFETY EVALUATION OF BWR VESSEL AND INTERNALS PROJECT, SAFETY EVALUATION OF PROPRIETARY EPRI REPORTS, "BWR VESSEL AND INTERNALS PROJECT, RAMA FLUENCE METHODOLOGY MANUAL (BWRVIP-114)," "RAMA FLUENCE METHODOLOGY BENCHMARK MANUAL-EVALUATION OF REGULATORY GUIDE 1.190 BENCHMARK PROBLEMS (BWRVIP-115)," "RAMA FLUENCE METHODOLOGY-SUSQUEHANNA UNIT 2 SURVEILLANCE CAPSULE FLUENCE EVALUATION FOR CYCLES 1-5 (BWRVIP-117)," "RAMA FLUENCE METHODOLOGY PROCEDURES MANUAL (BWRVIP-121)," AND "HOPE CREEK FLUX WIRE DOSIMETER ACTIVATION EVALUATION FOR CYCLE 1 (TWE-PSE-001-R-001)"

1.0 INTRODUCTION

1.1 Background

By letters dated June 11, 2003, June 26, 2003, August 5, 2003, October 29, 2003, and March 23, 2004, respectively, the Boiling Water Reactor Vessel and Internals Project (BWRVIP) submitted the following Electric Power Research Institute (EPRI) proprietary reports for staff review and approval, "BWR Vessel and Internals Project, RAMA Fluence Methodology Manual (BWRVIP-114)," "RAMA Fluence Methodology Benchmark Manual-Evaluation of Regulatory Guide 1.190 Benchmark Problems (BWRVIP-115)," "RAMA Fluence Methodology-Susquehanna Unit 2 Surveillance Capsule Fluence Evaluation for Cycles 1-5 (BWRVIP-117)," "RAMA Fluence Methodology Procedures Manual (BWRVIP-121)," and "Hope Creek Flux Wire Dosimeter Activation Evaluation for Cycle 1 (TWE-PSE-001-R-001)." These reports were supplemented by letter dated September 20, 2004, in response to the staff's request for additional information (RAI) dated April 20, 2004.

The BWRVIP-114 report describes the theory of the neutron transport calculation methodology and the uncertainty analysis. The BWRVIP-115 report documents benchmarking of the neutron fluence calculation methodology against two reactor pressure vessel (RPV) simulator measurements, a PWR surveillance capsule measurement and a calculational benchmark. The BWRVIP-117 and TWE-PSE-001-R-001 reports present plant-specific surveillance capsule neutron fluence benchmark comparisons for the Susquehanna and Hope Creek plants, respectively. The BWRVIP-121 report provides the standard procedures for carrying out neutron fluence calculations using this methodology.

The proposed methodology is essentially a new approach that has been developed by the BWRVIP for determining the fast ($E \geq 1.0$ MeV) neutron fluence accumulated by the RPV and internal components of BWR plants. The methodology employs the RAMA computer code for evaluating the neutron flux from the core through the downcomer, vessel internals and through the RPV wall. An important feature of the methodology is that the neutron transport calculation is 3-dimensional, rather than a synthesis of two 2-dimensional calculations that is used in the finite differences method on which presently approved methodologies are based. An additional feature of this approach is that the computer modeling of the physical geometry is represented without approximation. The RAMA code will be applied in the reactor beltline region defined by the top and bottom planes of the active fuel and the inside surface of the biological shield. The methodology employs the most recent BUGLE-96 nuclear transport and reaction-specific

ENCLOSURE

measured activity cross section data. The BWRVIP calculation and uncertainty methodology is summarized in Section 2. The technical evaluation is presented in Section 3, and the limitations and conclusions are provided in Section 4.

1.2 Purpose

The staff reviewed the reports discussed above to determine whether the BWRVIP's proposed methodology will provide an acceptable method for determining the fast ($E \geq 1.0$ MeV) neutron fluence accumulated by the RPV and internal components of BWR plants.

1.3 Regulatory Evaluation

The basis for this review is Regulatory Guide (RG) 1.190, "Radiation Embrittlement of Reactor Vessel Materials." RG 1.190 is based on General Design Criterion (GDC) 14, 30 and 31, and describes the attributes of neutron transport methodologies which are acceptable to the staff. The basic feature of an acceptable methodology is that the code is benchmarked by acquiring and evaluating a statistically significant database of measurement-to-calculation ratios and the resulting bias and uncertainty are within certain limits.

2.0 SUMMARY OF THE EPRI BWRVIP VESSEL NEUTRON FLUENCE METHODOLOGY

2.1 RPV Neutron Fluence Calculation Methodology

The BWRVIP neutron fluence calculational methodology employs the RAMA code to evaluate the neutron flux through the core, vessel internals, and vessel geometry. The code uses the BUGLE-96 cross-section library to calculate the neutron transport and to determine the reaction-specific measured activities. The RAMA code employs a combinatorial geometry method which allows an exact representation of geometrically complex components. This is accomplished by building the desired internal component using various primitive geometry elements (Ref. 8).

The neutron transport calculation is based on the following: (1) the three-dimensional transport equation is integrated by attenuating the neutron fluence along discrete rays according to the macroscopic cross-section and optical path in the intersected region, (2) a set of parallel rays are chosen in both a radial and axial plane and the neutron fluence is determined on this grid, (3) to account for the various possible directions of particle transport, rays are defined on a discrete set of angular quadratures, and (4) anisotropic scattering is treated using a Legendre expansion of the neutron scattering cross-section.

The neutron source is determined based on the core power density and the region-wise power distribution. The RAMA source accounts for the exposure dependence of the core neutron source and allows for a detailed pin power description of the source distribution. Typically, reflective boundary conditions are applied on the planes that define the angular sector of the geometry being calculated (typically, a core octant or quadrant), and vacuum boundary conditions are applied at the outer radial boundary (e.g., the outside wall of the RPV) and on upper and lower axial boundaries.

In order to facilitate comparisons of measurements to calculated values (as instructed by RG 1.190), RAMA calculates the corresponding quantities for the measured reaction rates. RAMA

determines the time-dependent neutron flux and tracks the target and reaction product nuclides.

The RAMA methodology includes a detailed neutron fluence uncertainty analysis. The parameters making a significant contribution to the neutron fluence calculation uncertainty are identified and RAMA is used to determine numerical sensitivity coefficients for these parameters. The uncertainty contribution from these parameters is determined by combining the numerical sensitivities with the estimates of the input parameter uncertainties. When making comparisons to benchmark measurements, the calculation-to-measurement (C/M) differences are combined using a covariance matrix to determine the uncertainty contribution from the measurements. The overall calculation uncertainty and bias are determined based on the C/M differences and the calculation input parameter uncertainties.

2.2 Calculation of the RPV Benchmarks

In validating the RAMA methodology, comparisons of RAMA predictions were performed for the following four benchmarks: (1) the Oak Ridge National Laboratory (ORNL) Pool Critical Assembly (PCA) benchmark experiment (Ref. 9), (2) the VENUS-3 engineering benchmark experiment (Ref. 10), (3) the H. B. Robinson-2 (HBR-2) RPV benchmark measurement (Ref. 11), and (4) the Brookhaven National Laboratory (BNL) RPV calculation benchmark of NUREG-6115 (Ref. 12). The PCA and VENUS-3 experiments are well-documented RPV mock-ups, including high accuracy dosimetry measurements. The PCA core includes twenty-five material test reactor (MTR) curved-plate type fuel assemblies and the simulator geometry includes a thermal shield, RPV, and void box outside the RPV. The PCA dosimetry measurements were made at positions in front and behind the thermal shield, at locations in front and behind the RPV, and at RPV internals locations. The PCA dosimetry measurements include the Np-237 (n, f), U-238 (n, f), In-115 (n, n'), Ni-58 (n, p) Co-58 and Al-27 (n, α) Na-24 reactions. The RAMA model is 3-dimensional and includes a radial quadrant of the PCA geometry, the full height of the core and the regions above and below the core. Detailed comparisons presented for both the thermal shield (or core shroud) and RPV locations indicate good agreement with the dosimetry measurements.

The VENUS-3 core consists of twelve 15x15 pressurized water reactor (PWR) fuel assemblies and the simulator geometry includes the baffle, core barrel, neutron pad and RPV simulator. The VENUS-3 dosimetry measurements include the Ni-58 (n, p) Co-58, In-115 (n, n'), and Al-27 (n, α) Na-24 reactions. The RAMA model is 3-dimensional and includes a radial quadrant of the simulator geometry, the full height of the core, and the regions above and below the core. Detailed comparisons are presented for the core, baffle, and core barrel and indicate good agreement with the measurements.

The HBR-2 benchmark experiment provides a well-documented set of dosimetry measurements for a full-height operating PWR, including core barrel, thermal shield and RPV. The HBR-2 dosimetry measurements include Np-237 (n, f), U-238 (n, f), Ni-58 (n, p) Co-58, Fe-54 (n, p) Mn-54, Ti-46 (n, p) Sc-46 and Cu-63 (n, α) Co-60. The measurements were made at an in-vessel capsule and at a cavity location. The HBR-2 RAMA model is 3-dimensional and provides a detailed representation of an octant of the problem geometry for a centrally-located axial region of the core. The model extends from the center of the core out to the outer surface of the biological shield. Detailed comparisons are presented for both the in-vessel surveillance capsule and the cavity measurements, and indicate good agreement with the measured data.

BNL NUREG-6115 provides the detailed specification and corresponding numerical solutions for a BWR RPV neutron fluence benchmark problem. The benchmark problem provides a reference calculation for a configuration that is typical of an operating BWR which includes the downcomer and RPV neutron fluences and the dosimeter response at an in-vessel surveillance capsule. The surveillance capsule dosimetry includes the Np-237 (n, f), U-238 (n, f), Ni-58 (n, p) Co-58, Fe-54 (n, p) Mn-54, Ti-46 (n, p) Sc-46, and Cu-63 (n, α) Co-60 reaction rates. The RAMA model is 3-dimensional and provides a detailed representation of an octant of the problem geometry over an axial region that includes the core as well as the regions above and below the core. The model extends from the center of the core out to the outer surface of the biological shield. Detailed comparisons are presented for both the RPV neutron fluences and the dosimetry reaction rates. The surveillance capsule comparisons indicate good agreement for all reaction rates. The downcomer and RPV neutron fluence comparisons indicate that RAMA is conservative relative to the reference solution.

2.3 Calculation of the Susquehanna Neutron Fluence Measurements

As part of the RAMA plant-specific qualification, RAMA transport calculations have been performed for the Susquehanna Unit 2 surveillance capsule that was removed at the end of Cycle 5. In order to validate the fast ($E \geq 1.0$ MeV) neutron fluence evaluations of the Susquehanna RPV, comparisons of the calculated and measured neutron fluence have been made to determine the neutron fluence calculational uncertainty and to identify any systematic bias in the neutron fluence predictions. The Cycle 5 surveillance capsule was located in the downcomer, radially at a position close to the innerwall of the RPV, and azimuthally 30° from the core flats. The surveillance capsule included three each of the following dosimeter wires: copper, nickel, and iron. The measured activities included the Cu-63 (n, α) Co-60, Ni-58 (n, p) Co-58, and Fe-54 (n, p) Mn-54 dosimetry reactions. The measurements were of high quality and were reported to have uncertainties on the order of a few percent.

The RAMA calculational model was based on detailed plant data provided by the Pennsylvania Power and Light (PPL) Company. The geometry data were taken from plant drawings and used to model the surveillance capsule and various core, core shroud, jet pump/riser and RPV components. RAMA provided a geometry model of high accuracy in which both the Cartesian geometry of the core boundary and the cylindrical geometry of the jet pump/riser components were represented without approximation. The RAMA model included a one-eighth (45°) azimuthal sector and the radial geometry from the center of the core out to the inner wall of the biological shield.

The core neutron source was based on the Susquehanna Cycles 1-5 operating history. Three-dimensional power, void and exposure distributions were constructed from the plant operating history files. The pin-wise gradient and exposure dependence of the neutron source for the fuel assemblies on the core periphery were included. Each cycle was described by a representative set of operating state-points. The neutron fluence accumulated by the capsule dosimeters was

determined by an appropriate weighting of the RAMA state-point calculations. An extensive set of sensitivity calculations was also performed to ensure the stability and convergence of the numerical solution.

RAMA calculations of the dosimeter activities were performed and compared with the measurements (dps/g). The average C/M overall measurement was found to be very close to unity indicating that there is no significant bias in the RAMA neutron fluence predictions. The standard deviation of all C/M values was less than 20% as recommended in RG 1.190 (Section 1.4.3). In order to provide an independent assessment of the accuracy of the RAMA neutron fluence prediction, a detailed analytic uncertainty analysis was also performed. The important input parameter uncertainties were identified and an estimate of the uncertainty in each parameter was determined. The uncertainty in each parameter was propagated through the RAMA calculation using numerical sensitivity calculations. The resultant analytic estimate of the RAMA neutron fluence calculation uncertainty, corresponding to the observed C/M standard deviation, was also shown to be less than 20%.

2.4 Calculation of the Hope Creek Neutron Fluence Measurements

RAMA transport calculations were performed for the surveillance capsule removed from the Hope Creek RPV at the end of the first cycle. In order to validate the fast ($E \geq 1.0$ MeV) neutron fluence evaluations of the RPV, comparisons of the calculated and measured neutron fluence have been made to determine the neutron fluence calculational uncertainty and to identify any systematic bias in the neutron fluence predictions. The first cycle surveillance capsule was located in the downcomer, radially at a position close to the innerwall of the RPV, and azimuthally at 33° from the core flats. It is noted that two additional capsules are located at 121° and 299°. The surveillance capsule included three copper and three iron flux wires. The measured activities included the Cu-63 (n, α) Co-60 and Fe-54 (n, p) Mn-54 dosimetry reactions. The measurements were reported to have uncertainties on the order of a few percent. The copper activity was corrected for the presence of Co-59 impurity of about 0.25 parts per million (ppm).

The RAMA calculational model was based on detailed plant data. The geometry data were taken from plant drawings and used to model the surveillance capsule, the core, core shroud, jet pump/riser, and RPV components. RAMA provided a geometry model of high accuracy in which both the Cartesian geometry of the core boundary and the cylindrical geometry of the jet pump/riser components were represented without approximation. The RAMA model included a one-eighth (45°) azimuthal sector and the radial geometry from the center of the core to the biological shield.

The core neutron source was based on the first cycle's operating history. Three-dimensional power, void, and exposure distributions were constructed from the plant operating history files. The pin-wise gradient and exposure dependence of the neutron source for the fuel assemblies on the core periphery were included. The neutron fluence accumulated by the capsule dosimeters was determined by an appropriate weighting of the RAMA state-point calculations. An extensive set of sensitivity calculations was also performed to ensure the stability and convergence of the numerical solution.

RAMA calculations of the dosimeter activities were performed and compared with the measurements (dps/gm). The average C/M overall measurement was found to be very close to

unity indicating that there is no significant bias in the RAMA neutron fluence predictions. The standard deviation of all C/M values was less than 20% as recommended in RG 1.190 (Section 1.4.3). In order to provide an independent assessment of the accuracy of the RAMA neutron fluence prediction, a detailed analytical uncertainty analysis was also performed. The important input parameter uncertainties were identified and an estimate of the uncertainty in each parameter was determined. The uncertainty in each parameter was propagated through the RAMA calculation using numerical sensitivity calculations. The resultant analytical estimate of the RAMA neutron fluence calculation uncertainty, corresponding to the observed C/M standard deviation, was also shown to be less than 20%.

3.0 TECHNICAL EVALUATION

The staff's review of the BWRVIP neutron fluence methodology focused on the details of the application of the neutron fluence calculation methodology and the qualification of the methodology provided by the benchmark comparisons and the plant-specific C/M database.

3.1 RPV Neutron Fluence Calculation Methodology

In the RAMA transport calculation, the neutron flux is determined by summing the contributions from a set of particle ray tracings through the problem geometry. The accuracy of this technique depends on the specific problem geometry, as well as the number and distribution of the rays used to track the neutrons through the geometry. In addition, the components that are associated with the problem geometry are represented with a discrete set of spatial regions (i.e., a spatial mesh). Because the neutron flux is averaged over these regions, a mesh-related uncertainty is introduced into the calculation. Since both of these numerical uncertainties are sensitive to the problem geometry, they require an evaluation that accounts for the geometry.

By letter dated April 20, 2004, the staff requested that the BWRVIP address the specific tests and criteria used to assure the adequacy of the number of rays and volumes used in the RAMA neutron fluence calculations for plant-specific applications. By letter dated September 29, 2004, the BWRVIP indicated that in plant-specific model applications of the RAMA fluence methodology, numerical sensitivity calculations will be performed to assure the adequacy of the number of particle tracking rays and the number of volumes used to represent component geometry in the RAMA neutron fluence evaluations. The staff found this approach acceptable.

The RAMA geometry model represents the individual components and regions of the problem geometry using a library of pre-calculated geometry elements. The modeling of the reflector region surrounding the core is particularly complicated in that it involves geometry elements that have both planar and cylindrical side boundaries. However, RAMA provides an exact representation of the true geometry (i.e., preserves the exact location, orientation and shape of all surfaces defining the physical geometry). For example, in the case of these reflector regions, the BWRVIP indicated in its letter dated September 29, 2004, that the geometry model allows for complex geometries, including the transition between the rectangular core and the cylindrical core shroud, to be precisely represented.

The RAMA code has the necessary mechanisms for geometrical representation, neutron scattering and neutron transport approximations. Therefore, the staff finds the RAMA code acceptable, based on its structural features.

3.2 Calculation of the RPV Benchmarks

The RPV benchmark calculations are performed to evaluate the accuracy of RAMA and to identify any systematic bias in the proposed licensing methodology. In order for the benchmark comparisons to reflect the difference between the benchmark and the proposed methodology, the methods used in the benchmark calculations must be the same as the proposed licensing methods. By letter dated April 20, 2004, the staff requested that the BWRVIP identify the differences between the methods used in performing the RAMA benchmark analyses in the BWRVIP-115 report and the methods that will be used in performing the calculations of the RPV and core shroud neutron fluence. By letter dated September 29, 2004, the BWRVIP indicated that the methods used in performing the RAMA benchmark analyses are the same as the methods that will be used in performing BWR RPV and core shroud neutron fluence calculations. The staff found this acceptable in that there would be no inconsistencies in the methods used.

The BWRVIP-115, BWRVIP-117, and TWE-PSE-001-R-001 reports present the RAMA analysis of a set of simulator calculations and operating reactor benchmarks which provide the basis of the Susquehanna and Hope Creek applications of the RAMA neutron fluence methodology. However, it is expected that as additional surveillance capsules are removed, new benchmark C/M data will become available. RG 1.190 requires that as new measurements become available, they shall be incorporated into the C/M database and the neutron fluence calculational bias and uncertainty estimates shall be updated as necessary.

By letter dated April 20, 2004, the staff requested that the BWRVIP address how it will ensure that new measurements are incorporated in the C/M database and that the neutron fluence bias and uncertainty will be updated in a timely manner. In its response by letter dated September 29, 2004, the BWRVIP stated that comparisons to measured surveillance capsule and benchmark dosimetry are maintained in a database that is updated as additional plant capsule evaluations are performed using the RAMA methodology. In addition, the BWRVIP stated that currently, TransWare Enterprises, Inc. (a primary contractor to the BWRVIP) maintains a surveillance capsule and benchmark dosimetry measurement database. The BWRVIP further stated that it would consider options of establishing a mechanism to collect and evaluate new C/M data. Based on the above, the staff found the BWRVIP's response acceptable.

The staff's review of this section established that the RAMA methodology is applied to the benchmarks in the same manner (approximations, cross-sections, etc.) as applied in plant-specific applications, therefore, the staff is in agreement that if a bias exists in the proposed code, it should appear in the benchmarks.

3.3 Results of the Susquehanna Dosimetry Measurements

The Susquehanna, Unit 2 surveillance capsule contained three of each of the following dosimeter wires; copper, iron and nickel. The RAMA calculated ratios and the corresponding measured specific activity (dps/g) C/M ratios are close to unity and display very good agreement. The individual ratios are well within the 20% limit specified in RG 1.190. In addition, the standard deviation is just a few percent.

In accordance with the guidance in RG 1.190, the BWRVIP-117 report includes an analytical neutron fluence uncertainty analysis. This analysis is important since it provides an independent estimate of the plant-specific Susquehanna RAMA neutron fluence calculational uncertainty. The uncertainty analysis requires that estimates of the major components of the uncertainty be determined and the uncertainties be propagated through the RAMA neutron fluence calculation. The uncertainty propagation is performed using numerical component sensitivity as calculated by RAMA. The important uncertainty components have been identified and include the following: (1) capsule and flux wire locations, (2) RPV inner radius, (3) core void fraction, (4) peripheral bundle power, and (5) iron cross-sections. In order to make an accurate determination of the RAMA uncertainty, reliable estimates of the component uncertainties are required.

By letter dated April 20, 2004, the staff requested that the BWRVIP discuss the basis for the parameter uncertainty for the components/locations listed above. In its letter dated September 29, 2004, the BWRVIP indicated that the uncertainty estimates for these components/locations is based on the following: (1) as-built measurements, (2) design drawing tolerances,
(3) experience estimates of ±5% variation in computed void fraction, (4) reported accuracy of core simulation analysis, and (5) experience estimates of ±5% in the cross section, respectively. In addition, the staff noted that Table 5-3 of the BWRVIP-117 report provided the values of the calculated bias and total uncertainty. The BWRVIP also displayed the calculation of the total uncertainty and bias from the C/M and the analytic uncertainty with weighting factors inversely proportional to the analytic and C/M variances in the BWRVIP-117 report. The staff finds the BWRVIP's response to the staff's request for additional information and the values of the bias and uncertainty, as provided in the BWRVIP-117 report, acceptable because the values are well within the limits set forth in RG 1.190.

3.4 Results of the Hope Creek Dosimetry Measurements

The Hope Creek surveillance capsule contained three copper dosimeter wires and three iron dosimeter wires. The surveillance capsule was irradiated during the first cycle for 377.9 effective full power days. The RAMA code calculated the specific dosimeter activity to the corresponding measured specific activity (dps/g). The C/M ratios are close to unity and displayed very good agreement. The individual dosimeter ratios are well within the 20% limit, as specified in RG 1.190, and the standard deviation is just a few percent. However, it was noted that unlike the Susquehanna case, the Hope Creek calculation does not include an analytical uncertainty and bias calculation.

4.0 CONCLUSION

4.1 BWR RPV Neutron Fluence

Based on the staff's review of the BWRVIP-114, -115, -117, and -121 reports, the TWE-PSE-001-R-001 report, and the supporting documentation, the staff concludes that the BWRVIP methodology, as described in these reports, provides an acceptable best-estimate plant-specific prediction of the fast (E $\geq$1.0 MeV) neutron fluence for BWR RPVs. This acceptance is limited to the axial region defined by the core active fuel height. The best-estimate RPV neutron fluence prediction is determined using the RAMA transport code, detailed plant-specific geometry, core operating history, and the BUGLE-96 nuclear data library with a minimum of a P_3 Legendre polynomial approximation in the iron inelastic scattering.

With respect to the calculation of BWR RPV neutron fluence, the staff concludes that based on the plant-specific benchmark data presently available, no calculational bias is required for the application of the methodology to plants of similar geometrical design to Susquehanna and Hope Creek, i.e., BWR-IV plants. However, in order to provide continued confidence in the proposed neutron fluence methodology for the BWR RPVs, the acceptance of this methodology is subject to the following conditions for plants which do not have geometries similar to the cited BWR-IV's:

- To apply the RAMA methodology to plant groups which have geometries that are different than the cited BWR-IV's, at least one plant-specific capsule dosimetry analysis must be provided to quantify the potential presence of a bias and assure that the uncertainty is within the RG 1.190 limits

  and

- Justification is necessary for a specific application based on geometrical similarity to an analyzed core, core shroud, and RPV geometry. That is, a licensee who wishes to apply the RAMA methodology for the calculation of RPV neutron fluence must reference, or provide, an analysis of at least one surveillance capsule from a RPV with a similar geometry.

4.2 Reactor Internals

EPRI's stated objective for this submittal included neutron fluence calculations for reactor internals. Neutron fluence values for reactor internal components are used to either quantify irradiation assisted stress corrosion cracking (IASCC) susceptibility, or to quantify helium formation which could affect the weldability of reactor internals components. IASCC depends on fast (E $\geq$ 1.0 MeV) neutron fluence, while helium formation is a function of thermal, epithermal, and fast neutron fluence. The calc ulational accuracy requirements for reactor internals are not the same as those for the RPV, and are not covered by the guidance in RG 1.190. In addition, the submittal does not include any benchmarking for reactor internals' neutron fluence calculations. Therefore, the staff will review qualification of RAMA for reactor internals applications on a case-by-case basis, based on consideration of C/M values and the associated accuracy requirements.

Licensees who wish to use the RAMA methodology for the calculation of neutron fluence at reactor internals locations must reference, or provide, an analysis which adequately benchmarks the use of the RAMA methodology for uncertainty and calculational bias based on the consideration of: (1) the location at which the neutron fluence is being calculated, (2) the geometry of the reactor, and, (3) the accuracy required for the application. In addition, if a licensee qualifies RAMA for calculating, for example, helium generation at one location (e.g., the core shroud), this qualifies RAMA for the same reactor and purpose at other reactor internals locations (e.g., at the location of the jet pumps).

4.3 Assembling a Statistically Significant Database

EPRI stated that efforts are underway to assemble a database which will enable the staff to remove any limitations placed on the use of the RAMA methodology. For such an effort to be successful, the staff expects that the neutron fluence uncertainty analysis and determination of the calculational bias for the relevant fleet of plants will be updated, as additional measurements are taken and as additional data become available. The results of the updated analysis, including the C/M ratios, should be submitted to the staff for review and approval.

5.0 REFERENCES

1. Letter from C. Terry, Electric Power Research Institute to US Nuclear Regulatory Commission "Project No. 704 - BWRVIP-114: BWR Vessel and Internals Project, RAMA Fluence Methodology Manual" June 11, 2003.

2. BWRVIP-115, "BWR Vessel and Internals Project, RAMA Fluence Methodology Benchmark Manual - Evaluation of Regulatory Guide 1.190 Benchmark Problems," EPRI, Palo Alto, CA: June 26, 2003.

3. BWRVIP-117, "BWR Vessel and Internals Project, RAMA Fluence Methodology-Susquehanna Unit 2 Surveillance Capsule Fluence Evaluation for Cycles 1 - 5," July 2003.

4. BWRVIP-121, "BWRVIP Vessel and Internals Project RAMA Fluence Methodology Procedures Manual," August 2003.

5. Letter from W. A. Eaton: Hope Creek Flux Wire Dosimeter Activation Evaluation for Cycle 1 Using the RAMA Fluence Methodology, March 23, 2004.

6. J. E. White, D. T. Ingersoll, C. O. Slater, R. W. Roussin, "BUGLE-96: A Revised multigroup Cross-section Library for LWR Applications Based on ENDF/B-VI Release 3," presented at the American Nuclear Society Radiation & Shielding Topical Meeting, April 21-25, 1996, Falmouth, MA, April 1996.

7. Office of Nuclear Regulatory Research, "Calculational and Dosimetry Methods for Determining Pressure Vessel Neutron Fluence," Regulatory Guide 1.190, U.S. Nuclear Regulatory Commission, April 2001.

8. J. T. West, M. B. Emmett, "MARS: A Multiple Array System Using Combinatorial Geometry," Oak Ridge National Laboratory, Radiation Shielding Information Center Report, December 1980.

9. W. N. McElroy, Editor, "LWR Pressure Vessel Surveillance Dosimetry Improvement Program: PCA Experiments and Blind Test," NUREG/CR-1861 (Hanford Engineering Development Laboratory, HEDL-TME 80-87), July 1981.

10. P. D'hondt, et al., "Contributions of the Venus-Engineering Mock-Up Experiments to the LWR-PV Surveillance, 'Proceedings of the 7th ASTM-Euratom Symposium on Reactor Dosimetry,'" Strasbourg, France, August 1990.

11. I. Remec and F. B. K. Kam, "H. B. Robinson-2 Pressure Vessel Benchmark," NUREG/CR-6453 (Oak Ridge National Laboratory, ORNL/TM-13204), February 1998.

12. "Pressure Vessel Fluence Calculation Benchmark Problems and Solutions," NUREG/CR-6115 (BNL NUREG-52395), Brookhaven National Laboratory, September 2001.

13. Letter from S. Coffin, US Nuclear Regulatory Commission to B. Eaton, Chairman BWRVIP, "Request for Additional Information - Review of BWR Vessel and Internals Project Reports, BWRVIP-114, BWRVIP-115, BWRVIP-117, and BWRVIP-121, and TransWare Enterprises Inc. Report TWE-PSE-001-R-001, Revision 0," April 20, 2004.

14. Letter from W.A. Eaton to US Nuclear Regulatory Commission Document Control Desk "Project No. 704 - BWRVIP Response to NRC Request for Additional Information on BWRVIP-114, -115, 117, and -121," September 29, 2004.

CITATIONS

This report was prepared by

Electric Power Research Institute
3420 Hillview Avenue
Palo Alto, CA 94304

TransWare Enterprises Inc.
1565 Mediterranean Dr.
Sycamore, IL 60178

Principal Investigators
K. E. Watkins
D. B. Jones

This report describes research sponsored by the Electric Power Research Institute (EPRI) and its BWRVIP participating members.

The report is a corporate document that should be cited in the literature in the following manner:

BWRVIP-114-A: BWR Vessel and Internals Project, RAMA Fluence Methodology Theory Manual. EPRI, Palo Alto, CA: 2009. 1019049.

This report is based on the previously published report:

BWRVIP-114: BWR Vessel and Internals Project, RAMA Fluence Methodology Theory Manual. EPRI, Palo Alto, CA: 2003. Technical Report 1003660, prepared by Trans Ware Enterprises Inc., principal investigator Ken Watkins.

PRODUCT DESCRIPTION

This report describes the theoretical and technical basis implemented in the RAMA Fluence Methodology for application to boiling water reactors (BWRs). A previous version of this report was published as BWRVIP-114 (1003660). This report (BWRVIP-114-A) incorporates changes proposed by the BWRVIP in response to the U.S. Nuclear Regulatory Commission (NRC) Requests for Additional Information, recommendations in the NRC Safety Evaluation (SE), and other necessary revisions identified since the previous publication of the report. All changes to the report except corrections to typographical errors are marked with margin bars. In accordance with an NRC request, the report number includes an "A" to indicate the version of the report accepted by the NRC staff.

Results and Findings

The RAMA Fluence Methodology contains the following software components: the transport code, parts model builder (PMB) code, state-point model builder (SMB) code, fluence calculator, and the nuclear data library. The methodology includes an advanced three-dimensional nuclear particle transport theory code that performs neutron and gamma flux calculations. It couples a three-dimensional, multi-group deterministic nuclear transport theory method with a combinatorial geometry modeling capability to provide a flexible and accurate tool for determining fluxes for any light water reactor design. The code supports the method of characteristics transport theory solution technique, a three-dimensional ray-tracing method, combinatorial geometry, a fixed source iterative solution, anisotropic scattering, thermal group upscattering treatments, and a nuclear cross-section data library based on the ENDF/B-VI data file. The software is written in conformance with the Fortran 95 programming language standard for ease of portability between computing platforms. The methodology adheres to the requirements set forth in NRC Regulatory Guide 1.190 for pressure vessel neutron fluence determinations.

Challenges and Objectives

The project had the following objectives:

- Develop a state-of-the-art method for calculating fluence in a BWR.
- Adhere to the requirements of NRC Regulatory Guide 1.190.
- Validate the methodology against specific benchmark problems identified in the regulatory guide and perform plant-specific analyses.
- Develop a system of software codes for application by utilities.

Applications, Value, and Use

The RAMA Fluence Methodology software package is used to determine neutron fluence in BWR components in compliance with the requirements and guidelines provided in NRC Regulatory Guide 1.190. RAMA Version 1.0 is designed to calculate the fluence for surveillance capsules, the reactor pressure vessel (RPV) within the active fuel height, and the core shroud within the active fuel height. Future versions of RAMA will be developed to extend the methodology to other internal components that are beyond the active fuel height.

EPRI Perspective

Accurate neutron fluence determinations for BWRs are required for several reasons:

- To determine neutron fluence within the RPV and at surveillance capsule locations to address vessel embrittlement issues
- To determine neutron fluence on the core shroud in order to determine fracture toughness and crack growth rate for use in flaw evaluation calculations
- To determine neutron fluence at other internal components for structural integrity assessments or to evaluate repair technologies

The RAMA Fluence Methodology is a state-of-the-art and versatile tool for calculating the fluence of the BWR pressure vessel and internals.

Approach

The BWRVIP conducted an extensive review and evaluation of existing technologies employed to determine the fluence of light water reactors. The three-dimensional nuclear particle transport theory, combinatorial geometry methods, and additional advanced features of the RAMA methodology provide capabilities not available in other existing technologies to accurately calculate the fluence of complex BWR internal components. Therefore, RAMA was selected as the methodology to address the needs of the BWRVIP. A key aspect of this work was to ensure that the RAMA methodology adheres to the requirements set forth in NRC Regulatory Guide 1.190 for pressure vessel neutron fluence determinations. To accomplish this, the methodology was verified and validated against specific benchmark problems identified in the regulatory guide, and plant-specific analyses were performed. Results of benchmark analyses will be presented in another BWRVIP report.

Keywords

Fluence
Embrittlement
Boiling water reactor
Vessel and internals
Reactor pressure vessel

ABSTRACT

This document describes the technical basis implemented in the RAMA Fluence Methodology software package. The RAMA Fluence Methodology contains the following software components: the transport code, parts model builder (PMB) code, state-point model builder (SMB) code, fluence calculator and the nuclear data library.

The RAMA Fluence Methodology software package is used to determine neutron fluence in BWR Priority 1 components in compliance with the requirements and guidelines provided in U.S. Nuclear Regulatory Commission Regulatory Guide 1.190. The BWR Priority 1 components include surveillance capsules, the reactor pressure vessel within the active fuel height, and the core shroud within the active fuel height.

The RAMA Fluence Methodology includes an advanced three-dimensional nuclear particle transport theory code that performs neutron and gamma flux calculations. RAMA couples a three-dimensional, multi-group deterministic nuclear transport theory method with a combinatorial geometry modeling capability to provide a flexible and accurate tool for determining fluxes for any light water reactor design. The code supports the method of characteristics transport theory solution technique, a three-dimensional ray-tracing method, combinatorial geometry, a fixed source iterative solution, anisotropic scattering, thermal-group upscattering treatments, and a nuclear cross-section data library based upon the ENDF/B-VI data file. The software is written in conformance to the Fortran 95 programming language standard for ease of portability between computing platforms.

RECORD OF REVISIONS

Revision Number	Revisions
BWRVIP-114	Original Report (1003660)
BWRVIP-114-A	This report is based on a previous report published as BWRVIP-114 (1003660) that was reviewed by the U.S. Nuclear Regulatory Commission (NRC). This report (BWRVIP-114-A) incorporates changes proposed by the BWRVIP in response to the NRC Requests for Additional Information, recommendations in the NRC Safety Evaluation (SE), and other necessary revisions identified since the last issuance of the report. All changes to the report except corrections to typographical errors are marked with margin bars. In accordance with a NRC request, the report number includes an "A" indicating the version of the report accepted by the NRC staff. NRC Safety Evaluation added to Front matter Appendices A-B added: NRC correspondence Details of the revisions can be found in Appendix C

CONTENTS

1 INTRODUCTION 1-1
1.1 Utility Need 1-1
1.2 Scope 1-1
1.3 Critical Characteristics 1-2
1.4 Documentation 1-2
1.5 Requisite Skills 1-3
1.6 Quality Assurance 1-3
1.7 Target Platforms 1-3
1.8 Document Organization 1-3
1.9 Implementation Requirements 1-4

2 OVERVIEW OF PROGRAM ARCHITECTURE 2-1

3 OVERVIEW OF GEOMETRY MODELING 3-1
3.1 Combinatorial Geometry Model 3-1
3.2 General Geometries 3-2
3.2.1 ARB - Arbitrary Convex Polyhedron 3-2
3.2.2 BOX - General Box 3-3
3.2.3 ELL - Ellipsoid 3-4
3.2.4 RAW - Right Angle Wedge 3-5
3.2.5 RCC - Right Circular Cylinder 3-5
3.2.6 REC - Right Elliptical Cylinder 3-6
3.2.7 RPP - Rectangular Parallelepiped 3-7
3.2.8 SPH - Sphere 3-8
3.2.9 TRC - Truncated Right Angle Cone 3-9

4 TRANSPORT METHODS 4-1
4.1 Geometry 4-1
4.1.1 Coordinate System 4-1

4.1.2 Reactor Models 4-2
4.1.2.1 Combinatorial Geometry Models 4-3
4.1.2.2 Geometry Symmetry 4-4
4.1.2.3 Meshing 4-4
4.1.3 Material Descriptions 4-4
4.2 Flux Calculation Methods 4-4
4.2.1 Particle Transport Equation 4-4
4.2.2 Characteristics Solution Methodology with Anisotropic Scattering 4-5
4.2.2.1 Ray Tracing Methodology 4-9
4.2.2.2 Neutron Source Due to Fissions 4-9
4.2.2.3 Boundary Condition Calculation 4-10
4.2.3 Flux Edits Methods 4-11

5 GEOMETRY MODEL BUILDING METHOD 5-1
5.1 Generating the Reactor Core Region Geometry Model 5-1
5.1.1 Fuel Assembly Meshing and Volume Calculations 5-2
5.2 Generating the Core Reflector Region Geometry Model 5-2
5.2.1 Core Reflector Meshing and Volume Calculations 5-2
5.3 Generating the Core Shroud Region Geometry Model 5-3
5.3.1 Shroud Meshing and Volume Calculations 5-3
5.4 Generating the Downcomer and Jet Pump Region Geometry Model 5-3
5.4.1 Downcomer and Jet Pump Meshing and Volume Calculations 5-3
5.5 Generating Geometry Models Containing Pipe Elements 5-4
5.5.1 Pipe Element Meshing and Volume Calculations 5-4
5.6 Radial and Azimuthal Meshing in Cylindrical Parts 5-4
5.7 Volume and Material Identifiers 5-5

6 MATERIAL PROCESSING METHOD 6-1
6.1 Fuel Assembly Homogenization 6-1
6.2 Volume Weighted Averaging 6-1
6.2.1 Homogenization of the Relative Powers 6-2
6.2.2 Homogenization of the Channel and Bypass Regions 6-5
6.3 Fuel Assembly RPP Types 6-5

7 ACTIVATION, FLUENCE, AND UNCERTAINTY METHODS 7-1
7.1 Activation Evaluation 7-1

7.1.1 Nuclide Activation 7-1
7.1.2 Accumulated Activation 7-2
7.1.3 Activation Reaction Rates 7-5
7.1.4 Reactions Per Atom 7-5
7.1.5 Equivalent ^{235}U Fission Spectrum Flux and Cross Section 7-6
7.1.6 Response Function Nuclide Number Densities and Decay Constants 7-6
7.2 Neutron Flux and Fluence Evaluations 7-6
7.2.1 Neutron Flux Energy Cutoff 7-6
7.2.2 Accumulated Neutron Fluence 7-9
7.2.3 Effective Full Power Time 7-9
7.2.4 Cumulative Power Factor 7-10
7.2.5 Average Neutron Flux 7-10
7.2.6 Rated Power Neutron Flux 7-11
7.3 Uncertainty Analysis Methodology 7-11
7.3.1 Analytical Uncertainty 7-11
7.3.2 Comparison Uncertainty 7-14
7.3.3 Calculational Uncertainty 7-16
7.3.4 Best Estimate Fluence 7-17

8 NUCLEAR DATA GENERATION METHOD 8-1
8.1 BUGLE-96 Data 8-1
8.2 Nuclide Identifiers 8-1
8.3 Legendre Order of Scattering 8-2
8.4 Cross Section Generation 8-2
8.4.1 Generation of Resonance Self-shielded Actinide Cross Sections 8-3
8.4.2 Generation of Broad Group Shielded Cross Sections 8-5
8.4.3 Creation of ANISN BCD Nuclear Data 8-6
8.4.4 Generation of the RAMA Nuclear Data Library 8-7

9 REFERENCES 9-1

A NRC REQUEST FOR ADDITIONAL INFORMATION A-1

B BWRVIP RESPONSE TO NRC REQUEST FOR ADDITIONAL INFORMATION B-1

C RECORD OF REVISIONS C-1

LIST OF FIGURES

Figure 2-1 RAMA Fluence Methodology Software Architecture Flow Diagram 2-2
Figure 3-1 Arbitrary Convex Polyhedron Geometry 3-3
Figure 3-2 General Box Geometry 3-4
Figure 3-3 Ellipsoid Geometry 3-4
Figure 3-4 Right Angle Wedge Geometry 3-5
Figure 3-5 Right Circular Cylinder Geometry 3-6
Figure 3-6 Right Elliptical Cylinder Geometry 3-7
Figure 3-7 Rectangular Parallelepiped Geometry 3-8
Figure 3-8 Sphere Geometry 3-8
Figure 3-9 Truncated Right Angle Cone Geometry 3-9
Figure 4-1 BWR Reactor Assembly Coordinate System 4-2
Figure 4-2 Cutaway View of a BWR Pressure Vessel Showing the Axial Zones 4-3
Figure 6-1 Rectangular Parallelepiped (RPP) Types 6-6
Figure 7-1 Reactor Operating History Example 7-3
Figure 8-1 SCAMPI Cross Section Processing Flow Diagram 8-4
Figure 8-2 RAMA Nuclear Data Library Generation Flow Diagram 8-5

LIST OF TABLES

Table 7-1 Default Target Nuclide Number Densities 7-8
Table 7-2 Default Product Nuclide Decay Constants 7-9
Table 7-3 Sample Input Parameter Set 7-14
Table C-1 Revision Details C-2

1 INTRODUCTION

1.1 Utility Need

Utilities have a need for a standard methodology, acceptable to the U.S. Nuclear Regulatory Commission (NRC), that can be used to perform accurate neutron fluence calculations in Boiling Water Reactors (BWR). Accurate neutron fluence determinations are required for a number of reasons: 1) to determine neutron fluence within the reactor pressure vessel (RPV) and at surveillance capsule locations to address vessel embrittlement issues; 2) to determine neutron fluence on the core shroud in order to determine fracture toughness and crack growth rate for use in flaw evaluation calculations; and 3) to determine neutron fluence at other internal components for structural integrity assessments or to evaluate repair technologies.

EPRI, under the direction of the BWR Vessel and Internals Project (BWRVIP) has developed the RAMA Fluence Methodology for predicting fluence in a manner that meets the NRC requirements. Fluence predictions are potentially required at many components within the reactor. However, there is a near term need for fluence calculations at surveillance capsule locations, within the vessel wall and the core shroud at elevations within the height of the active fuel. These "Priority 1" locations are addressed by the current methodology. In the future, the BWRVIP intends to extend the methodology for applicability to other internal components that are outside the elevation of the active core height.

1.2 Scope

The current methodology described herein predicts neutron fluence at all Priority 1 locations. The methodology includes computerized analysis tools to perform the fluence calculations, modeling guidelines describing the use of the methodology, and benchmark reports that document the capability of the methodology to predict neutron fluence.

The methodology includes a neutron transport code that is capable of accurately representing the reactor geometry and performing neutron flux calculations in true three-dimensional geometry, a nuclear data library which contains cross-section data and activation response factors which are suitable for neutron fluence determinations in BWR plants, and auxiliary processing codes to facilitate building detailed analysis models and determining dosimeter activities, neutron fluence, and uncertainties. The methodology adheres to the requirements set forth in NRC Regulatory Guide 1.190 [1] for pressure vessel neutron fluence determinations. This has been demonstrated by validating the methodology against specific benchmark problems identified in the regulatory guide and performing a plant-specific analysis.

The system of analysis tools developed for the BWR fluence methodology is provided in a software package referred to as the "RAMA Fluence Methodology". The RAMA Fluence Methodology includes the transport code that performs neutron transport calculations, the nuclear data library, and three supporting codes that were initially developed by TransWare Enterprises, Inc.: the RAFTER code that performs activation and uncertainty calculations, and the Parts Model Builder (PMB) and State-point Model Builder (SMB) codes that automate the process of preparing detailed computer models for the RAMA transport code.

1.3 Critical Characteristics

The RAMA Fluence Methodology performs fluence calculations for BWR Priority 1 components in a manner that meets Regulatory Guide 1.190. Following is a summary of key features and capabilities of the RAMA Fluence Methodology:

- Three-dimensional, multi-group transport code for calculating neutron flux. The transport methodology includes the capability to determine neutron source terms from input isotopic data and an anisotropic scattering treatment that is important for handling neutron transport from the in-core regions to the ex-core regions.
- Nuclear data that conforms to the cross sections and activation response functions contained in the industry standard BUGLE-96 nuclear data library [2].
- Accurate modeling and prediction of neutron fluence in the following specific BWR Priority 1 components: surveillance capsules, the reactor pressure vessel over the active fuel height (including axial and azimuthal profiles), and the core shroud over the active fuel height (including axial and azimuthal profiles).
- Capability to calculate dosimeter activation rates and to apply fluence trending evaluations, uncertainty, and bias adjustments identified in Regulatory Guide 1.190.
- Geometry and material model building tools to assist the user in constructing detailed reactor models.

1.4 Documentation

The following reports describe the RAMA Fluence Methodology software:

A Theory Manual (this report) describes the technical basis for the methodologies implemented in the RAMA computer codes. The Theory Manual also includes the technical basis for the methodologies used to generate the nuclear data library.

A User's Manual describes the installation, user interface, and input data requirements of the RAMA computer codes. The User's Manual also includes user information for the nuclear data library.

A Procedures Manual provides guidelines for the use of the methodology to perform neutron fluence, uncertainty and bias calculations in BWR Priority 1 components. The Procedures Manual also contains example problems that illustrate the process for building reactor models and performing fluence calculations.

A Benchmark Manual describes the benchmark problems and results. These benchmark problems provide an assessment of the accuracy and capabilities of the RAMA Fluence Methodology.

1.5 Requisite Skills

The RAMA Fluence Methodology is a technical tool that requires an understanding of reactor physics, computer modeling techniques, nuclear plant operation, fluence determinations, and uncertainty and bias determinations. The user of the software should have sufficient knowledge and experience in these technical areas in order to apply the software package correctly and to interpret the results generated by the software package. In general, the user should have a minimum Bachelor of Science degree in Nuclear Engineering or a related discipline.

1.6 Quality Assurance

The RAMA Fluence Methodology has been developed in accordance with 10CFR50 Appendix B and 10CFR21 requirements.

1.7 Target Platforms

The computer codes in the RAMA Fluence Methodology are written in conformance with the ISO/IEC Standard Fortran 95 [3] and ANSI Standard C [4] programming languages. Therefore, the software can be installed on any computer system supporting standard Fortran 95 and C compilers.

For this Project, the RAMA software shall be developed and maintained on desktop workstations employing Intel microprocessors and running the Linux operating system.

1.8 Document Organization

The remaining sections of this document describe the methodologies employed by the components of the RAMA Fluence Methodology to determine neutron fluence.

Section 2 provides an overview of the program architecture. A flow diagram illustrates how the code components work together and what data inputs are required.

Section 3 describes the geometry models employed in the transport code.

Sections 4-7 describe the methods used by RAMA, including the PMB, SMB, and RAFTER modules, respectively.

Section 8 describes the methods used to generate the nuclear data library.

Section 9 contains the references used in this document.

1.9 Implementation Requirements

This report is provided for information only. Therefore, the implementation requirements of Nuclear Energy Institute (NEI) 03-08, Guideline for the Management of Materials Issues, are not applicable.

2
OVERVIEW OF PROGRAM ARCHITECTURE

This section provides a brief description of the RAMA Fluence Methodology software architecture and logic flow.

The software is designed to perform neutron and gamma ray flux calculations, determine neutron fluence, and calculate nuclide activation for BWR nuclear reactor assemblies. Each component of the software package is implemented to execute as a stand-alone program module. A top-level flow diagram of the software package is presented in Figure 2-1.

As Figure 2-1 shows, input to the software system comes from mechanical design drawing information and plant operating history data. The PMB tool processes the mechanical design inputs and generates the geometry information to build the geometry model for the desired component. The geometry data file generated by the PMB is then input into the transport code module.

The plant operating data is collected by the utility. Each utility has its own database for storing data. The utility generates a data file in a compatible format that will link with the SMB tool. The SMB tool processes the operating data and generates a material composition data file for input to the transport code. RAMA retrieves the geometry and material data, accesses nuclide cross section data from the nuclear data library and performs the neutron and gamma-ray flux calculations.

During the performance of a flux calculation, RAMA generates two additional files that provide data for subsequent executions of the same (or nearly the same) component geometry and state-point condition. These files are the Track Data File and the Flux Guess Data File. During an initial flux calculation, RAMA must convert the geometry and material information provided by the model builder tools, using ray tracing methods, to a format that can be used by the flux calculation. RAMA also uses standard flat flux guesses when performing an initial flux calculation. As a result of the initial flux calculation, RAMA generates a Track Data File that contains component geometry and material data in the form used directly by the flux calculation. It also generates a Flux Guess Data File that contains modified flux guesses generated specifically for that component during the flux calculation. These files allow RAMA to execute much faster when running a restart case because they provide data that was calculated in a previous run and does not need to be re-calculated in the present run.

During code execution, RAMA generates output list and ASCII data files containing the flux and dose rate data. The ASCII data files are retrieved by the RAFTER module for use in performing neutron fluence calculations. RAFTER also uses the plant operating history data for given state-points and dosimeter activity measurements to determine nuclide activation rates. The uncertainty methodology in RAFTER then adjusts the neutron fluence determination to provide an accurate neutron fluence for the given reactor component.

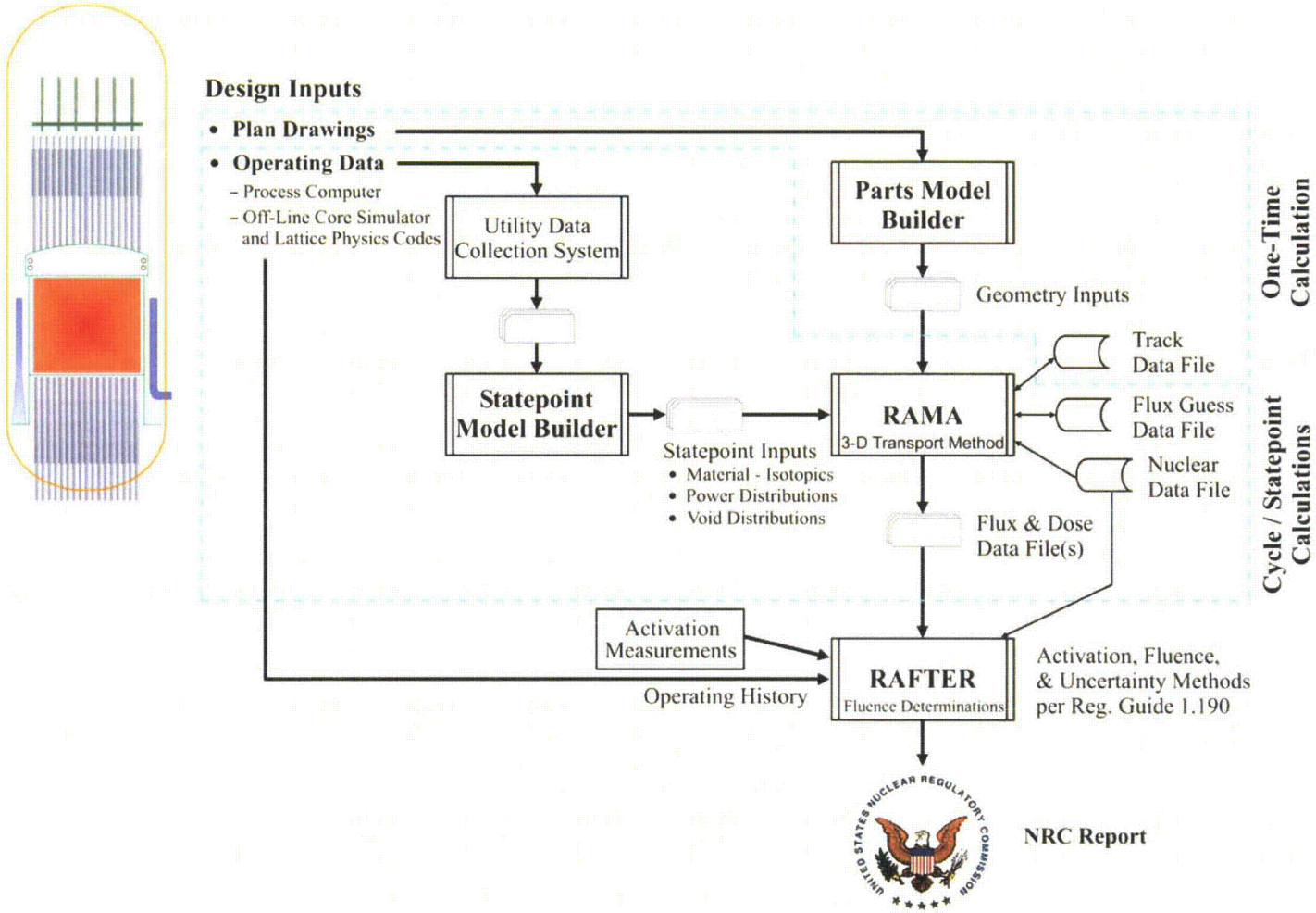

Figure 2-1
RAMA Fluence Methodology Software Architecture Flow Diagram

3
OVERVIEW OF GEOMETRY MODELING

This section provides an overview of the geometry modeling capabilities of the transport code. In essence, RAMA employs a geometry modeling capability that allows the user to describe the mechanical design of a reactor component at any desired level of modeling detail. To facilitate the use of the code, RAMA has a special input block that allows the user to easily describe very complex geometries with simple engineering inputs. The following subsections describe the geometry modeling method and provide examples of various parts models that are easily described using the geometry input data block. The User's Manual provides detailed descriptions for the geometry input data block.

3.1 Combinatorial Geometry Model

RAMA employs a combinatorial geometry modeling capability, similar to the methods used in Monte Carlo codes, that allows the user to describe problem geometries at any level of mechanical design detail. The geometry model is based on the combination of primitive geometry elements, e.g., rectangular parallelepipeds, right circular cylinders, right angle wedges, etc., to form geometry components having combinations of linear and curvilinear surfaces. A simple geometry component, or part, is described by a single geometry element. Complex geometry components, or parts, are described by specifying the differences and intersections of two or more primitive geometry elements. The primitive geometry elements most commonly used to describe geometry models are:

- arbitrary polyhedron,
- general box,
- ellipsoid,
- right angle wedge,
- right circular cylinder,
- right elliptical cylinder,
- rectangular parallelepiped,
- sphere, and
- truncated right angle cone.

The geometry model is similar in application to the combinatorial geometry techniques described in the MARS [5] geometry modeling system and used in various Monte Carlo codes such as SAM-CE [6]. The RAMA geometry model is very flexible. It allows the user to describe one or several unique individual parts in a local coordinate system. One or more instances of these parts are then placed in the proper absolute coordinates of the final solution geometry using positioning vectors. In restart cases, the user may easily replace any part in the solution geometry with another part using simple user input options.

The flexibility of the combinatorial geometry model can result in geometry descriptions that are very large and complex. To facilitate the use of the RAMA geometry modeling capability, RAMA supports an input data block that uses simple engineering data to describe the parts by dimensions, materials and meshing options. The code then automatically builds the parts descriptions in combinatorial geometry terms.

The following subsections describe the general geometry shapes used in RAMA to model any reactor component to detailed design descriptions. A discussion of how the Parts Model Builder combines these basic shapes to construct models of reactor components is provided in Sections 4 and 5. Additional information for building geometry models is provided in the User's Manual.

3.2 General Geometries

3.2.1 ARB - Arbitrary Convex Polyhedron

The arbitrary convex polyhedron body, "ARB", is a flexible geometry that can define 4, 5, and 6 sided bodies. A 6-sided arbitrary convex polyhedron body is illustrated in Figure 3-1.

The ARB body requires 30 values to describe the arbitrary convex polyhedron geometry. The first 8 sets of 3 values (24 values) define 8 vertices, $\vec{V}_1 - \vec{V}_8$, in (x, y, z) coordinates. These vertices are used to describe the shape and dimensions of the sides of the body. The remaining 6 values define the faces of the body. Each face is described by a 4-digit number, where each digit corresponds to an index of a vertex. For example, the value "1234" corresponds to the face defined by the vertices, $\vec{V}_1$, $\vec{V}_2$, $\vec{V}_3$, and $\vec{V}_4$. The faces may be specified in any order; however, the indexes for a face must be entered in either clockwise or counterclockwise order.

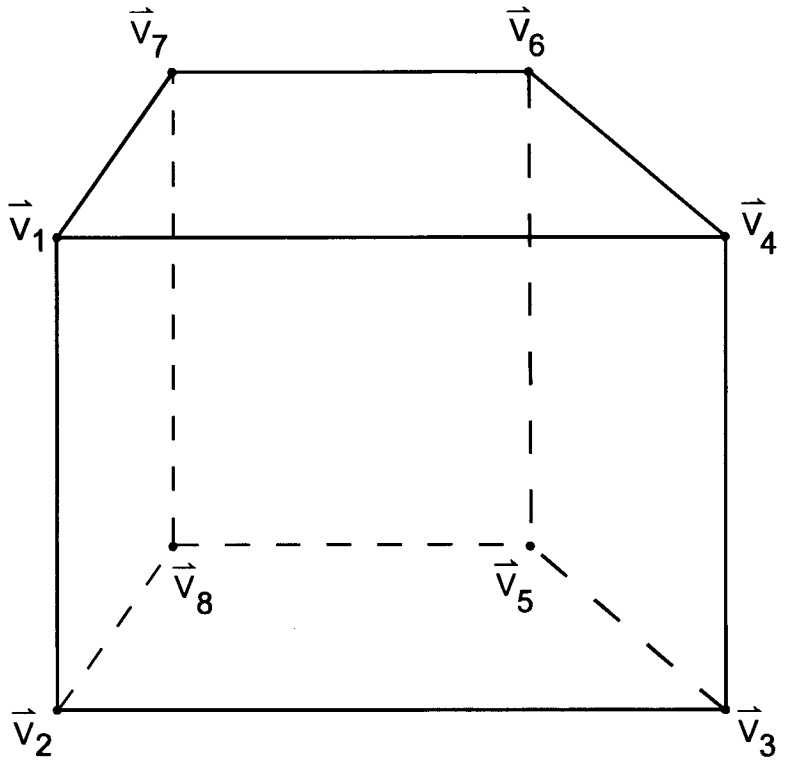

Figure 3-1
Arbitrary Convex Polyhedron Geometry

3.2.2 BOX - General Box

The general box body, "BOX", is a rectangular parallelepiped body that may be oriented arbitrarily relative to the coordinate axes. The general box body is illustrated in Figure 3-2.

The BOX body requires twelve values to describe the general box geometry. The first set of 3 values defines the origin of the body, (V_x, V_y, V_z). The following 3 sets of 3 values define mutually perpendicular sides of the body, (H_{1x}, H_{1y}, H_{1z}), (H_{2x}, H_{2y}, H_{2z}), and (H_{3x}, H_{3y}, H_{3z}) where, for example, the three components of H1 describe the length and orientation of H1 with respect to the coordinate system.

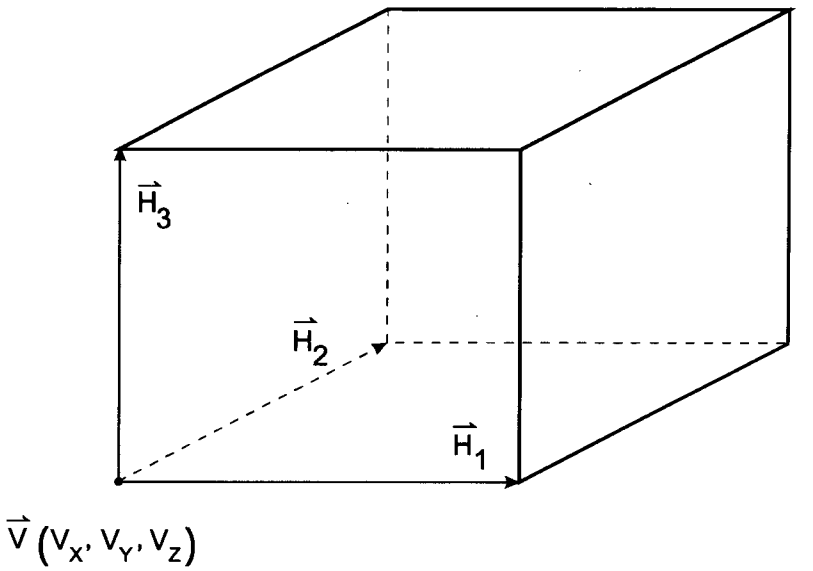

Figure 3-2
General Box Geometry

3.2.3 ELL - Ellipsoid

The ellipsoid body, "ELL", is illustrated in Figure 3-3. The ELL body requires seven values to describe the ellipsoid geometry. The first two sets of 3 values, $\vec{V}_1$ and $\vec{V}_2$ define the vertices of the foci in (x, y, z) coordinates. The last value is a scalar value, R, which defines the length of the major axis.

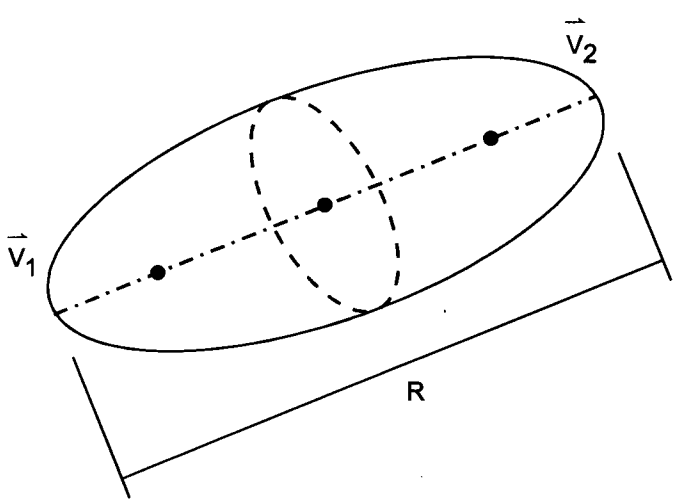

Figure 3-3
Ellipsoid Geometry

3.2.4 RAW - Right Angle Wedge

The right angle wedge body, "RAW", is illustrated in Figure 3-4. The RAW body requires twelve values to describe the right angle wedge geometry. The first set of 3 values defines the vertex of the RAW body, (V_x, V_y, V_z). The right angles that describe the faces of the wedge will be defined relative to the vertex point. The next two sets of 3 values define the vectors, (H_{1x}, H_{1y}, H_{1z}) and (H_{2x}, H_{2y}, H_{2z}), that describe the directions and dimensions for the sides of the body. The last set of 3 values defines a perpendicular vector, (B_x, B_y, B_z), that describes the height of the wedge body.

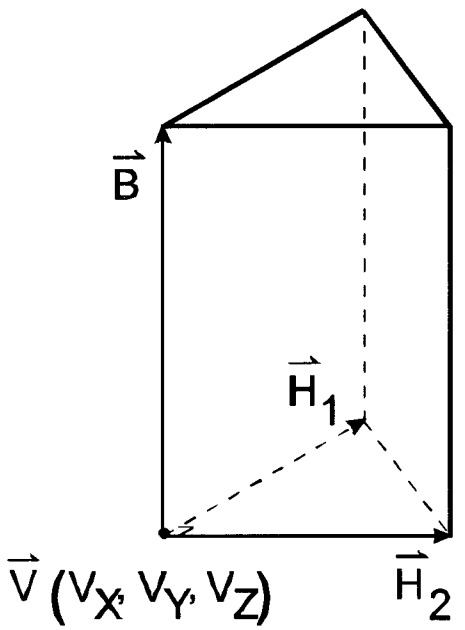

Figure 3-4
Right Angle Wedge Geometry

3.2.5 RCC - Right Circular Cylinder

The right circular cylinder body, "RCC", is illustrated in Figure 3-5. The RCC body requires seven values to describe the right circular cylinder geometry. The first set of 3 values, (V_X, V_Y, V_Z) defines the origin of the base plane of the cylinder. The second set of 3 values, (H_X, H_Y, H_Z) specifies the height and direction of the cylinder perpendicular to the base plane. The last value, R, defines the radius of the cylinder.

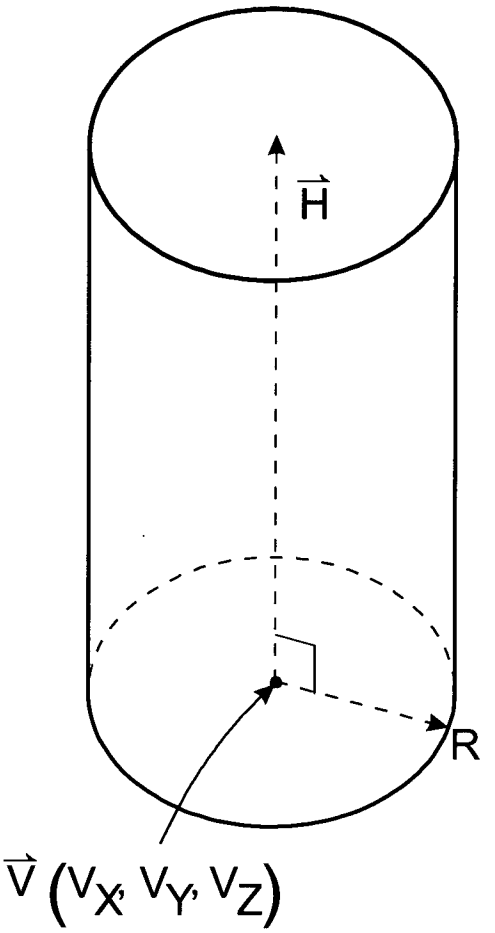

Figure 3-5
Right Circular Cylinder Geometry

3.2.6 REC - Right Elliptical Cylinder

The right elliptical cylinder body, "REC", is similar to an RCC body (see Section 3.2.5) except that the shape of the cylinder is elliptical instead of circular. Figure 3-6 illustrates a REC body. The REC body requires twelve values to describe the right elliptical cylinder geometry. The first set of 3 values, (V_X, V_Y, V_Z), defines the center of the elliptical cylinder in the base plane. The second set of 3 values, (H_X, H_Y, H_Z), specifies the height and direction of the elliptical cylinder. The last two sets of 3 values, (R_{1x}, R_{1y}, R_{1z}) and (R_{2x}, R_{2y}, R_{2z}), define the direction and length of the major and minor axes of the elliptical cylinder.

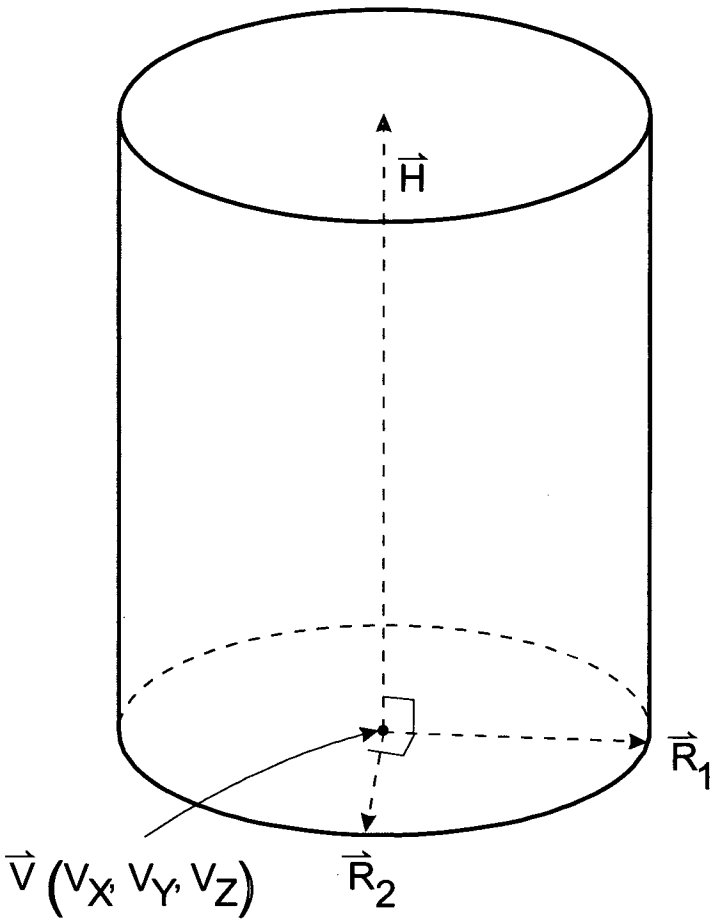

Figure 3-6
Right Elliptical Cylinder Geometry

3.2.7 RPP - Rectangular Parallelepiped

The rectangular parallelepiped body, "RPP", is similar to the BOX body (see Section 3.2.2) except the sides of the RPP body are parallel to the coordinate axes. The rectangular parallelepiped body is illustrated in Figure 3-7.

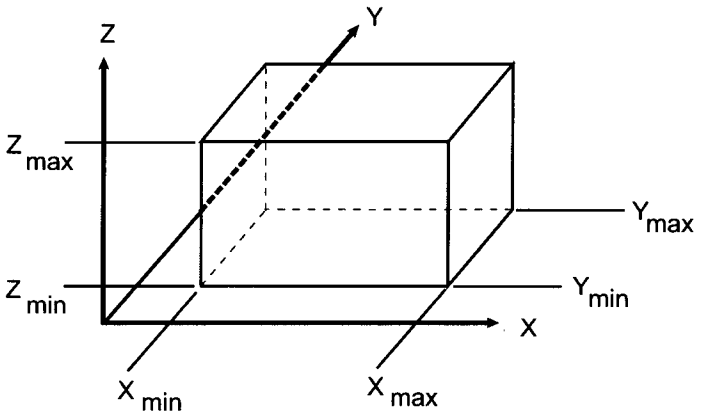

Figure 3-7
Rectangular Parallelepiped Geometry

The RPP body requires six values to describe the rectangular parallelepiped geometry. The first set of two values, X_{min} and X_{max}, define the minimum and maximum coordinates on the x-axis. The second set of two values, Y_{min} and Y_{max}, define the minimum and maximum coordinates on the y-axis. The third set of two values, Z_{min} and Z_{max}, define the minimum and maximum coordinates on the z-axis.

3.2.8 SPH - Sphere

The sphere body, "SPH", is illustrated in Figure 3-8. The SPH body requires four values to describe the sphere geometry. The first set of 3 values, (V_X, V_Y, V_Z), defines the centroid of the sphere. The fourth value, R, defines the radius of the sphere.

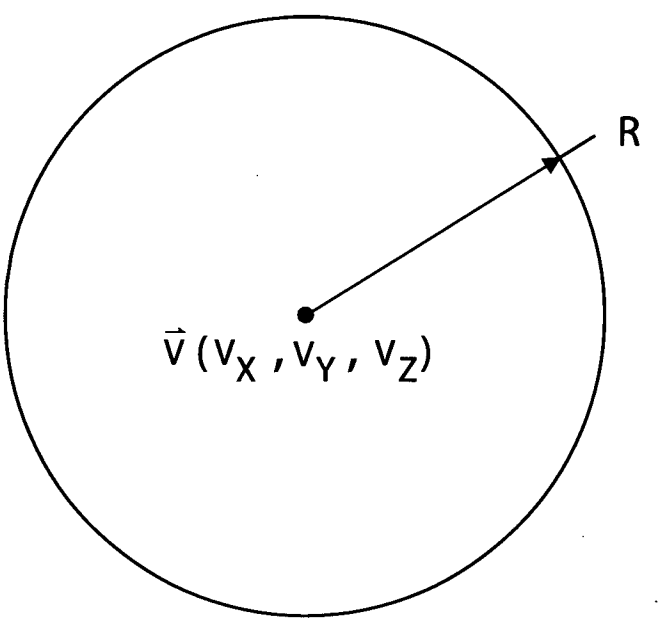

Figure 3-8
Sphere Geometry

3.2.9 TRC - Truncated Right Angle Cone

The truncated right angle cone body, "TRC", is illustrated in Figure 3-9. The TRC body requires eight values to describe the truncated right angle cone geometry. The first set of 3 values, (V_X, V_Y, V_Z), defines the centroid of the base plane of the cone. The second set of 3 values, (H_X, H_Y, H_Z), defines the height and direction of the cone. The seventh and eighth values, R_1 and R_2, define the lower and upper radii of the cone.

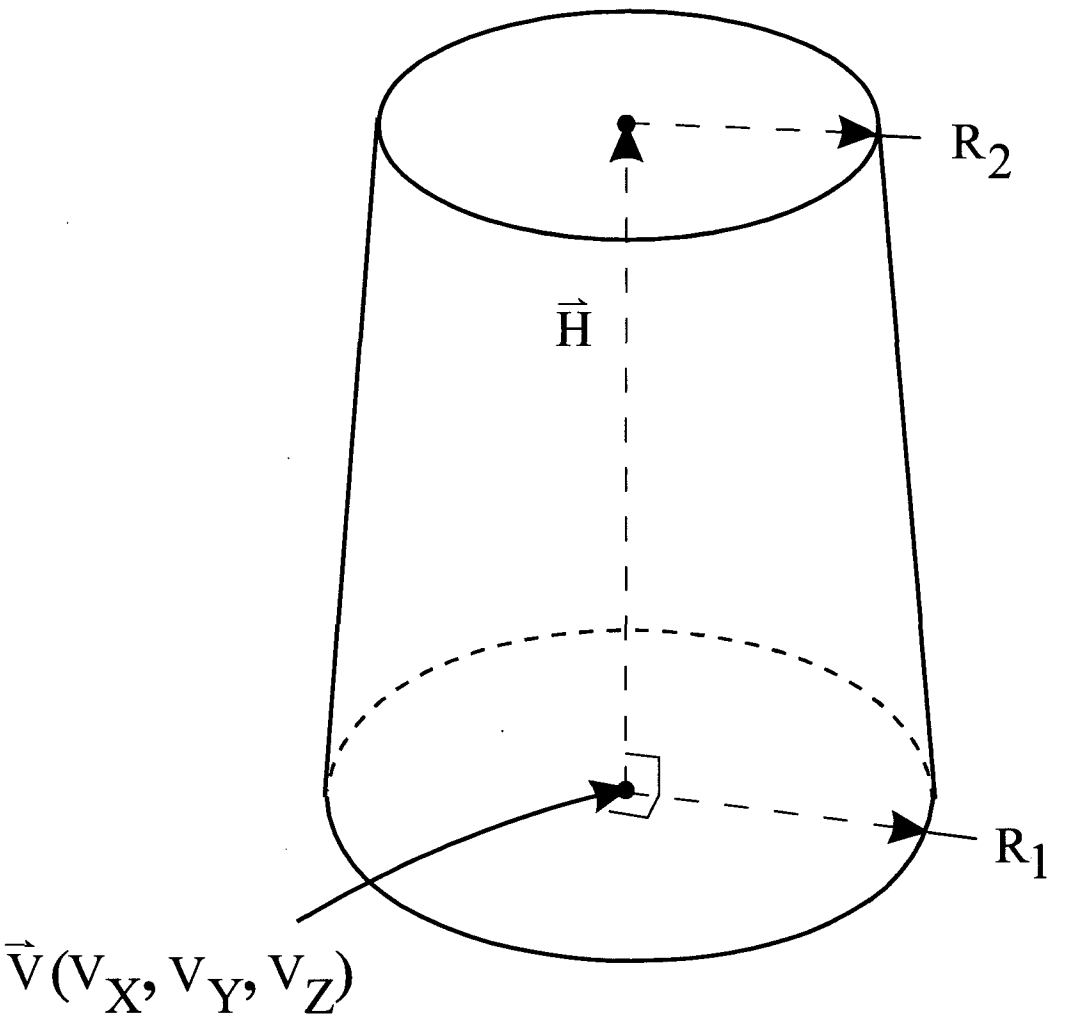

Figure 3-9
Truncated Right Angle Cone Geometry

4
TRANSPORT METHODS

This section describes the geometry models and solution methodologies that are employed by the RAMA transport code.

Section 4.1 describes the geometry modeling capabilities of the transport code. RAMA employs a geometry modeling technique that allows the user to model virtually any geometry problem in true three-dimensional detail.

Section 4.2 describes the nuclear transport methods used to solve the neutron and gamma-ray flux distribution problems. The transport theory is based upon the method of characteristics. The unique methods implemented in the code include treatments for three-dimensional spatial flux calculations and anisotropic scattering.

4.1 Geometry

RAMA employs a geometry modeling capability that is based upon combinatorial geometry techniques, similar to those in many Monte Carlo transport codes. This capability allows the user to describe virtually all parts of a reactor assembly in true three-dimensional design detail. This section describes the geometry coordinate system for a typical Boiling Water Reactor (BWR) assembly.

4.1.1 Coordinate System

Figure 4-1 illustrates the absolute coordinate system for a BWR reactor assembly model. RAMA uses the Cartesian coordinate system to describe the orientation of the reactor pressure vessel in space. The origin of the coordinate system is located on the inner surface of the vessel wall and is centered at the bottom drain plug. The z-axis is oriented along the vertical axis of the vessel. The xy-plane is perpendicular to the z-plane.

Individual reactor assembly parts may be described in a local Cartesian coordinate system for the modeling convenience of the user. The local coordinate system must then be defined such that the parts can be moved into the absolute coordinate system using simple positional vectors.

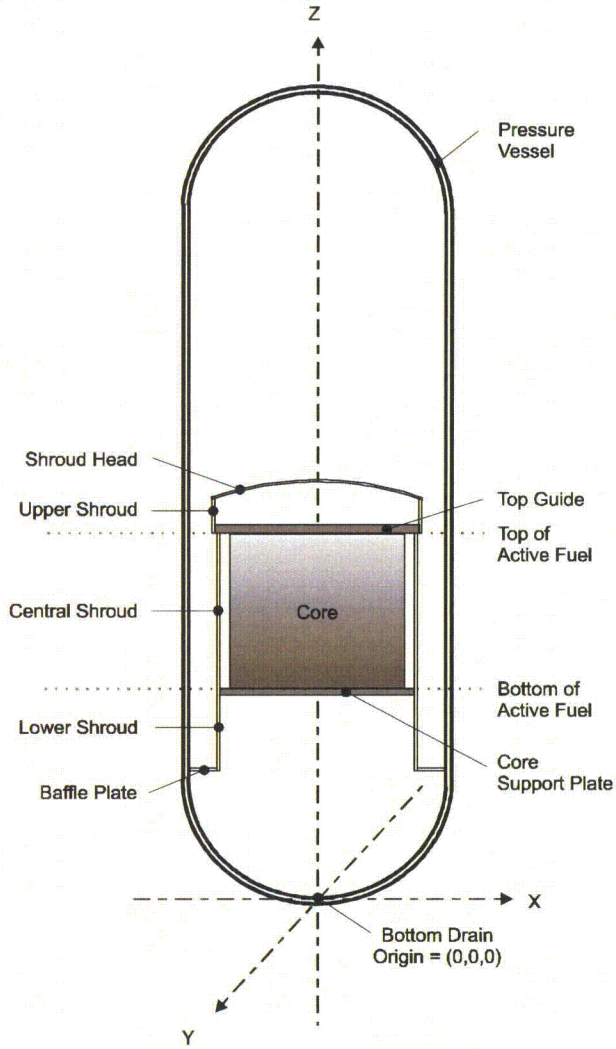

Figure 4-1
BWR Reactor Assembly Coordinate System

4.1.2 Reactor Models

The RAMA transport code is used to model the BWR system to calculate neutron flux. For modeling convenience, the BWR system is described in three axial zones. The first zone is comprised of the reactor core, pressure vessel components and coolant regions that lie between the axial elevations defined as the bottom of active fuel and top of active fuel. The second zone is comprised of the pressure vessel components and coolant regions that lie above the top of active fuel and the third zone is comprised of all components and coolant regions that lie below the bottom of active fuel. Figure 4-2 illustrates the three axial zones used in the RAMA models.

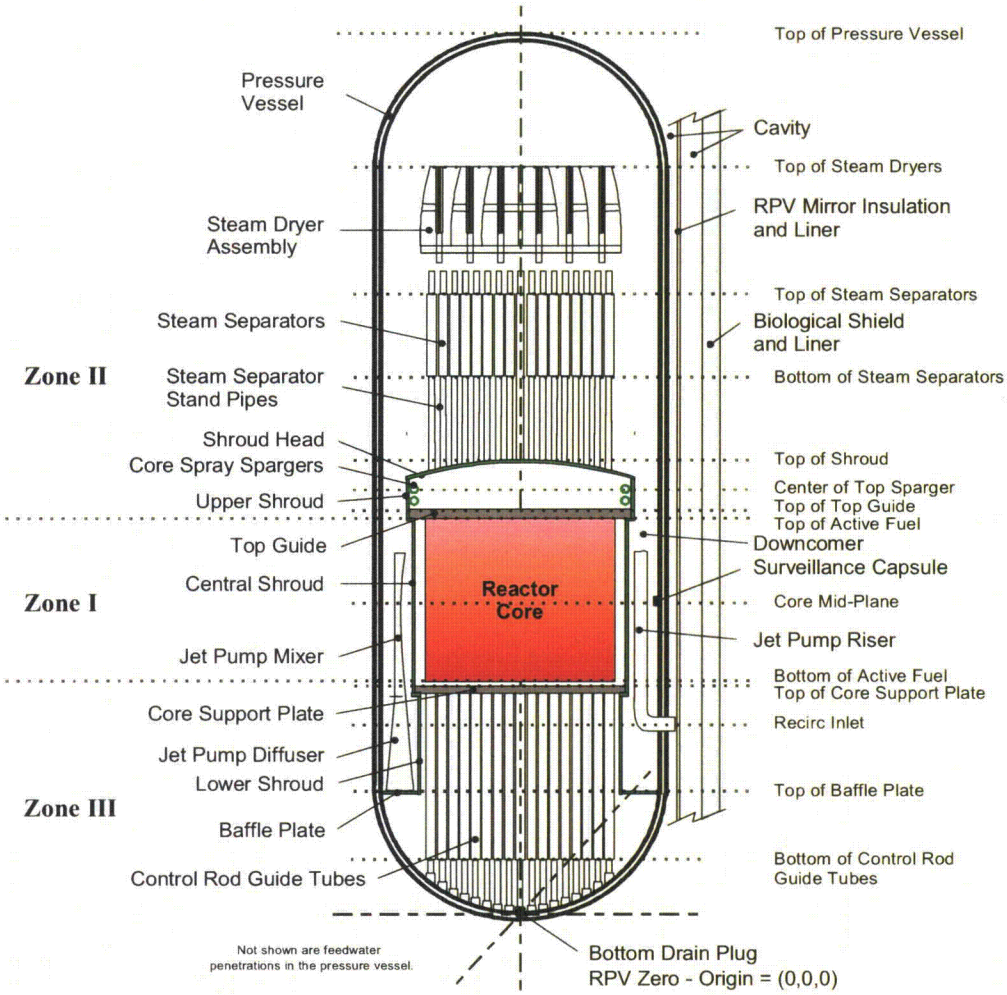

Figure 4-2
Cutaway View of a BWR Pressure Vessel Showing the Axial Zones

The Priority 1 components of interest in BWRs are all located within Zone 1. The major Priority 1 components and regions that must be represented in the RAMA transport calculation include the reactor core, central shroud, central downcomer, jet pump assemblies, dosimetry/surveillance capsules, and pressure vessel. The BWR Priority 1 model may also include representations for the pressure vessel mirror insulation, cavity, and biological shield (concrete wall), as required, to provide radial boundary conditions for the neutron transport calculation.

4.1.2.1 Combinatorial Geometry Models

RAMA employs a geometry modeling capability that allows the user to describe any part in the reactor assembly in true mechanical design detail. Accurate representations of straight and curved surfaces at any orientation are supported. The geometry model is coupled with a ray-tracing method that allows the code to determine accurate transmission probabilities of neutron and gamma-ray particles through material regions.

RAMA's geometry modeling capability is based upon three-dimensional combinatorial geometry techniques. The geometry modeling capability supports appropriate ray-tracing calculation methods to permit interfacing with the nuclear transport theory methods.

4.1.2.2 Geometry Symmetry

RAMA supports the capability to model problem geometries of any symmetrical form, thus allowing a reduced model for calculations.

4.1.2.3 Meshing

The geometry modeling capability allows parts to be described by one or more sub-volumes for purposes of meshing the problem.

4.1.3 Material Descriptions

RAMA has the capability to assign materials to all regions of the problem geometry. Material regions are described with the following attributes:

- Material type (e.g., SS304),
- Nuclides and nuclide concentrations in atoms/barn-cm, and
- Relative power term of the material in the material region.

4.2 Flux Calculation Methods

4.2.1 Particle Transport Equation

The basic equation that describes neutron transport is the Boltzmann equation [7]. The steady state form of this equation can be expressed as

$$\vec{\Omega} \cdot \nabla \psi(\vec{r},\vec{\Omega},E) + \Sigma'(\vec{r},E)\psi(\vec{r},\vec{\Omega},E) = q(\vec{r},\vec{\Omega},E) \tag{4-1}$$

with

$$q(\vec{r},\vec{\Omega},E) = \int\int \Sigma^s(\vec{r};\vec{\Omega}',E' \rightarrow \vec{\Omega},E)\psi(\vec{r},\vec{\Omega}',E')d\vec{\Omega}'dE' + Q(\vec{r},\vec{\Omega},E) \tag{4-2}$$

where $\psi(\vec{r},\vec{\Omega},E)$ is the angular flux in the $\vec{\Omega}$ direction at location $\vec{r}$ with energy E, $\Sigma'(\vec{r},E)$ is the total interaction cross-section at location $\vec{r}$ with energy E, $\Sigma^s(\vec{r};\vec{\Omega}',E' \rightarrow \vec{\Omega},E)$ is the cross-section at location $\vec{r}$ for scattering from direction $\vec{\Omega}'$ with energy E' to direction $\vec{\Omega}$ with energy

E, and $Q(\bar{r},\bar{\Omega},E)$ is the neutron or gamma, as appropriate, source at location $\bar{r}$ in the $\bar{\Omega}$ direction with energy E.

Equation (4-1) is a first order differential equation that forms the basis for determining the angular particle densities in a general geometry system. (Note that technically, Equation (4-1) is an integro-differential equation, since the RHS contains an integral scattering source term.) A discrete solution of Equation (4-1) can be obtained by any of several means. Historically, discrete ordinates methods [7] have been utilized to solve the angular particle transport equation for regular mesh geometry problems. Unfortunately, discrete ordinates methods are not well suited to combinatorial geometry modeling and require fine geometry meshing due to the loose coupling of the various meshed solution regions. For applications that require general geometry modeling capabilities, it is desirable to solve Equation (4-1) by means of a more robust solution technique, such as the method of characteristics solution methodology used in RAMA.

4.2.2 Characteristics Solution Methodology with Anisotropic Scattering

A formulation of the Boltzmann equation that is suited to problems with a large number of solution regions (i.e., greater than a few hundred solution regions) has been developed utilizing an implementation that is similar to a characteristic solution methodology which preserves the angular dependence of the transport equation in three-dimensional geometry.

Equation (4-1) can be simplified by noting that all of the streaming must occur along the $\bar{\Omega}$ direction; thus the first term can be expressed as a directional derivative in direction $\bar{\Omega}$. Defining the position vector in terms of distance, s, along the $\bar{\Omega}$ vector such that $\bar{r} = \bar{r}_0 + s\bar{\Omega}$ leads to the simplification

$$\bar{\Omega} \cdot \nabla \psi \rightarrow \frac{d}{ds}\psi(\bar{r}_0 + s\bar{\Omega},\bar{\Omega},E) \tag{4-3}$$

where r_0 is a reference point (usually chosen on the outer boundary) for the origin of a ray in the direction of $\bar{\Omega}$. This allows Equation (4-1) to be written as

$$\frac{d}{ds}\psi(\bar{r}_0 + s\bar{\Omega},\bar{\Omega},E) = \Sigma'(\bar{r}_0 + s\bar{\Omega},E)\psi(\bar{r}_0 + s\bar{\Omega},\bar{\Omega},E) = q(\bar{r}_0 + s\bar{\Omega},\bar{\Omega},E) \tag{4-4}$$

The derivation of the characteristic solution methodology consists of integrating the basic transport equation presented in Equation (4-4) along rays (i.e., straight lines) in the characteristic direction $\bar{\Omega}$ with distance along the ray denoted by the variable s. It is convenient to consider the application of Equation 4-4 to any ray passing through a volume, V_i, where the volume is sufficiently small that the material properties are constant throughout the volume (i.e., the cross sections do not vary spatially within the volume) and the distance variable, s, is considered to be measured relative to the entry point of the ray in the volume. The differential equation that defines the angular flux along any such ray within volume V_i can be written as:

$$\frac{d}{ds}\psi_i(s,\vec{\Omega},E)+\Sigma_i^t(\vec{\Omega},E)\psi_i(s,\vec{\Omega},E)=q(s,\vec{\Omega},E) \tag{4-5}$$

where the source term in Equation (4-5) can be expressed as:

$$q_i(s,\vec{\Omega},E)=\iint\Sigma_i^s(\vec{\Omega}',E'\rightarrow\vec{\Omega},E)\psi_i(s,\vec{\Omega}',E')d\vec{\Omega}'dE'+Q(s,\vec{\Omega},E) \tag{4-6}$$

At this point it is convenient to convert Equations (4-5) and (4-6) into a form that consists of a discrete set of angular directions and energy groups. Letting the discrete form of the angular flux be defined as:

$$\Phi_{i,k.g}(s)\equiv\int_{\Delta E_g}\int_{\Delta\Omega_k}\psi_i(s,\vec{\Omega},E)d\vec{\Omega}\,dE \tag{4-7}$$

where ΔE_g is the energy range corresponding to energy group g and $\Delta\Omega_k$ is a differential solid angle about direction $\vec{\Omega}_k$.

Integrating both sides of Equation (4-5) over the discrete solid angle $\Delta\Omega_k$ and the discrete energy group range ΔE_g, and assuming that the nuclear cross sections at any location are constant within the differential solid angle and energy group, yields:

$$\frac{d}{ds}\int_{\Delta E_g}\int_{\Delta\Omega_k}\psi_i(s,\vec{\Omega},E)d\vec{\Omega}\,dE+\Sigma_{i,g}^t\int_{\Delta E_g}\int_{\Delta\Omega_k}\psi_i(s,\vec{\Omega},E)d\vec{\Omega}\,dE=\int_{\Delta E_g}\int_{\Delta\Omega_k}q_i(s,\vec{\Omega},E)d\vec{\Omega}\,dE \tag{4-8}$$

where $\Sigma_{i,k,g}^t$ is the total interaction cross section in the differential solid angle $\Delta\Omega_k$ and energy group range ΔE_g. Using the definition in Equation (4-7), Equation (4-8) can be expressed as:

$$\frac{d}{ds}\Phi_{i,k,g}(s)+\Sigma_{i,g}^t\Phi_{i,k,g}(s)=q_{i,k,g}(s) \tag{4-9}$$

The source term in Equation (4-9) can be determined by substituting Equation (4-6) into Equation (4-8) to yield:

$$q_{i,k,g}(s)=\int_{\Delta\Omega_k}d\vec{\Omega}\sum_{g'=1}^{G}\sum_{k'=1}^{K}\Sigma_{i,k'\rightarrow k,g'\rightarrow g}^{s'}\Phi_{i,k',g'}(s)+\int_{\Delta E_g}\int_{\Delta\Omega_k}Q_i(s,\vec{\Omega},E)d\vec{\Omega}\,dE \tag{4-10}$$

where $\Sigma_{i,k'\rightarrow k,g'\rightarrow g}^{s'}$ is the anisotropic scattering cross section for scattering from discrete angle k′ to discrete angle k and from energy group g′ to energy group g, and the integrals over all energy and all angular directions have been replaced by summations over the number of discrete angles (K) and the number of energy groups (G).

The anisotropic scattering cross section in Equation (4-10) can be represented by a partial expansion of Legendre polynomials [7]. Letting

$$\Sigma^{s}_{i,k'\to k,g'\to g} \approx \sum_{m=0}^{M} (2m+1)\Sigma^{(m)}_{i,g'\to g} P^{(m)}\left(\mu_{k'\to k}\right) \tag{4-11}$$

allows the anisotropic scattering term to be written as:

$$\Sigma^{s'}_{i,k'\to k,g'\to g} = \frac{\Sigma^{s'}_{i,k'\to k,g'\to g}}{4\pi} \tag{4-12}$$

where $\Sigma^{(m)}_{i,g'\to g}$ is the m-th order scattering moment from energy group g' to energy group g, $P^{(m)}$ is the m-th order Legendre polynomial and $\mu_{k'\to k}$ is the cosine of the angle between $\bar{\Omega}_{k'}$ and $\bar{\Omega}_{k}$ that is

$$\mu_{k'\to k} = \bar{\Omega}_{k'} \cdot \bar{\Omega}_{k} \tag{4-13}$$

If particle production is assumed to be from an isotropic source (e.g., neutron production from fissions) that is uniform throughout volume V_i, then the production term can be represented as:

$$\int_{\Delta\Omega_k}\int_{\Delta E_g} Q_i\left(s,\bar{\Omega},E\right)dEd\bar{\Omega} = Q_{i,g}\frac{\int_{\Delta\Omega_k} d\bar{\Omega}}{4\pi} \tag{4-14}$$

where $Q_{i,g}$ is the uniform particle production rate in energy group g within volume V_i.

Substituting Equations (4-12) and (4-14) into Equations (4-9) and (4-10) results in the following expression for the angular flux in volume V_i to be written in the form:

$$\frac{d\Phi_{i,k,g}(s)}{ds} + \Sigma_{i,k,g}\Phi_{i,k,g}(s) = \hat{q}_{i,k,g} \tag{4-15}$$

where

$$\Sigma_{i,k,g} = \Sigma^{t}_{i,g} - W_k\Sigma^{s}_{i,k,g} \tag{4-16}$$

$$\hat{q}_{i,k,g} = W_k\left(Q_{i,g} + \sum_{\substack{g'=1\\ g',k'\neq g,k}}^{G}\sum_{k'=1}^{K}\Sigma^{s}_{i,k'\to k,g'\to g}\overline{\Phi}_{i,k',g'}\right) \tag{4-17}$$

and

$$W_k = \frac{\int_{\Delta\Omega_k} d\bar{\Omega}}{4\pi} = \frac{\Delta\Omega_k}{4\pi} \tag{4-18}$$

Equation (4-17) has been made a constant along the entire length of the ray within volume V_i by approximating the angular flux values in all angular directions except the $\bar{\Omega}_k$ direction by the average angular flux in volume V_i. As a result, at a given solution iteration the particle angular flux contributions to the source term in Equation (4-17) are held constant. Under this assumption, the average particle angular flux along a given ray in the $\bar{\Omega}_k$ direction can be determined by direct integration of Equation (4-15) to yield

$$\overline{\Phi}^r_{i,k,g} = \frac{\Phi^{I,r}_{i,k,g} - \frac{\hat{q}_{i,k,g}}{\Sigma_{i,k,g}}}{\tau^r_{i,k,g}}\left(1 - e^{-\tau^r_{i,k,g}}\right) + \frac{\hat{q}_{i,k,g}}{\Sigma_{i,k,g}} \tag{4-19}$$

where $\Phi^{I,r}_{i,k,g}$ is the value of the angular flux along ray r at the entrant boundary and $\tau^r_{i,k,g}$ is the optical distance through volume V_i for a particle traveling along ray r in energy group g, as given by:

$$\tau^r_{i,k,g} \equiv \Sigma_{i,k,g} d^r_i \tag{4-20}$$

where d^r_i is the distance through volume V_i.

Now consider the situation wherein more than one parallel ray traverses volume V_i in the $\bar{\Omega}_k$ direction. Because the flux physically corresponds to the track length within the volume, the total average angular flux in volume V_i in the $\bar{\Omega}_k$ direction in energy group g can be expressed as the volume weighted contribution of the incremental average flux values from each ray, such that

$$\overline{\Phi}_{i,k,g} = \frac{\sum_{r=1}^{R} \overline{\Phi}^r_{i,k,g} \Delta V_r}{\sum_{r=1}^{R} \Delta V_r} \tag{4-21}$$

where R is the total number of parallel rays through volume V_i, and the differential volume subtended by ray r as it traverses the volume, denoted by ΔV_r, is given by

$$\Delta V_r = d^r_i \Delta A_r \tag{4-22}$$

where ΔA_r is the cross-sectional area subtended by ray r. The scalar flux can be determined from Equation (4-21) to be:

$$\phi_{i,g} = \sum_{k=1}^{K} \overline{\Phi}_{i,k,g} \tag{4-23}$$

The value of the angular flux at the exit boundary of volume V_i, along ray r, denoted by $\Phi^{0,r}_{i,k,g}$ can also be determined from the solution of Equation (4-15) to be:

$$\Phi^{0,r}_{i,k,g} = \left(\Phi^{I,r}_{i,k,g} - \frac{\hat{q}_{i,k,g}}{\Sigma_{i,k,g}} \right) e^{-\tau^{r}_{i,k,g}} + \frac{\hat{q}_{i,k,g}}{\Sigma_{i,k,g}} \tag{4-24}$$

Note that this value is also the value of the angular flux at the entrant boundary of the volume adjacent to volume V_i along a given ray.

4.2.2.1 Ray Tracing Methodology

The application of the characteristic solution methodology described in Section 4.2.2, consists of saturating the solution geometry with sets of parallel rays that are projected through the geometry in various directions defined by an angular quadrature set. The rays provide the characteristic directions along which integration of the particle angular flux is determined. Individual parts of the geometry may be sub-meshed to form suitably sized solution volumes. The points of intersection of the various rays with the surface of each subvolume are identified by using routines similar to those used in Monte Carlo calculations. These intersections, along with the angular scattering relationship specified by the angular scattering equation, are used to determine particle interactions throughout the modeled geometry. By utilizing the Legendre expansion form of the scattering cross-section, defined in Equation (4-11), the angular dependence of scattering source can be maintained in the solution process.

4.2.2.2 Neutron Source Due to Fissions

It is possible to utilize any known external particle source term in the solution process. However, a source of a special nature that deserves unique treatment is encountered when neutron transport in the vicinity of fission sources is being evaluated. In this case, the power distribution is typically known for external calculations, such as from three-dimensional nodal simulator codes. The corresponding neutron source terms must be determined by relating the fission source to the generated power in the fission regions.

In any operating reactor system, the source of neutrons can be assumed to be exclusively the result of the fission process in the core region. It is also reasonable to assume that the fission process emits neutrons isotropically. Under these assumptions, the neutron source term can be expressed in the form:

$$Q_{i,g} = p_i P_D \frac{\sum_{n=1}^{N_i} \chi_{n,g} \sum_{g'=1}^{G} \left(\nu\Sigma^f\right)_{n,g'} \phi_{i,g'}}{\sum_{g'=1}^{G} \sum_{n=1}^{N_i} \kappa_n^f \Sigma_{n,g'}^f \phi_{i,g'}} \tag{4-25}$$

where p_i is the relative power (normalized to a core volume average value of 1.0) in volume V_i, P_D is the power density (watts/cm^3) in the core region, $\chi_{n,g}$ is the fraction of neutrons emitted into energy group g from a fission of nuclide n, $\left(\nu\Sigma^f\right)_{n,g'}$ is the fission production cross section for nuclide n in energy group g', κ_n is the energy produced from a fission of nuclide n (joules/fission), $\Sigma_{n,g'}^f$ is the fission cross section of nuclide n in energy group g', and N_i is the total number of fissioning nuclides in volume V_i.

The transport solution assumes an initial scalar flux distribution, which, from Equation (4-25) provides an estimate of the actual neutron fission source distribution. This distribution, in turn, produces an updated scalar neutron flux. The resulting scalar neutron flux provides an improved estimate of the fission source term. The outer iteration process is continued until acceptable accuracy is obtained.

4.2.2.3 Boundary Condition Calculation

Two boundary conditions are treated in the method of characteristics solution methodology: vacuum boundaries and reflective boundaries.

Vacuum boundaries are quite easy to incorporate into the method of characteristics solution. By definition, there is no entering particle current at a vacuum boundary. As a result, there can be no entering angular flux for any ray that emanates from a vacuum boundary. In a method of characteristics solution process, this condition is equivalent to using an entrant angular flux value of zero (i.e., $\Phi_{1,k,g}^{l,r} = 0$).

Reflective boundaries are handled by reflecting each ray that emanates from a reflective boundary back into the body. The process is repeated at each reflective boundary of the problem until the total number of mean free paths measured from the entrant reflective surface exceeds a user defined maximum value.

The entrant angular flux at the start of a ray that emanates from a reflective boundary can be determined by noting that an alternative solution to the method of characteristics governing equation, i.e., Equation (4-4), can be written as the integral transport expression [7]:

$$\Phi\left(\vec{r},\vec{\Omega},E\right) = \int_0^{\infty} e^{-\int_0^{s'} \Sigma\left(\vec{r}-s''\vec{\Omega},E\right)ds''} q\left(\vec{r}-s'\vec{\Omega},\vec{\Omega},E\right)ds' \tag{4-26}$$

The corresponding angular flux at the entrant to volume V_i can be expressed as:

[[

Content Deleted
EPRI Proprietary Information

]] **TS**

where the subscripts denote successive regions encountered along the reflected portion of the ray, starting at the reflective boundary and progressing backward until the accumulated optical distance is greater than a user-defined maximum value.

4.2.3 Flux Edits Methods

Most reactor system component damage assessments are based upon flux values that are greater than a cutoff energy level, e.g., ϕ(E>1 MeV). If the energy cutoff value falls on a group boundary, the resulting flux that is greater than the energy cutoff value is simply the sum of the fluxes in the energy groups with lower energy range values that are above the cutoff value. In this case, the resulting neutron flux is given by:

$$\phi_{E_0} = \sum_{g \le G} \phi_g \tag{4-28}$$

where ϕ_{E_0} is the total flux with energy greater than the cutoff energy E_0, G is the energy group whose lower boundary value coincides with the cutoff energy value, g is the group index, and ϕ_g is the neutron flux in energy group g.

If the cutoff energy value does not coincide with a group boundary, then it is necessary to determine the contribution to the neutron flux from the energy group in which the cutoff energy value lies. In this case, the resulting neutron flux can be expressed as:

$$\phi_{E_0} = \sum_{g < G} \phi_g + \delta_G \tag{4-29}$$

where G is the energy group that the cutoff energy lies in and δ_G is the contribution from energy group G to the neutron flux that is greater than the cutoff energy. [[

Content Deleted
EPRI Proprietary Information

]] **TS**

[[

Content Deleted
EPRI Proprietary Information

]] **TS**

5
GEOMETRY MODEL BUILDING METHOD

The RAMA transport code employs a geometry modeling capability that is based upon combinatorial geometry techniques. This capability allows the user to describe all parts of a reactor assembly in accurate three-dimensional design detail.

The Parts Model Builder (PMB) tool uses geometry elements to describe regions of the reactor. Nodal geometry modeling techniques are used when describing the reactor core region. Other regions of the reactor, such as the central shroud region or the downcomer region, are cylindrical in shape; therefore curvilinear geometry elements accurately describe these areas. Once a geometry element is selected to model a specific region, the PMB automatically regenerates these elements until the geometry model satisfies the dimensional specifications given by the user.

The PMB uses the basic geometry types described in Section 3.2 of this manual to generate geometries for the following parts and regions of a reactor model:

- fuel assemblies in the reactor core region;
- core reflector regions adjacent to, below, and above the reactor core region;
- the core shroud around the reactor core region;
- the downcomer region, including the jet pumps, between the core shroud and pressure vessel walls; and
- general cylindrical-shaped regions that include the pressure vessel, pressure vessel mirror insulation, cavity, and biological shield regions.

5.1 Generating the Reactor Core Region Geometry Model

The core geometry is described in (x,y)-coordinates. The fuel assembly locations are numbered beginning with (01,01) in the lower left corner of the geometry, and incrementing by +01 across the x-axis and +01 up the y-axis. The last region is in the upper right corner and has the value (NN,NN), where NN is the dimension of the reactor core.

The reactor core region is built using the fuel assembly descriptions input by the user. Fuel assembly parameters include assembly geometry type specifications, dimensions, and meshing options. Fuel assemblies are assumed to be square in the x-y plane and are built with the rectangular parallelepiped (RPP) bodies. The fuel assembly part may be specified as a nodal element corresponding to a fully-homogenized fuel assembly, or as sub-meshed elements corresponding to a supported fuel assembly geometry type.

5.1.1 Fuel Assembly Meshing and Volume Calculations

Fuel assembly meshing options range from pin-wise to fully homogenized. Fuel assemblies may be homogenized over the entire pitch of the fuel assembly region, or the fuel pins may be homogenized in the fuel bundle region preserving the channel and water gap regions around the fuel bundle that are present in BWR fuel assembly designs. Optionally, the fuel assemblies residing in the interior regions of the core may be modeled as a bulk region; thus, reducing the number of regions in the problem. A different mesh type may be specified for each fuel assembly location in the core region.

The volumes of fuel assemblies are calculated simply as length x width x height. Volumes for meshed fuel assemblies are calculated according to the mesh option used. Volumes for fuel assemblies that lie on symmetry lines are also calculated according to the symmetry of the region.

5.2 Generating the Core Reflector Region Geometry Model

The core reflector region is built in the radial plane beside the core region. The reflector region is bounded by the rectangular boundary of the core region and the curvilinear boundary of the core shroud. The parts generated by the PMB provide for the transition from rectangular to cylindrical form in the model. This is accomplished by intersecting rectangular parallelepiped (RPP) with right circular cylinder (RCC) bodies in the combinatorial geometry specification to form solution regions that have both planar and cylindrical faces.

5.2.1 Core Reflector Meshing and Volume Calculations

Meshing of the core reflector parts is determined in three steps. First, a reflector part is built as a series of RPP regions, or sub-volumes, where each region has an equal volume in accordance with the meshing parameters specified by the user. Second, the RPP regions that are intersected by a RCC body are recalculated. Last, the regions affected by the RCC intersection are evaluated to determine if "extremely small" volumes result. If a small volume is formed, then the region with the small volume is joined with a neighboring region to form a larger volume. The region volumes are then re-evaluated to determine the acceptability of the meshing. If the joined region exceeds the meshing limits, the region is halved and the volumes are re-evaluated again. This process continues until acceptable volumes are attained for all mesh regions. Assuming that a nominal mesh region has the volume, V_{nom}, the following criteria are used to evaluate the acceptability of the calculated mesh volume, V_{mesh}:

[[

Content Deleted
EPRI Proprietary Information]] TS

5.3 Generating the Core Shroud Region Geometry Model

The core shroud is a cylindrical part in design and is built using RCC and right angle wedge (RAW) bodies. The RCC body provides the cylindrical shape and sub-annuli meshing of the shroud wall and the RAW body provides the sub-meshing of the circular parts to form arcs of equal azimuthal angle.

5.3.1 Shroud Meshing and Volume Calculations

The methods for determining the meshing in the shroud part are described in Section 5.6, *Radial and Azimuthal Meshing in Cylindrical Parts.*

5.4 Generating the Downcomer and Jet Pump Region Geometry Model

The downcomer water region is built in three radial zones. The inner zone lies in the annulus between the core shroud and jet pump assemblies, and spans all azimuthal angles in the problem geometry. The outer zone lies in the annulus between the jet pump assemblies and pressure vessel, and spans all azimuthal angles in the problem geometry. Both zones are formed from simple right circular cylinder (RCC) and right angle wedge (RAW) bodies.

The central zone lies in the annulus of the downcomer region between the inner and outer zones. It is constructed from two part types. The first part type is a column of arc meshes that spans the radial distance between the inner and outer zones. These parts are formed from simple right circular cylinder (RCC) and right angle wedge (RAW) bodies. The second part type is RCC bodies that describe the jet pump riser and mixer pipes and the water in the pipes. The method for calculating the meshing in these parts is described in Section 5.6.

5.4.1 Downcomer and Jet Pump Meshing and Volume Calculations

The methods for determining the meshing in the inner and outer zone regions of the downcomer are described in Section 5.6, *Radial and Azimuthal Meshing in Cylindrical Parts.*

Meshing in the central zone parts is determined in three steps. First, the meshing, or regions, for the part is determined using the technique described in Section 5.6 for right circular cylinders. Second, the regions are adjusted to account for the presence of the jet pump pipes. Last, the regions affected by the intersection of the jet pump pipes are evaluated to determine if "extremely small" volumes result. If a small volume is formed, then the region with the small volume is joined with a neighboring region to form a larger volume. The region volumes are then re-evaluated to determine the acceptability of the meshing. If the joined region exceeds the meshing limits, the region is halved and the volumes are re-evaluated again. This process continues until acceptable volumes are attained for all mesh regions. Assuming that a nominal mesh region has the volume, V_{nom}, the following criteria are used to evaluate the acceptability of the calculated mesh volume, V_{mesh}:

[[

Content Deleted
EPRI Proprietary Information

]] TS

5.5 Generating Geometry Models Containing Pipe Elements

PMB uses pipe elements for certain geometry models. Typical components that use pipe elements include the reactor pressure vessel, pressure vessel mirror insulation, biological shield (concrete wall), and cavity region.

Pipe parts are circular in design and are built with RCC and RAW bodies. RCC bodies describe the inner and outer radii of the pipes. RCC bodies are also used to describe sub-annulus meshing in the pipe wall. The RAW body is used to sub-mesh the pipe wall into arcs of equal azimuthal angles.

5.5.1 Pipe Element Meshing and Volume Calculations

The methods for determining the meshing in pipe elements are described in Section 5.6, *Radial and Azimuthal Meshing in Cylindrical Parts*.

5.6 Radial and Azimuthal Meshing in Cylindrical Parts

The PMB code calculates radial and azimuthal meshing in cylindrical parts in accordance with meshing parameters specified by the user. The cylindrical parts are built using RCC bodies. The cylindrical parts are meshed into arcs using RAW bodies. The RCC body provides the cylindrical shape and radial meshing of the part and the RAW body provides the azimuthal meshing of the part.

Radial sub-meshing is accomplished by determining an appropriate number of RCC bodies in the circular part. Radial meshing may be determined using either the equal radius or equal volume method.

Radial meshing, ΔR, in the equal radii method is determined as:

$$\Delta R = \frac{R_{outer} - R_{inner}}{N} \tag{5-1}$$

where R_{outer} is the outer radius of the cylinder part, R_{inner} is the inner radius of the part, and N is the number of sub-annuli in the part.

Radial meshing in the equal volume method is determined in two steps. First, the volume per unit height of a mesh region, ΔV, is determined as:

$$\Delta V = \frac{\pi(R^2{}_{outer} - R^2{}_{inner})}{N} \tag{5-2}$$

The radii for the mesh volumes are then determined by consecutively adding the mesh volume, ΔV, to the volume formed by the immediately preceding region, V_{n-1}, and calculating the new radius, R_n:

$$R_n = \sqrt{\frac{V_{n-1} + \Delta V}{\pi}} \tag{5-3}$$

Azimuthal meshing is applied to the part by intersecting the cylindrical bodies that were formed by the RCC bodies with right angle wedge (RAW) bodies using the combinatorial geometry operation "RCC -RCC + RAW". The azimuthal mesh size is uniform in the part and is determined by calculating the delta angle, ΔA, from the input specifications provided by the user.

$$\Delta A = \frac{A_1 - A_0}{M} \tag{5-4}$$

where A_1 is the ending angle, A_0 is the starting angle, and M is the number of azimuthal meshes between the angles.

5.7 Volume and Material Identifiers

Parts and regions generated by the PMB code are identified using volume and material identifiers that are compatible with the RAMA model specifications. Volume identifiers are 32-character strings that allow parts and regions to be identified by a familiar name. Material identifiers are 32-character strings that describe the materials in the model.

The fully-qualified form of a volume identifier is:

PartName: PartNo.VolumeNo

where:

PartName	is a sub-string that identifies a part, or region, in the model;
":"	is a required field separator;
PartNo	is an integer value that identifies a specific instance of the part;
"."	is a required field separator; and

VolumeNo	is an integer value that identifies a sub-volume in the part.

Several parts with the same part name, *PartName*, may exist in a model. The different instances of the part are identified using part numbers, *PartNo*, starting with the integer value "1". A part may be composed of one or more sub-volume elements, *VolumeNo*, that are numbered starting with the integer value "1".

The fully-qualified form of a material identifier is:

MatName: MatNo

where:

MatName	is a sub-string that identifies a type of material;
":"	is a required field separator; and
MatNo	is an integer value that identifies a specific type of the material.

Several materials with the same material name, *MatName*, may exist in a model. The different instances of a material are identified using material numbers, *MatNo*, starting with the integer value "1".

6
MATERIAL PROCESSING METHOD

The purpose of the State-point Model Builder (SMB) code is to process reactor operating data and materials for assignment to the geometry model generated by the Parts Model Builder (PMB) code. The discrete materials and powers from the reactor operating data may be homogenized in the process. The material data handled by SMB includes nuclear fuel compositions for the reactor core region, steel compositions for structural components, and water compositions for the coolant flow regions.

The SMB provides the user with the capability to generate a homogenized bulk-core region and homogenized fuel elements that helps to reduce the model detail. Various types of fuel element homogenization are available. The homogenization methodology in SMB is based on volume weighted averaging of materials and powers. The subsections that follow describe the calculations performed in the State-point Model Builder code as a part of the homogenization process.

6.1 Fuel Assembly Homogenization

The reactor operating data from the utility generally contains considerable detail for the core region. Powers factors are provided for every fuel pin in every assembly, and compositions are provided for every fuel pin, water pin, channel and coolant bypass region in every assembly. These data may be homogenized into a single assembly, an assembly with fewer regions, or a bulk region. Full detail maybe preserved if desired.

The final result of the homogenization is determined by the geometry information in the PMB model files and, possibly, a PMB core region bulk homogenization file. The SMB code converts the reactor operating data into a form that matches the PMB geometry.

6.2 Volume Weighted Averaging

All homogenization is done using volume weighted averaging. Volume weighted averaging can be described by the equation:

$$\alpha = \frac{1}{V}\sum_{i=1}^{N} V_i \alpha_i \tag{6-1}$$

where V_i is the sub-volume, α_i is a property of that sub-volume, V is the total volume, and α is the homogenized property. The total volume is simply the sum of the sub-volumes:

Material Processing Method

$$V = \sum_{i=1}^{N} V_i \tag{6-2}$$

For example, to calculate the number density of a nuclide contained in the homogenized material, the product of the number density and volume for each composite region is summed over all regions and divided by the total volume. This is done for all the nuclides that are present.

6.2.1 Homogenization of the Relative Powers

The homogenization of the relative powers is handled somewhat differently than the other material properties. The approach is to conserve the power produced in the power producing regions in the homogenized region. RAMA generates the local region power density by taking the product of the global power density term and the local relative power factor. Thus the local region power density is determined by:

$$(pd)_i = r_i(PD) \tag{6-3}$$

where $(pd)_i$ is the power density in the i-th local region being modeled, r_i is the local relative power factor (field 3 in the RAMA GAT input block) for the i-th local region, and (PD) is the core average power density. Usually the global power density (PD) is specified as the average core power density for the plant, although this is a convention rather than a requirement. The only true requirement is that the product of the global power density and the local relative power factor in any region should produce the correct power density in that region.

The local power density of the i-th region in a RAMA model is defined as:

$$(pd)_i \equiv \frac{P_i}{V_i} \tag{6-4}$$

where P_i is the total power being produced in the i-th local region and V_i is the volume of the i-th local region as it is modeled in RAMA. The corresponding local relative power factor is obtained from Eqs. (6-3) and (6-4) as:

$$r_i = \frac{P_i}{V_i(PD)} \tag{6-5}$$

A check to confirm that the local relative power factors are consistent is to note that:

$$(PD)\sum_{i=1}^{N} r_i V_i = P_{TOT} \tag{6-6}$$

where N is the total number of modeled power producing regions in the core and P_{TOT} is the total power in the core (or total power in the modeled region of the core if the model is a subset of the full core).

The pin powers reported by the utilities are, invariably, the product of a nodal assembly relative power and a pin relative power, where the pin powers are normalized such that the average pin power taken over all pins results in the nodal power factor. The nodal power factor is the total nodal power divided by the power in an "average" core node. (Note that there is no dependence on volume in any of the utility reported power factors, other than the fact that the pin relative power factors are summed exclusively over the fuel pins, not all pincell regions in the node.)

This method of computing a relative pin power is somewhat inconsistent with the RAMA relative power term. This inconsistency shows up when the power in a given pin is computed using the utility definition of relative pin power versus the RAMA relative pin power definition. From the utility pin power definition, the total power in any pin node is given by:

$$P_i = p_i\left(\frac{P_{node}}{N_{pins}}\right) = p_i\left(\frac{P_{core}}{N_{nodes}N_{pins}}\right) \tag{6-7}$$

where p_i is the utility-specified relative pin power, P_{node} is the power in an average core node, P_{core} is the core power, N_{pins} is the number of fuel pins in the core node, and N_{nodes} is the number of nodes in the core (since all power nodes represented in the nodal codes have the same size).

The nodal pin total power computed by the RAMA definition is:

$$P_i = r_iV_i(PD) = r_iV_i\left(\frac{P_{core}}{V_{core}}\right) \tag{6-8}$$

where r_i is the RAMA relative pin power, V_i is the modeled volume of the pin, and V_{core} is the total core volume which is usually defined in RAMA runs as the total homogenized core volume, such that

$$V_{core} = N_{nodes}V_{node} \tag{6-9}$$

with V_{node} being the homogenized volume of a fuel node. From Eqs. (6-7), (6-8), and (6-9), the RAMA relative nodal pin power can be expressed as a function of the utility-supplied relative power as:

$$r_i = p_i\left(\frac{V_{node}}{V_iN_{pins}}\right) \tag{6-10}$$

Material Processing Method

If Eq. (6-10) is applied at the pin-by-pin level and if all fuel region volumes are assumed to be of equal size, then the RAMA relative pin powers are related to the utility-supplied relative pin powers by the following relationship:

$$r_i = p_i \left(\frac{V_{node}}{V_{fuel}} \right) \tag{6-11}$$

where V_{fuel} is the volume of fuel (i.e., power producing regions) in the modeled core node. It is important to note that Eq. (6-11) is applicable regardless of how the fuel pin volumes are considered in a model (i.e., the pins may be considered as discrete fuel rods, pincells within a channel, or even homogenized pincells over the entire core node). The only important thing is that, at the pin level, each fuel region can be represented with equal volumes.

Subsequent core node homogenization can now be accomplished using the "adjusted" RAMA pin powers from Eq. (6-11) as a starting point. The power in homogenized fuel regions should be determined using a volume weighted average of the individual regions that make up the homogenized region (including non-power producing regions). For example, a homogenized region consisting of N "pin" regions (some of which may have zero powers) would have a homogenized power of:

$$r_h = \frac{\sum_{i=1}^{N} r_i V_i}{\sum_{i=1}^{N} V_i} \tag{6-12}$$

where r_i is zero for non-power producing regions and the other individual region relative powers in Eq. (6-12) are related to the utility-supplied relative pin powers using Eq. (6-11). It should be noted that Eq. (6-12) can also be applied to situations involving homogenization of regions that lie on a diagonal symmetry line, which is commonly encountered in octant core models. The volume of those regions that are split by the symmetry line will have half the volume of the regions that are not split by the symmetry line.

As a simple example of the use of Eqs. (6-11) and (6-12), consider the case of an 8x8 fuel assembly node that has a nodal power factor of 0.3 with 62 fuel pins each having a relative power (normalized to the nodal average) of 1.0 and two water rods. The utility-supplied relative pin powers for this node would be 0.3 for all power-producing fuel pins in the assembly node. Assuming the RAMA model consists of fuel pincells that are homogenized over the entire nodal volume (i.e., the channel and water gaps are not modeled as separate regions), then the ratio of the node volume to the fuel volume in Eq. (6-11) is given by:

$$\left(\frac{V_{node}}{V_{fuel}} \right) = \left(\frac{64 * V_{pincell}}{62 * V_{pincell}} \right) = 1.0323 \tag{6-13}$$

The equivalent RAMA relative pin powers for a pin-by-pin representation of this assembly are 0.30968 [=0.3 * 1.0323] for each of the power-producing fuel regions.

Now consider the case of homogenizing the assembly node into quadrants composed of 4x4 fuel regions. Two of the quadrants will consist of 16 fuel rods and the other two quadrants will consist of 15 fuel rods and one water rod. The corresponding RAMA relative powers for the homogenized regions, from Eq. (6-12), are 0.30968 [=0.30968*16/16] in the quadrants containing 16 fuel rods and 0.29032 [= (15*0.30968+1*0.0)/16] in the quadrants containing 15 fuel rods and 1 water rod. Note that even this homogenization can be further homogenized to a single core node that has a RAMA relative power of 0.3000 [= (2*0.30968+2*0.29032)/4] or equivalently, [=(62*0.30968+2*0.0)/64]. If the entire assembly node is homogenized to a single region, then the RAMA relative power is equal to the assembly nodal relative power, as expected, regardless of how the homogenization is performed.

6.2.2 Homogenization of the Channel and Bypass Regions

In the case where the fuel assembly is homogenized into a single region or part of the bulk-core region, the materials of the channel and bypass are homogenized into the aggregate material using volume weighted averaging as outlined above. In the case where the fuel assembly (target geometry) has sub-regions or some form of pin detail and no channel or bypass detail, the materials of the channel and bypass must be distributed among the sub-regions according to the volume of the sub-regions. If the sub-regions are of equal volume, such as in full pin detail, the materials of the channel and bypass can be distributed evenly among the sub-regions, otherwise the relative volumes of the sub-regions must be considered.

6.3 Fuel Assembly RPP Types

Fuel assembly parts are described using Right Parallelepiped (RPP) bodies. A fuel assembly may be described as a single RPP region, as a set of RPP regions describing full pin detail, or as a special RPP type. Special RPP types allow partial assembly detail to be used. Some of the more commonly utilized RPP types are shown in Figure 6-1 and are identified as types 0, 1, 20, 26 and 28.

RPP type 0 has no sub-assembly detail, type 1 has full pin detail, and types 20, 26 and 28 have some form of homogenized detail. The actual size of the sub-regions in types 20, 26 and 28 depends on the geometry of the incoming data (i.e., the source or utility geometry).

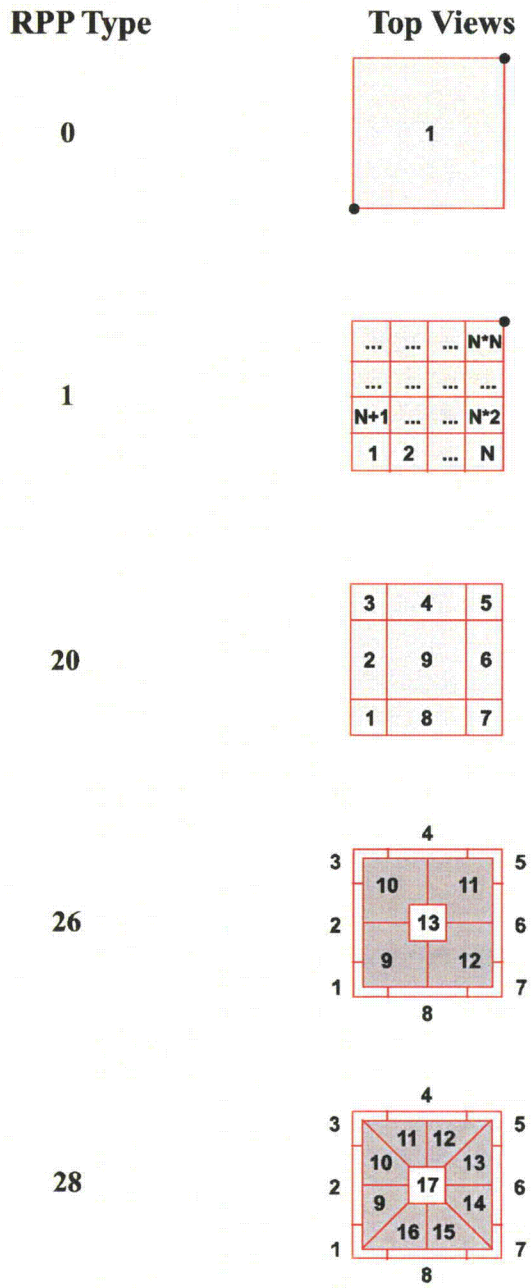

Figure 6-1
Rectangular Parallelepiped (RPP) Types

7
ACTIVATION, FLUENCE, AND UNCERTAINTY METHODS

The RAFTER code module of the RAMA Fluence Methodology calculates activation, fluence, and uncertainties for reactor components and regions in the reactor system. The methods used by RAFTER to perform these calculations and to determine nuclide activation and neutron fluence are presented in this section.

7.1 Activation Evaluation

Activation of material in surveillance capsules or other regions of the reactor system results from neutron absorption by a target nuclide to form a product nuclide that is radioactive. The activity resulting from the combined production and decay of the product nuclide provides a measure of the neutron fluence accumulated during the irradiation period. It is possible to predict the level of activation of the sample provided an estimate of the neutron flux is available.

7.1.1 Nuclide Activation

The differential equation that describes the rate of change in the number density of the target nuclide is given by:

$$\frac{dN_t}{dt} = -\sigma_a^t \phi N_t \tag{7-1}$$

where N_t is the number density of the target nuclide, σ_a^t is the absorption cross section for the target nuclide, and ϕ is the neutron flux. Note that the absorption is actually a function of energy, given by the expression:

$$\sigma_a^t \phi \equiv \sum_{g=1}^{\#groups} \sigma_{a_g}^t \phi_g \tag{7-2}$$

where $\sigma_{a_g}^t$ is the energy group-dependent absorption cross section of the target nuclide, and ϕ_g the group dependent neutron flux (that is assumed to be constant over the time interval of interest). Letting N_{t_0} be the target nuclide number density at time $t=t_0$, and assuming that the neutron flux is constant over the time interval $t > t_0$, then the target nuclide number density at time t ($t > t_0$) is determined from integration of Eq. (7-1) to be:

$$N_t(t) = N_{t_0} e^{-\sigma_a^t \phi (t - t_0)} \tag{7-3}$$

The differential equation that describes the rate of change in the number density of the product nuclide can be expressed in terms of production and loss of product nuclides as:

$$\frac{dN_p}{dt} = \sigma_R \phi N_t - (\lambda_p + \sigma_a^p \phi) N_p \tag{7-4}$$

where N_p is the number density of the product nuclide, λ_p is the product nuclide decay constant, σ_a^p is the absorption cross section of the product nuclide, and σ_R is the reaction response cross section (i.e., the cross section for product production from target irradiation). Note that the reaction response cross section for product production from fissions is equal to the target nuclide fission cross section multiplied by the product nuclide fission yield. Both the product absorption term and the reaction response term are also energy group dependent and are given by expressions similar to Eq. (7-2) by substituting the appropriate group-dependent cross section for the target absorption cross section in Eq. (7-2).

Substituting Eq. (7-3) into Eq. (7-4) yields:

$$\frac{dN_p}{dt} + (\lambda_p + \sigma_a^p \phi) N_p = \sigma_R \phi N_{t_0} e^{-\sigma_a^t \phi (t - t_0)} \tag{7-5}$$

Eq. (7-5) can be solved to yield:

$$N_p(t) = \left(N_{p_0} - \frac{\sigma_R \phi N_{t_0}}{\lambda_p + \sigma_a^p \phi - \sigma_a^t \phi} \right) e^{-(\lambda_p + \sigma_a^p \phi)(t - t_0)} + \left(\frac{\sigma_R \phi N_{t_0}}{\lambda_p + \sigma_a^p \phi - \sigma_a^t \phi} \right) e^{-\sigma_a^t \phi (t - t_0)} \tag{7-6}$$

where N_{p_0} is the product number density at time $t=t_0$. It should be noted that the product absorption rate is generally negligible while the target absorption rate is often negligible except for certain thermal reactions (such as ^{10}B absorption).

The activity resulting from the decay of the product nuclide is then given by:

$$A(t) = \lambda_p N_p(t) \tag{7-7}$$

for time $t \geq t_0$.

7.1.2 Accumulated Activation

The measured activity of dosimetry samples is the result of irradiation of the samples at varying flux magnitudes and energy distributions over a defined irradiation period. Variations in flux spatial and energy distributions result from reactor power variations and fuel exposure

accumulation. Reactor power and exposure effects must be accounted for in order to accurately estimate the activity of dosimetry samples at the end of the irradiation period.

One method of dealing with these operating history effects is to assume that the reactor power history can be treated as a series of step changes in power over time. The magnitude of the flux at these different power levels is assumed to be directly proportional to the reactor power. Since exposure effects are accumulated rather slowly throughout the irradiation period, it is also reasonable to assume that the energy distributions of the flux are relatively constant over several adjacent power steps.

Figure 7-1 shows an example of reactor power history over a period of time ranging from T_0 to T_{11}. In this example, the operating history is composed of ten discrete power levels that span three "state points". Each state point represents a period of time wherein the flux space and energy distributions are assumed to be constant.

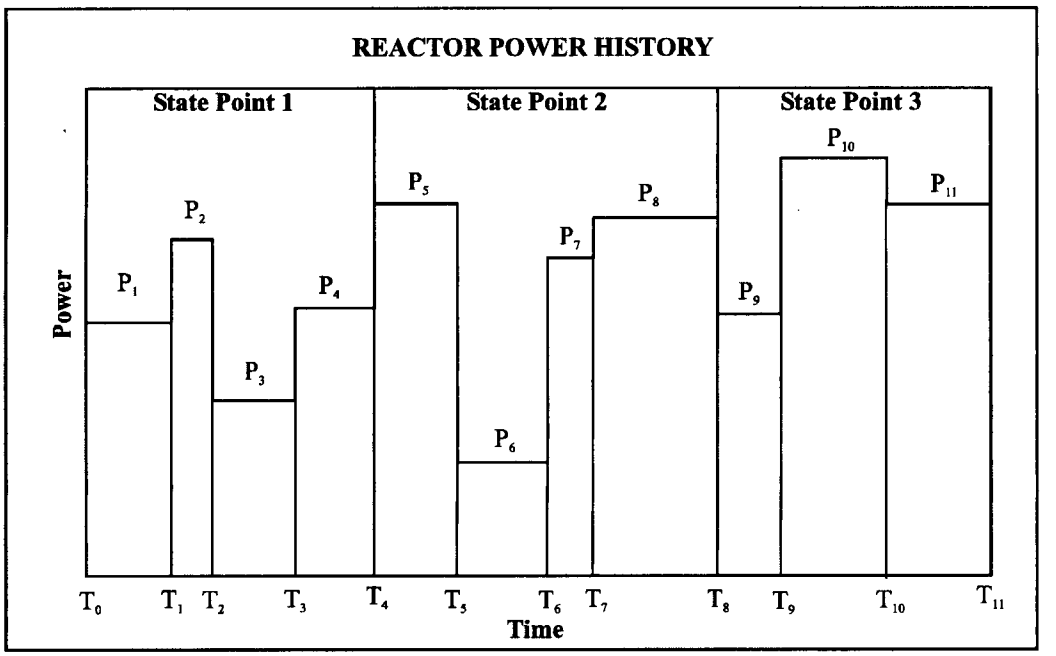

Figure 7-1
Reactor Operating History Example

In theory, large changes in reactor power would be expected to have an impact on the space and energy distributions of the flux, (e.g., due to variations in number densities) even if the changes occurred over small time periods. As a result, adjacent power steps with significantly different power levels would be expected to be represented by somewhat different state points. In practice, however, the selection of state points is often restricted to selected times with documented reactor operating conditions (such as process computer edit times). In addition, the irradiation of dosimetry located at the RPV or beyond is influenced less by the core interior bundles (that would be expected to be significantly more affected by the power changes) than by the core periphery bundles.

The estimation of accumulated activity in surveillance samples is accomplished by direct application of Eqs. (7-3), (7-6) and (7-7) to each time step in the history. The target and product number densities at the end of each time step are the corresponding initial number densities for the subsequent time step. A particle transport evaluation is performed for each state-point condition to obtain the reference state-point flux for each state-point condition. The flux in each power step is the corresponding state-point flux scaled by the ratio of the time step reactor power to the state-point reactor power, i.e.:

$$\phi_i = \phi_{i,s} p_i \left(\frac{P_R}{P_s} \right) \tag{7-8}$$

where ϕ_i is the flux at the surveillance sample location during the i-th power step, ϕ_s is the reference flux at the surveillance capsule location from the s-th state point particle transport evaluation that applies to the i-th time step, P_R is the rated reactor power, P_s is the reactor power used for the s-th state point particle transport evaluation, and p_i is the reactor fractional power during the i-th time step given by:

$$p_i = \frac{P_i}{P_R} \tag{7-9}$$

where P_i is the reactor power during the i-th time step. Since the reference state point flux is assumed to be directly proportional to the reactor power, it is common to use the reactor rated power in the reference state point particle transport evaluation, even if the actual reactor power at the state-point time is not the rated power. In this way, the power ratio in Eq. (7-8) is unity.

Utilizing the approach of representing the reactor power history as a set of constant power time steps allows the target and product nuclide number densities at the end of the i-th time step to be expressed as:

$$N_{t_i} = N_{t_{i-1}} e^{-\sigma_a^t \phi_i \Delta T_i} \tag{7-10}$$

and

$$N_{p_i} = \left(N_{p_{i-1}} - \frac{\sigma_R \phi_i N_{t_{i-1}}}{\lambda_p + \sigma_a^p \phi_i - \sigma_a^t \phi_i} \right) e^{-(\lambda_p + \sigma_a^p \phi_i)\Delta T_i} + \left(\frac{\sigma_R \phi_i N_{t_{i-1}}}{\lambda_p + \sigma_a^p \phi_i - \sigma_a^t \phi_i} \right) e^{-\sigma_a^t \phi_i \Delta T_i} \tag{7-11}$$

The accumulated activity in the dosimeter region is then given by:

$$A = \lambda_p N_{p_T} \tag{7-12}$$

where N_{p_T} is the product nuclide number density at the end of irradiation.

7.1.3 Activation Reaction Rates

Various neutron fluence experiments report the measured activation of the dosimetry in terms of the activation reaction rates of the irradiated material in the dosimeter. The reaction rate (reactions/sec per cm^3) is given by:

$$R = \frac{1}{T}\int_0^T N_t(t)\sigma_R\phi(t)dt \tag{7-13}$$

or, utilizing the concept of the reactor power history, as:

$$R = \frac{1}{T}\sum_{i=1}^{\#timesteps} \sigma_R\phi_i \int_{T_{i-1}}^{T_i} N_t(t)dt \tag{7-14}$$

where T is the total irradiation time (seconds) determined by summing the individual time step durations. Substituting Eq. (7-3) into Eq. (7-14) and performing the indicated integration over each time step yields:

$$R = \frac{1}{T}\sum_{i=1}^{\#timesteps} \frac{\sigma_R\phi_i N_{t_{i-1}}(1-e^{-\sigma_a^t\phi_i\Delta T_i})}{\sigma_a^t\phi_i} \tag{7-15}$$

where ΔT_i is the duration of the i-th time step.

Note that it would appear that the flux in the numerator and denominator of Eq. (7-15) would cancel, however, that is not the case since the product of the cross section and the flux actually represents a summation of the energy group dependent values over all energy groups as noted in Eq. (7-2).

In the case of numerical benchmarks, it is common practice to use a single state point with no operating power history to determine the predicted activation reaction rates in dosimeter regions of the problem. When this is the case, the activation reaction rate takes the form:

$$R = \sigma_R\phi_s N_{t_0} \tag{7-16}$$

7.1.4 Reactions Per Atom

The total number of reactions per target atom may be used either as an alternate means of determining irradiation damage, such as displacements per atom (dpa), or for determining the accumulation of product nuclides, such as helium accumulation resulting from irradiation of boron impurities in steel. The total reactions per atom over the period of irradiation is given by:

$$R_A = \sum_{i=1}^{\#timesteps} \sigma_R\phi_i\Delta T_i \tag{7-17}$$

7.1.5 Equivalent ^{235}U Fission Spectrum Flux and Cross Section

A common means of reporting benchmark activation rates is through the use of the "equivalent ^{235}U fission spectrum flux". This equivalent flux utilizes an equivalent ^{235}U fission spectrum dosimeter cross section defined as:

$$\sigma_{eq} = \sum_{g=1}^{\#energygroups} \sigma_{R_g} \chi_g \tag{7-18}$$

where χ_g is the energy group dependent ^{235}U fission production spectrum. The equivalent ^{235}U fission spectrum flux is then defined as:

$$\phi_{eq} = \frac{\sum_{g=1}^{\#energygroups} \sigma_{R_g} \phi_g}{\sigma_{eq}} \tag{7-19}$$

7.1.6 Response Function Nuclide Number Densities and Decay Constants

In order to facilitate the computation of activation reactions in support of RPV fluence and surveillance capsule evaluations, the RAFTER computer program includes default values of target nuclide number densities and product nuclide decay constants for the BUGLE-96 [2] response reactions. The target number densities given in Table 7-1 are based upon the natural abundance of the target nuclide. Table 7-2 contains the corresponding product decay constants for the various response reactions.

7.2 Neutron Flux and Fluence Evaluations

Determining the neutron fluence in component regions of reactor systems is an essential element in the assessment of component damage resulting from neutron irradiation. Generally, the evaluation is restricted to a reduced energy range since low energy neutrons are substantially less likely to inflict irradiation damage than are high-energy neutrons. Material damage assessments are usually restricted to neutron energies > 0.1 MeV, with neutron energies > 1 MeV being even more commonly used to express the extent of irradiation damage.

7.2.1 Neutron Flux Energy Cutoff

Since most reactor system component damage assessments are based upon flux values that are greater than a cutoff energy level, it is necessary to be able to compute flux values that do not span the entire energy spectrum used in the particle transport calculation. If the energy cutoff value falls on a group boundary, the resulting flux that is greater than the energy cutoff value is simply the sum of the fluxes in the energy groups with lower energy range values that are above the cutoff value. In this case, the resulting neutron flux is given by:

$$\phi_{i,E_0} = \sum_{g \le G} \phi_{i,g} \tag{7-20}$$

where ϕ_{i,E_0} is the flux in the i-th state point with energy greater than the cutoff energy, E_0, G is the energy group whose lower boundary value coincides with the cutoff energy value, g is the group index, and $\phi_{i,g}$ is the neutron flux in energy group g for the i-th state point.

If the cutoff energy value does not coincide with a group boundary, then it is necessary to determine the contribution to the neutron flux from the energy group in which the cutoff energy value lies. In this case, the resulting neutron flux can be expressed as:

$$\phi_{i,E_0} = \sum_{g < G} \phi_g + \delta_G \tag{7-21}$$

where G is the energy group that the cutoff energy lies in and δ_G is the contribution from energy group G to the neutron flux that is greater than the cutoff energy. This contribution is determined in the same manner as described in Section 4.2.3.

Table 7-1
Default Target Nuclide Number Densities

Target Nuclide	Number Density (atoms/b-cm)
^{27}Al	6.0242E-02
^{197}Au	5.9074E-02
^{10}B	2.6276E-02
^{59}Co	9.0951E-02
^{63}Cu	5.8738E-02
^{65}Cu	2.6180E-02
^{54}Fe	4.9249E-03
^{56}Fe	7.7882E-02
^{58}Fe	2.3776E-04
^{127}I	2.3396E-02
^{115}In	3.6694E-02
^{6}Li	3.4750E-03
^{55}Mn	8.1451E-02
^{23}Na	2.5437E-02
^{58}Ni	6.2166E-02
^{60}Ni	2.3946E-02
^{237}Np	5.1448E-02
^{239}Pu	4.9967E-02
^{240}Pu	[1]
^{241}Pu	[1]
^{242}Pu	[1]
^{103}Rh	7.2629E-02
^{32}S	3.6949E-02
^{45}Sc	4.0042E-02
^{232}Th	3.0419E-02
^{46}Ti	4.5666E-03
^{47}Ti	4.1670E-03
^{48}Ti	4.2126E-02
^{234}U	2.5891E-06
^{235}U	3.4090E-04
^{236}U	[1]
^{238}U	4.7599E-02

[1] These nuclides do not have a naturally occurring nuclide number density.

Table 7-2
Default Product Nuclide Decay Constants

Product Nuclide	Decay Constant (1/sec)
^{198}Au	2.976E-06
^{58}Co	1.133E-07
^{60}Co	4.166E-09
^{64}Cu	1.516E-05
^{59}Fe	1.803E-07
^{4}He	Stable
^{126}I	6.118E-07
^{115m}In	4.292E-05
^{116m}In	2.128E-04
^{27}Mg	1.221E-03
^{54}Mn	2.569E-08
^{56}Mn	7.467E-05
^{24}Na	1.287E-05
^{57}Ni	5.407E-06
^{32}P	5.626E-07
^{103m}Rh	2.059E-04
^{46}Sc	9.575E-08
^{47}Sc	2.401E-06
^{48}Sc	4.409E-06
^{233}Th	5.180E-04
^{239}U	4.926E-04

7.2.2 Accumulated Neutron Fluence

The accumulated fluence greater than an energy cutoff value of E_0 in a region is given by:

$$\varphi_{E_0} = \sum_{i=1}^{\#timesteps} \phi_{i,E_0} \Delta T_i \tag{7-22}$$

where ΔT_i is the duration of the i-th time step in seconds and ϕ_{i,E_0} is the accumulated neutron flux above the energy cutoff value E_0 as determined from Eq. (7-20) or Eq. (7-21).

7.2.3 Effective Full Power Time

The effective full power time (seconds) is given by:

$$T_E = \sum_{i=1}^{\#timesteps} p_i \Delta T_i \tag{7-23}$$

where ΔT_i is the duration in seconds of the i-th time step and p_i is the fractional power factor given in Eq. (7-9).

7.2.4 Cumulative Power Factor

The cumulative power factor is the average fractional power of the reactor over the period of irradiation and is given by:

$$\overline{p} = \frac{\sum_{i=1}^{\#timesteps} p_i \Delta T_i}{T} = \frac{T_E}{T} \tag{7-24}$$

where T_E is the effective full power time given by Eq. (7-23) and T is the total time of irradiation given by the sum of the duration of all time steps in the irradiation period. This value is analogous to the plant capacity factor for the period.

7.2.5 Average Neutron Flux

When reactor power history is provided, the region average neutron flux for energy above an energy cutoff value of E_0 is given by:

$$\overline{\phi}_{E_0} = \frac{\sum_{i=1}^{\#timesteps} \phi_{i,E_0} \Delta T_i}{T} \tag{7-25}$$

where T is the total irradiation time given by the sum of the duration of all time steps in the irradiation period.

When no reactor power history is provided, the region average neutron flux for energy above an energy cutoff value of E_0 can be determined directly from the state-point flux value:

$$\overline{\phi}_{E_0} = \phi_{s,E_0} \tag{7-26}$$

where ϕ_{s,E_0} is the state-point flux above the energy cutoff value of E_0 computed using Eq. (7-20) or Eq. (7-21) as appropriate.

7.2.6 Rated Power Neutron Flux

The rated power neutron flux above an energy cutoff value of E_0 provides a means for estimating the end of life fluence of the reactor components. The rated power neutron flux is given by:

$$\phi_{R,E_0} = \frac{\sum_{i=1}^{\#timesteps} \phi_{i,E_0} \Delta T_i}{\sum_{i=1}^{\#timesteps} p_i \Delta T_i} = \frac{\sum_{i=1}^{\#timesteps} \phi_{i,E_0} \Delta T_i}{T_E} \tag{7-27}$$

where T_E is the effective full power time from Eq. (7-23).

7.3 Uncertainty Analysis Methodology

The neutron flux undergoes several decades of attenuation between the core and the reactor pressure vessel. Calculation of the neutron flux distribution is sensitive to material and geometric representation of the core and reactor internals, the neutron source, the nuclear cross-section data, and the numerical scheme used in the calculation. It is important to account for uncertainties in these parameters in determining the neutron fluence and in estimating the uncertainty in the calculated fluence.

The sources of uncertainty in determining the RPV fluence include analytical uncertainty and comparison uncertainty. These are combined to provide an estimate of the overall fluence bias and standard deviation that is used to determine the best-estimate RPV fluence from the calculated RPV fluence values. The methods used to calculate these forms of uncertainty are presented in the following subsections.

7.3.1 Analytical Uncertainty

The uncertainty analysis applied to the neutron fluence calculation is a function of several random, possibly correlated, input parameters. The calculated neutron fluence (>1 MeV) at any given location in the RPV can be expressed in functional form as:

$$\phi = \phi(x_1, x_2, \ldots, x_n) = \phi(\bar{x}) \tag{7-28}$$

where ϕ is the resultant neutron fluence that is a function of the N input parameters: x_1 , x_2, ... x_n (represented by the N-dimensional vector $\bar{x}$). Using a linear approximation (single term Taylor expansion), the fluence corresponding to a perturbed set of input parameters can be written as:

$$\phi(\bar{x} + \delta\bar{x}) = \phi(\bar{x}) + \delta\phi = \phi(\bar{x}) + \sum_{i=1}^{n} \frac{\partial\phi}{\partial x_i} \delta x_i \tag{7-29}$$

From Eq. (7-29), the deviation in fluence resulting from deviations in the input parameters can be written in matrix form as:

$$\delta\phi = S_a^T(\delta\bar{x}) \tag{7-30}$$

where S_a is the N-dimensional sensitivity vector corresponding to deviations in the analytical input parameters, $\delta\bar{x}$ is the N-dimensional vector of deviations in input parameter values, and the superscript T denotes the transpose of the vector. The sensitivity vector takes the general form of:

$$S_a = \begin{bmatrix} \frac{\partial\phi}{\partial x_1} \\ \cdots \\ \frac{\partial\phi}{\partial x_n} \end{bmatrix} \approx \begin{bmatrix} \frac{\Delta\phi}{\Delta x_1} \\ \cdots \\ \frac{\Delta\phi}{\Delta x_n} \end{bmatrix} \tag{7-31}$$

The statistical standard deviation corresponding to the analytical fluence evaluation can be determined from Eq. (7-30) to be:

$$\sigma_a \equiv \left[E\left\{(\delta\phi)(\delta\phi)^T\right\}\right]^{1/2} = \left[S_a^T E\left\{(\delta\bar{x})(\delta\bar{x})^T\right\}S_a\right]^{1/2} = \left[S_a^T C_a S_a\right]^{1/2} \tag{7-32}$$

where the notation E{} denotes the statistical expectation (i.e., an average over a probability distribution of possible deviations from the mean value) and C_a is the N x N uncertainty matrix (i.e., covariance matrix) that describes the uncertainty of the input parameters. The uncertainty matrix in Eq. (7-32) takes the form:

$$C_a = \begin{bmatrix} \sigma_1^2 & \sigma_{12}^2 & \cdots & \sigma_{1N}^2 \\ \sigma_{21}^2 & \sigma_2^2 & \cdots & \sigma_{2N}^2 \\ \cdots & \cdots & \cdots & \cdots \\ \sigma_{N1}^2 & \sigma_{N2}^2 & \cdots & \sigma_N^2 \end{bmatrix} \tag{7-33}$$

The diagonal elements of the uncertainty matrix are the statistical variances (i.e., squares of the standard deviations) of the corresponding input parameters. The off-diagonal elements are statistical covariances that describe the correlation between the input parameters, if any correlation exists. It should be noted that most of the input parameters that comprise the analytical uncertainty evaluation are uncorrelated, therefore, the corresponding off-diagonal elements of the uncertainty matrix are zero.

The fluence calculation methodology may result in an inherent analytical bias in the determination of the RPV fluence. It is possible to estimate the relative analytical bias from Eq. (7-30) as:

$$B_a = \frac{\phi(\bar{x}_{opt}) - \phi(\bar{x}_a)}{\phi(\bar{x}_a)} \approx \frac{S_a^T(\bar{x}_{opt} - \bar{x}_a)}{\phi(\bar{x}_a)} \tag{7-34}$$

where $\vec{x}_a$ is the vector of input parameters used in the analytical fluence evaluation and $\vec{x}_{opt}$ is the vector of "optimal" input parameters that, when used in the fluence evaluation, produce the best estimate of the fluence. The components of the "optimal" input parameter set consist of the mean value of input parameters that are bounded (such as parameters with tolerances or estimate uncertainty ranges) and the asymptotic value of input parameters that are unbounded (such as mesh interval parameters and angular quadrature set parameters). In general, the mean value of bounded input parameters is used in the standard fluence evaluation, so the contribution to the analytical fluence bias is zero for these parameters. However, it is not uncommon that values other than the true asymptotic value of unbounded input parameters are used in the standard fluence evaluation. This can result in a non-zero analytical bias.

The analytical input parameter set and the corresponding uncertainty in the input parameters is expected to be somewhat application specific. An example of a "typical" input parameter set that would be applicable to fluence evaluations in BWRs is shown in Table 7-3. The type of analysis used to obtain the sensitivity elements that comprise the sensitivity vector is also shown in Table 7-3. The spectral effects resulting from the flux attenuation through the RPV is accounted for in the analytical uncertainty analysis by computing individual bias and standard deviation values at the 0 T, ¼ T, ½ T, ¾ T, and T locations at the azimuth of peak vessel fluence (for 2-D sensitivity cases) and at the azimuth and axial location of peak vessel fluence (for 3-D sensitivity cases).

It should be noted that the analytical bias is typically an integral part of the observed deviation in the comparison of calculated to measured activation since the models used for fluence evaluations are the same as those used for the measurement comparisons. Thus the analytical bias is usually zero in RAMA fluence evaluations.

Table 7-3
Sample Input Parameter Set

[[

Content Deleted
EPRI Proprietary Information

]] **TS**

7.3.2 Comparison Uncertainty

The comparison uncertainty is determined from the comparison between measured and calculated dosimetry activation results obtained from the fluence benchmark and operating reactor surveillance capsule evaluations. Uncertainties in the comparison to measured values arise from (1) uncertainties in the predicted activities due to uncertainties in calculation input parameters, and (2) uncertainties in the measured activities. The comparison uncertainty analysis accounts for both of these contributions.

The calculated flux is used to determine calculated activities at the dosimeter locations. Uncertainties in the calculated activities are determined in a similar manner to the calculated vessel fluence uncertainties described in Section 7.3.1. Sensitivity evaluations are performed for each measurement in the benchmark and operating plant surveillance capsule database.

For a measurement database consisting of M measurements and a set of N significant input parameters used in the activation calculation, then the N x M sensitivity matrix obtained from sensitivity evaluations is given by:

$$S_I = \begin{bmatrix} \frac{\partial A_1}{\partial x_1} & \frac{\partial A_2}{\partial x_1} & \cdots & \frac{\partial A_M}{\partial x_1} \\ \frac{\partial A_1}{\partial x_2} & \frac{\partial A_2}{\partial x_2} & \cdots & \frac{\partial A_M}{\partial x_2} \\ \cdots & \cdots & \cdots & \cdots \\ \frac{\partial A_1}{\partial x_N} & \frac{\partial A_2}{\partial x_N} & \cdots & \frac{\partial A_M}{\partial x_N} \end{bmatrix} \approx \begin{bmatrix} \frac{\Delta A_1}{\Delta x_1} & \frac{\Delta A_2}{\Delta x_1} & \cdots & \frac{\Delta A_M}{\Delta x_1} \\ \frac{\Delta A_1}{\Delta x_2} & \frac{\Delta A_2}{\Delta x_2} & \cdots & \frac{\Delta A_M}{\Delta x_2} \\ \cdots & \cdots & \cdots & \cdots \\ \frac{\Delta A_1}{\Delta x_N} & \frac{\Delta A_2}{\Delta x_N} & \cdots & \frac{\Delta A_M}{\Delta x_N} \end{bmatrix} \tag{7-35}$$

where A_m is the predicted relative activity corresponding to the m-th measurement in the database, and x_n is the n-th significant input parameter in the sensitivity evaluation. The list of input parameters that are included in the comparison uncertainty sensitivity evaluation are generally similar to those utilized in the fluence analytical uncertainty sensitivity evaluation with some additional activity calculation specific parameters, such as detector location and activation cross sections.

Letting C_x be the N x N uncertainty matrix associated with the input parameters and C_m be the M x M uncertainty matrix associated with the measurements, then the uncertainty associated with the difference between calculated and measured results, C_d, is given by:

$$C_d = S_I^T C_x S_I + C_m \tag{7-36}$$

where it has been assumed that there is no correlation between the input parameters and the measured results. For a detailed derivation of Eq. 7-36, see [8]. If $\vec{d}$ is the M-dimensional vector whose elements are the differences between the calculated and measured activity results, then the overall comparison uncertainty (i.e., standard deviation) can be expressed as:

$$\sigma_b = \left[\vec{d}^T C_d \vec{d}\right]^{1/2} \tag{7-37}$$

The bias, based upon comparison of calculated to measured dosimeter results, is:

$$B_b = \frac{1}{M}\sum_{i=1}^{M} \frac{m_i - c_i}{c_i} = \frac{1}{M}\sum_{i=1}^{M}\left(\frac{m_i}{c_i} - 1\right) \tag{7-38}$$

where m_i is the i-th measured activation value in the database and c_i is the i-th calculated activation value. Note that an implicit assumption in Eq. (7-38) is that the relative bias based upon comparison to measured values applies to RPV locations as well.

The elements contributing to the comparison uncertainty analysis are generally quite different for the vessel simulator benchmark evaluations as opposed to operating light water reactor dosimetry evaluations. As a result, the bias and uncertainty (standard deviation) are determined using the above methodology for two different measurement databases: (1) the vessel simulator benchmark database consisting of comparison results for the PCA and VENUS-3 benchmark problems, and (2) the operating system database consisting of dosimetry measurement data from operating light water reactor plants.

The comparison databases must be evaluated to confirm their statistical validity for use in determining the RPV "best estimate" bias. Statistical valid databases must meet three criteria: (1) the database should provide a representative sample over the range of operating states for which the fluence evaluation methodology is to be applied, (2) the uncertainty in the database comparisons should be small compared to the comparison bias, and (3) the calculation and measurement errors of the comparison ratios must be uncorrelated (i.e., no systematic bias is present in the comparisons).

The method of evaluating the extent of correlated comparisons in the databases, and the method for removing the correlated bias is described in [9]. The database comparisons are expressed in a regression model of the form:

$$\left(\frac{m}{c}\right) = \mu_{m/c} + \sum_{k=1}^{K} c_k \alpha_k \tag{7-39}$$

where $\mu_{m/c}$ is the fitted mean of the comparisons, c_k are fit coefficients, and α_k are parameters that represent various possible correlation conditions, such as the type of detector, the location of the detector (e.g., in-vessel and behind jet pumps), the energy threshold of the detector, etc. The statistics of the fit parameters are used to determine correlated parameters. The regression model of Eq. (7-39) is used to remove the systematic bias from the measurement comparisons. The measurement comparisons are used to determine an adjusted bias, as in Eq. (7-38).

7.3.3 Calculational Uncertainty

[[

Content Deleted
EPRI Proprietary Information

]] **TS**

[[

Content Deleted
EPRI Proprietary Information

]] TS

7.3.4 Best Estimate Fluence

The calculational fluence bias and standard deviation determined from Section 7.3.3 are used to compute the best estimate neutron fluence from the calculated fluence as specified in [1] using the following methodology.

If the overall calculational bias, B_c, is not statistically significant, then the best estimate fluence is equivalent to the calculated fluence obtained from the RAMA fluence evaluation (i.e., the fluence estimate has a zero bias). To be statistically significant, the calculational bias should exceed ±2 times the overall calculational uncertainty, σ_c, obtained from Eq. (7-40).

If the bias is deemed to be statistically significant then the following approach is used to determine a best estimate of the neutron fluence. If the calculational uncertainty (1σ) is ≤20%, the best estimate neutron fluence is given by

$$\varphi = \varphi_c(1 + B_c) \tag{7-44}$$

where φ is the best estimate fluence and φ_c is the calculated neutron fluence. If the calculational uncertainty (1 ∫) is greater than 20% but less than 30%, the best estimate neutron fluence is given by

$$\varphi = \varphi_c\left(1 + B_c + \frac{\sigma_c(\%) - 20}{100}\right) \tag{7-45}$$

where σ_c is the calculational uncertainty obtained from Eq. (7-40).

8
NUCLEAR DATA GENERATION METHOD

The RAMA nuclear data library is derived from the BUGLE-96 [2] nuclear data library. BUGLE-96 is comprised of several data files containing material cross sections, response functions, and kerma factors that are appropriate for LWR shielding and pressure vessel dosimetry calculations. RAMA is a single data library file that contains the necessary data from the various BUGLE-96 data files. The following subsections describe the process for generating the RAMA nuclear data library.

8.1 BUGLE-96 Data

The BUGLE-96 and RAMA cross section data is represented in a coupled 47 neutron/20 gamma-ray broad-group, energy group structure with scattering cross section moments up to P_7. The 47 neutron/20 gamma-ray broad-group cross sections were derived from the fine-group VITAMIN-B6 [10] nuclear data library using the SCAMPI [11] code package. The BUGLE-96 library includes several sets of weighted broad-group data that are weighted according to location and flux spectra in the reactor. This means that the data that will be used in transport calculations has been collapsed from a fine-group to a broad-group structure using a flux spectrum that is appropriate for the region containing the material. As a consequence, several forms of the same material are included in the library, each weighted with a different flux spectrum. Collapsed data are included for the following reactor regions: BWR core, downcomer, pressure vessel, and concrete shield.

The broad-group cross section data, response functions, and kerma factors in the RAMA nuclear data library are derived directly from the BUGLE-96 nuclear data library. The cross section data is obtained from the self-shielded data with thermal up-scatter.

8.2 Nuclide Identifiers

The BUGLE-96 and RAMA nuclear data libraries use different identifiers to identify the materials and nuclides in the data libraries. BUGLE-96 uses "material numbers" and RAMA uses "nuclide identifiers". There is no direct correspondence of the BUGLE-96 material numbers with RAMA nuclide identifiers.

The material numbers used in the BUGLE-96 nuclear data library define one cross section set with one scattering moment for a nuclide. The material numbers are assigned in a somewhat arbitrary fashion; that is, the numbers do not necessarily identify a particular nuclide for the data. The only requirements for material numbers is that each material number in the data library must be unique in order to select the correct cross section set for a transport calculation.

The nuclide identifiers in the RAMA nuclear data library are specified to permit the data to be easily identified and associated with a particular nuclide. RAMA nuclide identifiers are specified by an integer value of the form "ZZAAAWW", where ZZ is the atomic number, AAA is the atomic weight, and WW is a spectrum weighting identifier. Whereas BUGLE-96 maintains separate material cross section tables for each Legendre scattering moment, RAMA maintains one nuclide identifier that represents all the scattering moments for that nuclide.

8.3 Legendre Order of Scattering

The cross section sets in the BUGLE-96 and RAMA nuclear data libraries include high-order scattering moments for treating anisotropic effects in the transport calculations. The order of scattering is based upon a Legendre expansion of the scattering term. The same order of scattering is used for both neutrons and gamma-rays. The highest moments in the RAMA and BUGLE-96 data libraries are P_7 for nuclides with Z=1 (hydrogen) to Z=29 (copper) and P_5 for the remainder of the nuclides.

RAMA is capable of performing anisotropic calculations using scattering moments from P_1 through P_7. The order of scattering may be specified by the user. Even though all cross sections are not tabulated with the same scattering moments (i.e., some nuclides have P_5 and some have P_7 tabulations), RAMA properly handles situations when higher order (greater than P_5) cross sections are mixed with lower order (less than or equal to P_5) cross sections.

8.4 Cross Section Generation

The BUGLE-96 nuclear data library includes nuclear cross section data that are specifically developed for light water reactor shielding and pressure vessel dosimetry calculations. These cross sections are generated from the VITAMIN-B6 nuclear data library using the SCAMPI code package. The process used to generate the light water reactor cross sections for both BWR and PWR reactors is described in the BUGLE-96 distribution documentation.

The RAMA nuclear data library contains cross section data for the same material nuclides as the BUGLE-96 nuclear data library. In addition, the RAMA data library includes BWR and PWR core-weighted cross section data for the following actinides: ^{239}Pu, ^{240}Pu, ^{241}Pu, and ^{242}Pu, as well as fission cross section data and fission spectrum data for ^{235}U, ^{238}U, ^{239}Pu, ^{240}Pu, ^{241}Pu, and ^{242}Pu. The additional BWR and PWR core-weighted actinide cross section data is generated from VITAMIN-B6 using the same basic process as that used to generate BUGLE-96. The methodology for generating the additional core-weighted RAMA cross sections from VITAMIN-B6 and for generating the composite RAMA nuclear data library involves four major steps:

1. Perform resonance shielding of the additional BWR and PWR actinide nuclides from the VITAMIN-B6 BCD data files using generic BWR or PWR pincell geometry and material composition, as appropriate.

2. Collapse the fine-group shielded working library cross sections to the desired broad-group structure (47 neutron / 20 gamma-ray) using the BUGLE-96 BWR or PWR core region collapsing flux spectra, as appropriate.

3. Create an ANISN BCD format library containing the broad-group cross sections.

4. Generate the RAMA binary nuclear data library using the BUGLE-96 light water reactor weighted cross-section data combined with the additional BWR and PWR core-weighted nuclear data generated in steps 1 through 3 above.

Figure 8-1 illustrates steps 1 through 3 that involves running the SCAMPI code modules to generate the additional BWR or PWR core-shielded cross sections in ANISN-format. The additional nuclear data is then combined with the remaining BUGLE-96 light water reactor data to form the RAMA nuclear data library. Figure 8-2 illustrates step 4 that involves running the RAMALIB code to generate the RAMA nuclear data library file.

The BUGLE-96 data library contains most of the nuclides required by the RAMA code system for light water reactor fluence calculations except plutonium and selected uranium nuclear data. Therefore, it is only necessary to run the SCAMPI code system to process additional uranium cross sections for the uranium nuclides ^{235}U and ^{238}U and the additional plutonium cross sections for the plutonium nuclides ^{239}Pu, ^{240}Pu, ^{241}Pu, and ^{242}Pu.

The four steps required to generate the RAMA nuclear data library file are described in more detail in subsections that follow.

8.4.1 Generation of Resonance Self-shielded Actinide Cross Sections

The SCAMPI code system is used to generate a working library that contains appropriately shielded corrections for common resonance nuclides.

Following is a description of the process involved in generating the resonance self-shielded cross sections for the BWR and PWR actinide nuclides:

1. The AIM and AJAX modules of SCAMPI are executed for each core nuclide to convert the VITAMIN-B6 BCD format data files into a binary unshielded master library.

2. Appropriately self-shielded core actinide cross sections are obtained by executing the BONAMI module of SCAMPI material and geometry definitions provided in [4] for BWR and PWR fuel pincells.

3. The AJAX module is again executed to produce a set of cross sections in AMPX binary master library format that contains the desired self-shielded actinide nuclides in the VITAMIN-B6 group structure (i.e., 199 neutron groups and 42 photon groups).

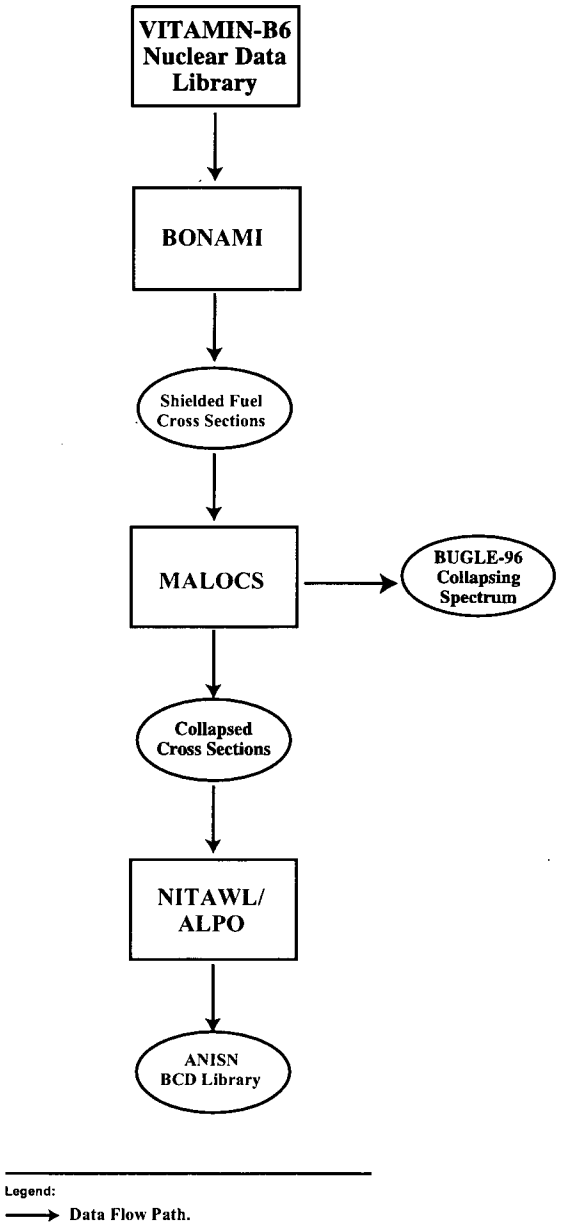

Figure 8-1
SCAMPI Cross Section Processing Flow Diagram

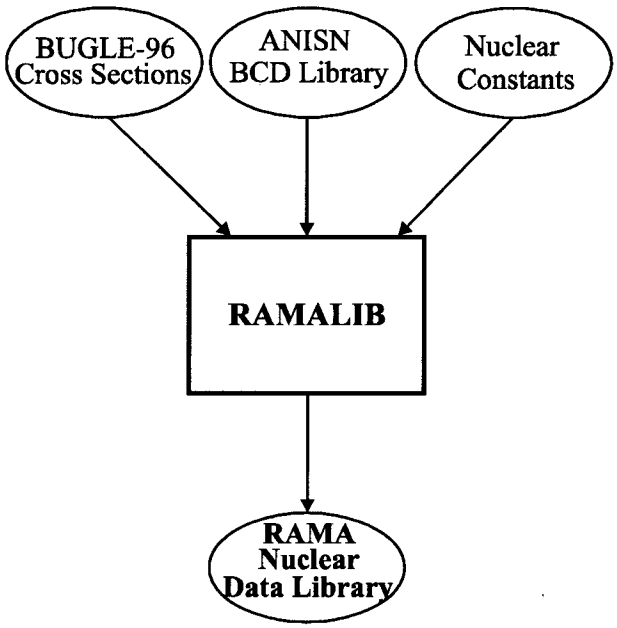

Legend:
→ Data flow path.

Figure 8-2
RAMA Nuclear Data Library Generation Flow Diagram

8.4.2 Generation of Broad Group Shielded Cross Sections

The self-shielded actinide cross sections obtained from step 1 are collapsed to the BUGLE-96 and RAMA broad-group structure (i.e., 47 neutron groups and 20 photon groups). The flux spectra used to collapse the cross sections are the same as those used to collapse the BUGLE-96 core-weighted nuclides. These spectra have been determined from generic 1-D BWR and PWR reactor system models using the XSDRNPM module of the SCAMPI package.

Following is a description of the process used to collapse the BWR and PWR self-shielded actinide cross sections obtained from the process described in Section 8.4.1 above to a set of BWR and PWR core-weighted nuclides in the AMPX working library format and BUGLE-96 energy group structure:

1. The MALOCS module of SCAMPI is executed to collapse the self-shielded actinide nuclide cross sections to the BUGLE-96 energy group structure. The collapsing process uses the appropriate collapsing flux spectra from [2] (i.e., the BWR flux distribution from region #57 of the XSDRNPM BWR reactor system model and the PWR flux distribution from region #37 of the XSDRNPM PWR reactor system model).

2. The collapsed core-weighted cross sections are converted to the AMPX working library format by the NITAWL module of SCAMPI.

3. The RADE module of SCAMPI is executed to perform consistency and validity checks on the collapsed set of cross sections to ensure that the data is free of obvious processing errors.

8.4.3 Creation of ANISN BCD Nuclear Data

The final RAMA library generation process requires that the nuclear data for all nuclides be in the ANISN BCD format (either fixed-format or free-format). The BUGLE-96 nuclear data is in ANISN BCD fixed format. The additionally processed actinide nuclear data must be converted to ANISN BCD format in order to be included in the RAMA nuclear data library.

Following is a description of the process used to convert the collapsed core-weighted BWR and PWR cross sections obtained from Section 8.4.2 above to ANISN BCD format libraries for incorporation in the RAMA nuclear data library generation process.

1. The conversion of the collapsed core-weighted cross sections to ANISN BCD format libraries is performed by the ALPO module of SCAMPI. In addition to the traditional cross section arrays that are typically provided with the BUGLE-96 nuclide data sets (i.e., absorption, nu-fission, total, and scattering matrix cross sections), additional data arrays (i.e., fission cross section and fission spectrum arrays) are included in the BWR and PWR actinide ANISN libraries. The resulting ANISN BCD libraries are assigned to named data files that are used along with the remaining BUGLE-96 nuclide data files to generate the RAMA nuclear data library as described in Section 8.4.4 of this manual.

2. To assist in verifying the validity of the created actinide ANISN libraries, the LAVA module of SCAMPI is used to convert the BCD libraries back into AMPX working library format cross-section sets.

3. The ALE module of SCAMPI is then used to display the nuclide data arrays (e.g., total cross section array, absorption cross section array, etc.). The data arrays for core-weighted ^{235}U and ^{238}U can then be compared to the corresponding data arrays obtained from the same BUGLE-96 nuclear data library.

8.4.4 Generation of the RAMA Nuclear Data Library

The RAMALIB code is used to generate the RAMA nuclear data library from the ANISN BCD cross section data files generated by the SCAMPI code system and other nuclear constants. RAMALIB uses one input file to describe all the data required for the RAMA nuclear data library. This input file includes references to the individual nuclide data files that contain the cross-section data for the nuclide. The file also provides for assigning kerma values, kappa values (i.e., energy release per fission), and the RAMA nuclide identifier to the individual nuclides.

9
REFERENCES

1. "Calculational and Dosimetry Methods for Determining Pressure Vessel Neutron Fluence," Nuclear Regulatory Commission Regulatory Guide 1.190, March 2001.

2. "BUGLE-96: Coupled 47 Neutron, 20 Gamma-Ray Group Cross Section Library Derived from ENDF/B-VI for LWR Shielding and Pressure Vessel Dosimetry Applications," RSICC Data Library Collection, DLC-185, March 1996.

3. "Programming Languages – Fortran," ISO/IEC, 1559-1:1997, International Organization for Standardization and International Electrotechnical Commission, October 21, 1997.

4. "C Programming Language," ANSI X3.159-1989, American National Standards Institute, Inc., December 14, 1989.

5. J. T. West, M. B. Emmett, "MARS: A Multiple Array System Using Combinatorial Geometry," Oak Ridge National Laboratory, Radiation Shielding Information Center report, December 1980.

6. H. Lichtenstein, et al, "The SAM-CE Monte Carlo System for Radiation Transport and Criticality Calculations in Complex Configurations," CCM-8, EPRI Research Project 972, 1980.

7. G. I. Bell and S. Glasstone, "Nuclear Reactor Theory," Van Nostrand Reinhold Company, 1970, p. 65.

8. B. L. Broadhead, C. M. Hopper, and C. V. Parks, "Sensitivity and Uncertainty Analyses Applied to Criticality Safety Validation," NUREG/CR-6655, Vol. 2, Nov. 1999.

9. J. Carew, S. Finch, and L. Lois, "Statistical Analysis of Reactor Pressure Vessel Fluence Calculation Benchmark Data Using Multiple Regression Techniques," *Nuclear Science and Engineering*, 143, 2003, pp. 158-163.

10. "VITAMIN-B6: A Fine-Group Cross Section Library Based on ENDF/B-VI Release 3 for Radiation Transport Applications," RSICC Data Library Collection, DLC-184, December 1996.

11. "SCAMPI: Collection of Codes for Manipulating Multigroup Cross Section Libraries in AMPX Format," RSICC Computer Code Collection, PSR-352, September 1995.

A
NRC REQUEST FOR ADDITIONAL INFORMATION

UNITED STATES
NUCLEAR REGULATORY COMMISSION
WASHINGTON, D.C. 20555-0001

April 20, 2004

Bill Eaton, BWRVIP Chairman
Entergy Operations, Inc.
Echelon One
1340 Echelon Parkway
Jackson, MS 39213-8202

SUBJECT: REQUEST FOR ADDITIONAL INFORMATION - REVIEW OF BWR VESSEL AND INTERNALS PROJECT REPORTS, BWRVIP-114, BWRVIP-115, BWRVIP-117, AND BWRVIP-121, AND TRANSWARE ENTERPRISES INC. REPORT TWE-PSE-001-R-001, REVISION 0 (TAC NO. MB9765)

Dear Mr. Eaton:

By applications dated August 1, August 5, October 23, and October 29, 2003, respectively, you submitted for NRC staff review, four Electric Power Research Institute (EPRI) proprietary reports, BWRVIP-114, "RAMA Fluence Methodology Theory Manual," BWRVIP-115, "RAMA Fluence Methodology Benchmark Manual-Evaluation of Regulatory Guide 1.190 Benchmark Problems," BWRVIP-117, "RAMA Fluence Methodology Plant Application-Susquehanna Unit 2 Surveillance Capsule Fluence Evaluation for Cycles 1-5," and BWRVIP-121, "RAMA Fluence Methodology Procedures Manual." In addition, by application dated March 23, 2004, you submitted for NRC staff review, TransWare Enterprises, Inc. Report, TWE-PSE-001-R-001, Revision 0, "Hope Creek Flux Wire Dosimeter Activation Evaluation for Cycle 1 Using the RAMA Fluence Methodology." These reports were submitted to the NRC as a means of exchanging information with the NRC for the purpose of supporting generic regulatory improvements related to methodologies to determine neutron fluence in BWR internal components.

The NRC staff has completed its initial review of the BWRVIP-114, BWRVIP-115, BWRVIP-117, and BWRVIP-121 reports, and the TransWare Enterprises, Inc. Report, TWE-PSE-001-R-001, Revision 0. As indicated in the attached request for additional

B. Eaton - 2 -

information (RAI), the NRC staff has determined that additional information is needed to complete the review. If you have any questions, please contact Meena Khanna at (301) 415-2150.

Sincerely,

Stephanie M. Coffin, Chief
Vessels & Internals Integrity and Welding Section
Materials and Chemical Engineering Branch
Division of Engineering
Office of Nuclear Reactor Regulation

Project No. 704

Enclosure: As stated

cc: BWRVIP Service List

cc:

Jim Meister, BWRVIP Vice-Chairman
Exelon Corp.
Cornerstone II at Cantera
4300 Winfield Rd.
Warrenville, IL 60555-4012

William C. Holston, Executive Chairman
BWRVIP Integration Committee
Constellation Generation Group
Nine Mile Point Nuclear Station
P.O. Box 63
Lycoming, NY 13093

Tom Mulford, EPRI BWRVIP
Integration Manager
Raj Pathania, EPRI BWRVIP
Mitigation Manager
Ken Wolfe, EPRI BWRVIP
Repair Manager
Larry Steinert, EPRI BWRVIP
Electric Power Research Institute
P.O. Box 10412
3412 Hillview Ave.
Palo Alto, CA 94303

Al Wrape, Executive Chairman
BWRVIP Assessment Committee
PPL Susquehanna, LLC
2 N. 9th St.
Allentown, PA 18101-1139

H. Lewis Sumner, Executive Chairman
BWRVIP Mitigation Committee
Vice President, Hatch Project
Southern Nuclear Operating Co.
M/S BIN B051, P.O. BOX 1295
40 Inverness Center Parkway
Birmingham, AL 35242-4809

Robert Carter, EPRI BWRVIP
Assessment Manager
Greg Selby, EPRI BWRVIP
Inspection Manager
EPRI NDE Center
P.O. Box 217097
1300 W. T. Harris Blvd.
Charlotte, NC 28221

Denver Atwood, Technical Chairman
BWRVIP Repair Focus Group
Southern Nuclear Operating Co.
Post Office Box 1295
40 Inverness Center Parkway (M/S B031)
Birmingham, AL 35242-4809

Robin Dyle, Technical Chairman
BWRVIP Integration Committee
Southern Nuclear Operating Co.
42 Inverness Center Parkway (M/S B234)
Birmingham, AL 35242-4809

Jeff Goldstein, Technical Chairman
BWRVIP Mitigation Committee
Entergy Nuclear NE
440 Hamilton Ave. (M/S K-WPO-11c)
White Plains, NY 10601

Dale Atkinson, BWRVIP Liason to EPRI Nuclear
Power Council
Energy Northwest
Columbia Generating Station (M/S PEO8)
Snake River Complex
North Power Plant Loop
Richland, WA 99352-0968

Richard Ciemiewicz, Technical Vice Chairman
BWRVIP Assessment Committee
Exelon Corp.
Peach Bottom Atomic Power Station
M/S SMB3-6
1848 Lay Road
Delta, PA 17314-9032

Gary Park, Chairman
BWRVIP Inspection Focus Group
Nuclear Management Co.
Monticello Nuclear Plant
2807 W. Country Road 75
Monticello, MN 55362-9635

George Inch, Technical Chairman
BWRVIP Assessment Committee
Constellation Nuclear
Nine Mile Point Nuclear Station (M/S ESB-1)
348 Lake Road
Lycoming, NY 13093

REQUEST FOR ADDITIONAL INFORMATION FOR THE REVIEW OF THE ELECTRIC POWER RESEARCH INSTITUTE (EPRI) RAMA METHODOLOGY FOR REACTOR PRESSURE VESSEL FLUENCE EVALUATION

BWRVIP-114: "BWR Vessel and Internals Project, RAMA Fluence Methodology Theory Manual"

RAI 114-1 In the plant-specific applications, what specific tests and criteria are used to assure the adequacy of the number of rays and the number of volumes used in the RAMA fluence calculations?

RAI 114-2 It is not evident that the RAMA geometry model described in Ref. 1 provides a correct representation of the true geometry (i.e., preserves the location, orientation and shape of all surfaces defining the physical geometry). For example, the modeling of the reflector region, surrounding the core, involves geometry elements that have both planar and cylindrical side boundaries. Since the geometry elements described in Ref. 1, Section 3.2, do not include bodies of this type, does RAMA introduce any distortion of the physical geometry in modeling the reflector and, if so, how is this distortion controlled to ensure acceptable accuracy?

RAI 114-3 The equation provided in Ref. 1, (Equation 7-38) for determining the M/C bias for the benchmark database requires an additional 1/M multiplicative normalization factor.

RAI 114-4 Equation 7-40 of Ref. 1 combines the analytical bias (B_a) and the benchmark bias (B_{bi}) to determine the overall calculational bias. The analytical bias (B_a), defined in Equation 7-34, provides the effect of not using the optimum asymptotic calculational input in the RAMA fluence calculation. Since the benchmark biases include the effect of the approximate calculational input used in the benchmark calculations (i.e., use of the standard input parameters rather than the asymptotic parameters), the analytical bias is only required when there is an inconsistency between the input used in the vessel fluence calculations and the benchmark calculations; e.g., when the calculations of the benchmark measurements are made with the asymptotic input values and the vessel fluence calculations are made with the standard input values. The staff requests that the BWRVIP clearly address the determination of the bias.

RAI 114-5 The weights defined in Equation 7-41 are not normalized (i.e., sum to unity), as required. Also, the weights should reflect the reliability of the bias estimates. If, for example, a weight of $1/\sigma^2$ is used, the σ should represent the standard deviation of the bias estimate, not the standard deviation of the M/C data about the mean.

ATTACHMENT

RAI 114-6 The values of σ_a, σ_{b1} and σ_{b2} of Equation (7-43) represent the (one standard deviation) uncertainty in the RAMA calculated fluence, based on the analytical estimate of the uncertainties, comparisons with simulator benchmarks, and comparisons with operating plant data, respectively. These three uncertainty values represent independent estimates of the RAMA calculational uncertainty.

Therefore, the staff requests that the BWRVIP, in calculating the final estimate of the RAMA calculational uncertainty, σ_c, use an appropriately weighted combination of these three values, where each weight reflects the reliability of the uncertainty estimate, and then normalize the weights. The staff requests that the BWRVIP address this issue and provide a justification.

BWRVIP-115, "BWR Vessel and Internals Project, RAMA Fluence Methodology Benchmark Manual - Evaluation of Regulatory Guide 1.190 Benchmark Problems"

RAI 115-1 Identify all differences between the methods used in performing the RAMA benchmark analyses of Reference 2 and the methods that will be used in performing the calculations of the vessel and shroud fluence. Also, address how the effects of these inconsistencies will be accounted for in determining the RAMA calculational bias and uncertainty.

RAI 115-2 (a) Regulatory Guide 1.190 requires that, as they become available, new measurements are to be incorporated into the M/C database and the fluence calculational bias and uncertainty estimates are to be updated, as necessary. The staff requests that the BWRVIP address how it will ensure that new measurements are incorporated in the M/C database and that the fluence bias and uncertainty will be updated in a timely manner.

(b) How many BWR samples (measurements) are currently available and when is it anticipated that a statistically significant set of measurements will be available to evaluate the overall bias?

RAI 115-3 In the calculation of the VENUS-3 benchmark, it is stated that the source is normalized to the experimental results. If the experimental results used for this normalization are the fluence measurements (which would erroneously reduce the M/C uncertainty), rather than the measurements of the core source distribution, discuss the effect that this simplification has on the calculational bias and uncertainty inferred from this benchmark comparison.

RAI 115-4 In Table 2-24, the sensitivity of the RAMA calculation of the NUREG-6115 benchmark problem to the axial distance between parallel rays has not been included (as in Table 2-16 for the H3R-2 calculation). Please discuss the sensitivity of the RAMA calculation to the axial distance between parallel rays. Please present your results on the same (or a similar) graph as Figures 5.4.6 or 5.4.8 of NUREG-6115.

BWRVIP-117, "BWR Vessel and Internals Project, RAMA Fluence Methodology Plant Application - Susquehanna Unit 2 Surveillance Capsule Fluence Evaluation for Cycles 1-5"

RAI 117-1 In Ref. 3, what criteria was used to select the sixty-three state points used to represent the Cycle 1-5 core operating history and what determination criteria was used in the weighing assignments of each state point calculation?

RAI 117-2 Was the Susquehanna Cycle 1-5 power, void and exposure distribution data based on calculational results or plant process computer data? If this data was the result of recent calculations, rather than the original historical calculations, discuss why new calculations were required and what differences were introduced in the calculations. Also, discuss the effect of any approximations used in representing the state-point dependence of the pin-wise source distribution of the peripheral fuel bundles.

RAI 117-3 Discuss the basis for the Table 5-3 parameter uncertainty for the following locations: (1) capsule and flux wire locations, (2) vessel inner radius, (3) core void fraction, (4) peripheral bundle power, and the (5) iron cross section.

RAI 117-4 Describe the spatial mesh used to represent the capsule and the capsule/vessel water gap.

RAI 117-5 What fluence uncertainty is introduced by the uncertainty in the Cu-63(n, α)Co-60, Fe-54(n, p)Mn-54 and Ni-58(n, p)Co-58 dosimetry cross sections?

RAI 117-6 Provide a discussion of the method used to determine the analytical modeling input bias and the associated uncertainty provided in Table 5-3.

RAI 117-7 In view of the fact that the uncertainty in the bias, inferred from the measurements of Table 5-4, is larger than the bias itself, provide justification for applying this bias to the RAMA calculated fluence.

RAI 117-8 In view of the fact that the RAMA calculation of the benchmark measurements used the "standard" fluence input parameters and the C/M comparisons (and the inferred C/M bias), address the effect of these parameters and provide justification for applying the analytical bias to the RAMA fluence calculation.

RAI 117-9 Discuss the methods used to measure the flux wire activations and conformance to ASTM E-263-93 (Ref. 4), ASTM E-263-93 (Ref. 5) and ASTM E-264-92 (Ref. 6). Also, discuss the basis for the 2.5% measurement accuracy.

BWRVIP-121, "BWR Vessel and Internals Project RAMA Fluence Methodology Procedures Manual"

RAI 121-1 Ref. 7 states that the BWR shroud is a "priority 1 component." However, no mention or attempt was made to demonstrate how RAMA performs in the evaluation of the shroud. Provide benchmarking data and calculations for the core shroud.

RAI 121-2 The staff requests that the BWRVIP provide a justification of the statement in the BWRVIP-121 report, "The nature of the guidelines is applicable to BWR plants without jet pumps..." In most BWRs, the dosimeters are placed behind the jet pump, which introduces spectral distortions, particularly for Fe and Ni dosimeters. If the BWRVIP report is indicating that the RAMA bias and uncertainties, based on jet pump plants, are applicable to plants without jet pumps, then the staff requests that the BWRVIP justify this statement.

TWE-PSE-001-R-001, "Hope Creek Flux Wire Dosimeter Activation Evaluation for Cycle 1"

1. The surveillance capsule is situated directly behind the jet pump. Given the "window" in the inelastic scattering of Fe in the 1.0 to 2.5 MeV range, what is the effect of the spectrum on the Fe, Ni, and Cu activation?

2. There is no mention of the estimation of the neutron spectrum in these calculations. The report states that there are 12 segments in the cycle, with different material compositions. It seems that the major differences in these segments are the decreasing concentration of U-235, the increasing concentration of Pu-239, and the increasing concentration of fission products. How do these changes affect the spectrum and how is it calculated?

3. What were the findings/results from the sensitivity study? Are the parameter default settings optimized?

4. Given the systematic underestimation of the Cu dosimeters, address whether an investigation shall be launched to determine if a dosimeter-specific bias exists?

5. The report states that the Cu discrepancy could be due to Co-59 impurity. The staff requests that the BWRVIP address that dosimeters supposed to be chemically and isotopically pure?

REFERENCES

1. BWRVIP-114, "BWR Vessel and Internals Project, RAMA Fluence Methodology Theory Manual," EPRI, Palo Alto, CA 2003 1003660.

2. "BWRVIP-115, "BWR Vessel and Internals Project, RAMA Fluence Methodology Benchmark Manual - Evaluation of Regulatory Guide 1.190 Benchmark Problems," EPRI, Palo Alto, CA 2003 1008063.

3. "BWRVIP-117, "BWR Vessel and Internals Project, RAMA Fluence Methodology Plant Application - Susquehanna Unit 2 Surveillance Capsule Fluence Evaluation for Cycles 1-5," EPRI, Palo Alto, CA 2003 1008065.

4. ASTM E-263-93, "Standard Test Method for Measuring Fast-Neutron Reaction Rates by Radioactivation of Iron," ASTM Standards, Section 12, American Society for Testing and Materials, Philadelphia, PA, 1995.

5. ASTM E-523-92, "Standard Test Method for Measuring Fast-Neutron Reaction Rates by Radioactivation of Copper," ASTM Standards, Section 12, American Society for Testing and Materials, Philadelphia, PA, 1995.

6. ASTM E-264-92, "Standard Test Method for Measuring Fast-Neutron Reaction Rates by Radioactivation of Nickel," ASTM Standards, Section 12, American Society for Testing and Materials, Philadelphia, PA, 1995.

7. BWRVIP-121, "BWR Vessel and Internals Project RAMA Fluence Methodology Procedures Manual," EPRI, Palo Alto, CA 2003 1008062.

B
BWRVIP RESPONSE TO NRC REQUEST FOR ADDITIONAL INFORMATION

ELECTRIFY THE WORLD

EPRI

BWRVIP BWR Vessel & Internals Project 2004-420

September 29, 2004

Document Control Desk
U. S. Nuclear Regulatory Commission
11555 Rockville Pike
Rockville, MD 20852

Attention: Meena Khanna

Subject: Project No. 704 – BWRVIP Response to NRC Request for Additional Information on BWRVIP-114, -115, -117 and -121

References:
1. Letter from Meena Khanna (NRC) to Bill Eaton (BWRVIP Chairman), "Request for Additional Information – Review of BWR Vessel and Internals Project Reports, BWRVIP-114, BWRVIP-115, BWRVIP-117, and BWRVIP-121, and Transware Enterprises Inc. Report TWE-PSE-001-R-001, Revision 0 (TAC NO. MB9765)," dated April 20, 2004.
2. Letter from Carl Terry (BWRVIP Chairman) to Document Control Desk (NRC), "Project 704 – BWRVIP-114: BWR Vessel and Internals Project, RAMA Fluence Methodology Theory Manual," dated June 11, 2003.

Enclosed are ten (10) copies of the BWRVIP response to the NRC Request for Additional Information (RAI) on the BWRVIP-114, -115, -117, -121 reports on the RAMA fluence methodology and a Transware Enterprises report on a Hope Creek flux wire dosimeter evaluation that was transmitted to the BWRVIP by the Reference 1 NRC letter identified above. The enclosure repeats each of the items from the NRC RAI verbatim followed by the BWRVIP response to that item.

Please note that the enclosed document contains proprietary information. Therefore, the request to withhold the BWRVIP-114 report from public disclosure transmitted to the NRC by the Reference 2 letter identified above also applies to the enclosed document.

If you have any questions on this subject, please contact George Inch (Constellation Energy, BWRVIP Assessment Committee Technical Chairman) by telephone at 315.349.2441.

Sincerely,

William A. Eaton

William A. Eaton
Entergy Operations
Chairman, BWR Vessel and Internals Project

CORPORATE HEADQUARTERS
3412 Hillview Avenue | Palo Alto CA 94304-1395 USA | 650.855.2000 | Customer Service 800.313.3774 | www.epri.com

EPRI Proprietary

REQUEST FOR ADDITIONAL INFORMATION FOR THE REVIEW OF THE ELECTRIC POWER RESEARCH INSTITUTE (EPRI) RAMA METHODOLOGY FOR REACTOR PRESSURE VESSEL FLUENCE EVALUATION

The U. S. Nuclear Regulatory Commission (NRC) has reviewed the RAMA Fluence Methodology documents submitted by the Boiling Water Reactor Vessel and Internals Project (BWRVIP) to qualify the application of the methodology for use in determining neutron fluence in BWR components. As a result of the review, twenty-seven Requests for Additional Information (RAIs) were identified in a letter transmitted to BWRVIP dated April 20, 2004. This report documents the response to these RAIs.

RAI 114-1 **Comment:** In the plant-specific applications, what specific tests and criteria are used to assure the adequacy of the number of rays and the number of volumes used in the RAMA fluence calculations?

Response: The adequacy of the RAMA fluence model parameters is assured by means of model sensitivity evaluations that are performed for each reactor model. A combination of 2-dimensional and 3-dimensional geometry and transport integration sensitivity evaluations are performed to ensure consistent results throughout the fluence model. Sections 4.6 and 4.7 of Ref. 7 describe the specific parametric cases and methodology for applying the 2-dimensional and 3-dimensional sensitivity evaluations, respectively, that are performed as a part of BWR vessel fluence calculations.

RAI 114-2 **Comment:** It is not evident that the RAMA geometry model described in Ref. 1 provides a correct representation of the true geometry (i.e., preserves the location, orientation and shape of all surfaces defining the physical geometry). For example, the modeling of the reflector region, surrounding the core, involves geometry elements that have both planar and cylindrical side boundaries. Since the geometry elements described in Ref. 1, Section 3.2, do not include bodies of this type, does RAMA introduce any distortion of the physical geometry in modeling the reflector and, if so, how is this distortion controlled to ensure acceptable accuracy?

Response: The solution regions in a RAMA geometry model are formed by combinations (i.e., intersections and differences) of the bodies described in Section 3.2 of Ref. 1. This allows complex geometries, including the transition between the rectangular core and the cylindrical shroud, to be precisely represented in a RAMA model. As

an example, a solution region can be formed by intersecting a right circular cylinder body with a rectangular parallelepiped body which results in a solution region that is cylindrical on one face and planar on the other faces. The use of these types of solution regions to transition between the planar core surfaces and the cylindrical shroud surface is illustrated in Figure 6-4 of Ref. 7.

RAI 114-3 **Comment:** The equation provided in Ref. 1, (Equation 7-38) for determining the M/C bias for the benchmark database requires an additional 1/M multiplicative normalization factor.

Response: The 1/M multiplicative factor was inadvertently omitted from the definition of the average value presented in Equation 7-38 of Ref. 1. The correct average value was used in the uncertainty evaluation presented in Ref. 3. Attachment 1 to this document contains a revised Page 7-16 from Ref. 1 illustrating the correct equation 7-38.

RAI 114-4 **Comment:** Equation 7-40 of Ref. 1 combines the analytical bias (B_a) and the benchmark bias (B_{b1}) to determine the overall calculational bias. The analytical bias (B_a), defined in Equation 7-34, provides the effect of not using the optimum asymptotic calculational input in the RAMA fluence calculation. Since the benchmark biases include the effect of the approximate calculational input used in the benchmark calculations (i.e., use of the standard input parameters rather than the asymptotic parameters), the analytical bias is only required when there is an inconsistency between the input used in the vessel fluence calculations and the benchmark calculations; e.g., when the calculations of the benchmark measurements are made with the asymptotic input values and the vessel fluence calculations are made with the standard input values. The staff requests that the BWRVIP clearly address the determination of the bias.

Response: It is acknowledged that the analytical bias that is determined from vessel fluence sensitivity evaluations is implicitly included in the benchmark and operating plant measurement bias. The theoretical basis for determining the analytical bias is included in the RAMA fluence methodology for completeness. In general practice, the analytical bias can be omitted from the uncertainty evaluation, but will be available if an analytical bias adjustment to the calculated fluence is required.

RAI 114-5 **Comment:** The weights defined in Equation 7-41 are not normalized (i.e., sum to unity), as required. Also, the weights should reflect the reliability of the bias estimates. If, for example, a weight of $1/\sigma^2$ is used,

the σ should represent the standard deviation of the bias estimate, not the standard deviation of the M/C data about the mean.

Response: An error existed in the definition of the weighting factor in Equation 7-42 in the original Ref. 1 document. A revision to the weighting factor definition was issued as: Errata for "BWRVIP-114: BWR Vessel and Internals Project, RAMA Fluence Methodology Theory Manual," 1003660 May 2003 and was transmitted to the NRC with a letter from Carl Terry, Chairman of the BWRVIP, dated August 21, 2003. The revision provides for weights that are normalized (i.e., sum to unity), as expected. Since the measurement bias estimate is based on the mean of the M/C data, using the standard deviation of the measurement data should provide a reasonable estimate of the standard deviation of the bias estimate. The revised equation is shown in Attachment 2.

RAI 114-6 **Comment:** The values of σ_a, σ_{b1} and σ_{b2} of Equation (7-43) represent the (one standard deviation) uncertainty in the RAMA calculated fluence, based on the analytical estimate of the uncertainties, comparisons with simulator benchmarks, and comparisons with operating plant data, respectively. These three uncertainty values represent independent estimates of the RAMA calculational uncertainty.

Therefore, the staff requests that the BWRVIP, in calculating the final estimate of the RAMA calculational uncertainty, σ_c, use an appropriately weighted combination of these three values, where each weight reflects the reliability of the uncertainty estimate, and then normalize the weights. The staff requests that the BWRVIP address this issue and provide a justification.

Response: It is correct that each of the three uncertainty values represents independent estimates of the RAMA calculational uncertainty. Using the unweighted contribution of the individual uncertainty values, as proposed in Ref. 1, is conservative in that it leads to an overestimate of the uncertainty. However, it is appropriate to estimate the overall uncertainty using a weighted mean of each of the three uncertainty estimates. Therefore, the BWRVIP intends to revise the computational process for determining the calculational uncertainty to incorporate a weighted treatment of the individual uncertainty components as shown in Equation 7-43 of Attachment 2. The weight factors of Equation 7-41 (w_a, w_b and w_c) are now multiplied by their respective variances to obtain a weighted mean.

EPRI Proprietary

The application of the revised uncertainty treatment will be documented in BWRVIP-117 (Ref. 3). Attachment 3 to this document contains revised Page 5-5 of Ref. 3 that illustrates the application of the revised uncertainty treatment.

RAI 115-1

Comment: Identify all differences between the methods used in performing the RAMA benchmark analyses of Ref. 2 and the methods that will be used in performing calculations of the vessel and shroud fluence. Also, address how the effects of these inconsistencies will be accounted for in determining the RAMA calculational bias and uncertainty.

Response: The methods used in performing the RAMA benchmark analyses in Ref. 2 are the same as the methods that will be used in performing BWR vessel and shroud fluence calculations. The methods are described in Ref. 7. The application of the methods to operating BWRs is described in Refs. 3 and 9.

RAI 115-2(a)

Comment: Regulatory Guide 1.190 requires that, as they become available, new measurements are to be incorporated into the M/C database and the fluence calculational bias and uncertainty estimates are to be updated, as necessary. The staff requests that the BWRVIP address how it will ensure that new measurements are incorporated in the M/C database and that the fluence bias and uncertainty will be updated in a timely manner.

Response: The comparisons to measured surveillance capsule and benchmark dosimetry are maintained in a database that is updated as additional plant capsule evaluations are performed using the RAMA methodology. The fluence bias and uncertainty are re-evaluated as new comparison data is added to the database. At present, TransWare Enterprises Inc., a primary contractor to EPRI and the BWRVIP, is performing fluence calculations using RAMA. TransWare also maintains a surveillance capsule and benchmark dosimetry measurement database. However, it is envisioned that in the future other organizations may choose to perform the fluence calculations and contribute to the database. Therefore, the BWRVIP will consider options for establishing a mechanism to collect and evaluate new M/C data and disseminate the information to all users of RAMA.

RAI 115-2(b)

Comment: How many BWR samples (measurements) are currently available and when is it anticipated that a statistically significant set of measurements will be available to evaluate the overall bias?

EPRI Proprietary

Response: The current RAMA comparison database includes comparisons to 15 measurement samples from two BWR-4 reactors and 237 measurement samples from three capsules in a BWR-2 reactor with no jet pumps. Work currently being performed includes comparison to measurements from three different BWR-4 reactors with jet pumps for the following measurements: 1) three additional surveillance capsules; 2) scrapings from various axial locations in the core shroud and top guide; and 3) samples from shroud head bolts. This work and other anticipated comparisons will provide a statistically significant set of measurements for both jet pump and non-jet pump BWRs when this work is completed (estimated to be within two years). This work will also demonstrate RAMA's capability to determine fluence for additional reactor system components.

RAI 115-3 **Comment:** In the calculation of the VENUS-3 benchmark, it is stated that the source is normalized to the experimental results. If the experimental results used for this normalization are the fluence measurements (which would erroneously reduce the M/C uncertainty), rather than the measurements of the core source distribution, discuss the effect that this simplification has on the calculational bias and uncertainty inferred from this benchmark comparison.

Response: The VENUS-3 measurement results reported by the experimenters included a normalization to an arbitrary source magnitude. The intent of the statement regarding the normalized source is to indicate that the same source magnitude used by the VENUS-3 experimenters was also used in the RAMA benchmark calculation. There was no normalization of the RAMA predicted activation to measured values.

RAI 115-4 **Comment:** In Table 2-24, the sensitivity of the RAMA calculation of the NUREG-6115 benchmark problem to the axial distance between parallel rays has not been included (as in Table 2-16 for the HBR-2 calculation). Please discuss the sensitivity of the RAMA calculation to the axial distance between parallel rays. Please present your results on the same (or a similar) graph as Figures 5.4.6 or 5.4.8 of NUREG-6115.

Response: The sensitivity of the RAMA calculation of the NUREG-6115 benchmark problem to the axial distance between parallel rays is determined by evaluating the >1.0 MeV neutron flux at the capsule location for various values of the parallel ray axial distance. The axial distance between parallel rays was varied over a range of 2 cm to 16 cm. Over the range of 2 cm to 9 cm the maximum observed deviation was ≤1%. Thus, the default value of 5 cm was conservatively used in

the RAMA calculation. Attachment 4 contains revised Pages 2-46 through 2-48 of Ref. 2. The sensitivity of the RAMA calculation of the NUREG-6115 benchmark problem to the axial distance between parallel rays is included in Table 2-24 of Attachment 4 and the plot that illustrates the sensitivity is provided in Figure 2-20 of Attachment 4.

RAI 117-1 **Comment:** In Ref. 3, what criteria was used to select the sixty-three state points used to represent the Cycle 1-5 core operating history and what determination criteria was used in the weighting assignments of each state point calculation?

Response: The guidelines and criteria for selecting the state points that are to be used in RAMA fluence evaluations are described in Section 5.2.1 of Ref. 7. Daily reactor power for the period over which a state point is deemed representative is used as the weighting assignment for each state point calculation.

RAI 117-2 **Comment:** Was the Susquehanna Cycle 1-5 power, void and exposure distribution data based on calculational results or plant process computer data? If this data was the result of recent calculations, rather than the original historical calculations, discuss why new calculations were required and what differences were introduced in the calculations. Also, discuss the effect of any approximations used in representing the state-point dependence of the pin-wise source distribution of the peripheral fuel bundles.

Response: The Susquehanna power, void, and exposure distribution data were based upon "core follow" calculations that were performed during the five cycles of operation. Restart edit cases were executed to retrieve the required data from the previous calculations, however, no recalculation of data was performed. The core calculations provide pin-wise power distributions for each bundle in the core for each state point that was used in the analysis. Thus no approximations were needed to represent the state-point dependence of the pin-wise source distribution of the peripheral fuel bundles.

RAI 117-3 **Comment:** Discuss the basis for the Table 5-3 parameter uncertainty for the following locations: (1) capsule and flux wire locations, (2) vessel inner radius, (3) core void fraction, (4) peripheral bundle power, and the (5) iron cross section.

EPRI Proprietary

Response: (1) The uncertainty in radial and axial locations of the capsule is based upon the design drawing tolerances. The uncertainty in capsule azimuthal location is based upon as-built measurements from a similar BWR. The uncertainty in the location of the flux wires is based upon the assumption that the flux wires can be located anywhere within the surveillance capsule. (2) The uncertainty in RPV inner radius is based upon design drawing tolerances. (3) The uncertainty in void fraction is based upon experience estimates of ±5% variation in computed void fraction. (4) The uncertainty in peripheral bundle power is based upon the reported accuracy of the core simulation analysis computer code. (5) The uncertainty in the iron cross section is based upon experience estimates of ±10% uncertainty in the cross section.

RAI 117-4 **Comment:** Describe the spatial mesh used to represent the capsule and the capsule/vessel water gap.

Response: Figures 4-1, 4-2, and 4-4 of Ref. 3 illustrate the location and size of the capsule in the Susquehanna fluence model. The capsule is positioned in the radial plane to provide for a water gap between the capsule and pressure vessel wall. The capsule geometry is represented with 12 mesh volumes of the following configuration: 3 azimuthal sectors, 2 radial annuli, and 2 axial planes. The water gap between the capsule and the pressure vessel wall is represented with 6 mesh volumes of similar configuration to the capsule with the exception that 1 annulus is used to represent the radial thickness of the gap.

RAI 117-5 **Comment:** What fluence uncertainty is introduced by the uncertainty in the Cu-63(n, α)Co-60, Fe-54(n, p) Mn-54 and Ni-58(n, p)Co-58 dosimetry cross sections?

Response: The dosimetry cross sections are used in the comparison of calculated activations to measurements so that the uncertainty introduced by the activation cross sections is inherently included in the comparison of calculations to measurements for the respective dosimetry reactions. As a result, no separate estimate of the uncertainty associated with activation cross sections is required.

RAI 117-6 **Comment:** Provide a discussion of the method used to determine the analytical modeling input bias and the associated uncertainty provided in Table 5-3.

Response: The method used to determine the analytical modeling uncertainty and bias estimation is described in Section 7.3.1 of Ref. 1 and in Section 8 of Ref. 7.

EPRI Proprietary

RAI 117-7 **Comment:** In view of the fact that the uncertainty in the bias, inferred from the measurements of Table 5-4, is larger than the bias itself, provide justification for applying this bias to the RAMA calculated fluence.

Response: The application of the bias in the case of the Susquehanna fluence evaluation is provided as an example of the bias application process. As described in Section 8.3.1 of Ref. 7, the application of a computed bias to the fluence evaluation should only be done when the bias is statistically significant. Section 5.4 of the Susquehanna fluence evaluation presented in Ref. 3 will be revised to be consistent with the anticipated application of the analytic (and overall) bias treatment in practice. Attachment 3 to this document provides a revised Page 5-5 that clarifies the intended treatment.

RAI 117-8 **Comment:** In view of the fact that the RAMA calculation of the benchmark measurements used the "standard" fluence input parameters and the C/M comparisons (and the inferred C/M bias), address the effect of these parameters and provide justification for applying the analytical bias to the RAMA fluence calculation.

Response: As noted in the response to RAI 114-4, the analytical bias is generally implicitly included in the measurement comparisons. The application of an analytical bias in the case of the Susquehanna fluence evaluation was carried out to demonstrate the application of an analytical bias should there be inconsistencies between the methodology used for the measurement comparisons and the fluence evaluation. In addition, any combined bias should be applied only if it is statistically significant (Section 8.3.1 of Ref. 7), which is not the case for the Susquehanna evaluation. Section 5.4 of the Susquehanna fluence evaluation presented in Ref. 3 will be revised to be consistent with the anticipated application of the analytic (and overall) bias treatment in practice. Attachment 3 to this document provides a revised Page 5-5 that clarifies the intended treatment.

RAI 117-9 **Comment:** Discuss the methods used to measure the flux wire activations and conformance to ASTM E-263-93 (Ref. 4), ASTM E-263-93 (Ref. 5) and ASTM E-264-92 (Ref. 6). Also, discuss the basis for the 2.5% measurement accuracy.

Response: The flux wire measurements were performed by GE. The methods used to measure the flux wire activations, measurement results, and measurement accuracy are described in Ref. 8.

EPRI Proprietary

RAI 121-1 **Comment:** Ref. 7 states that the BWR shroud is a "priority 1 component." However, no mention or attempt was made to demonstrate how RAMA performs in the evaluation of the shroud. Provide benchmarking data and calculations for the core shroud.

Response: The purpose of the Ref. 7 document is to provide general modeling guidelines that can be used to assist users in the application of RAMA to BWR component fluence evaluations. Application of the RAMA methodology to RPV vessel and surveillance capsule fluence evaluations, including comparison of calculated values to measurements, is described in Refs. 1, 2, and 3. Application of the RAMA Fluence Methodology to the core shroud in the active fuel region is straightforward since this region is modeled to obtain the RPV fluence. In Ref. 7 the shroud is evaluated using the same criteria as the RPV in the geometry meshing sensitivity studies. A benchmark evaluation is currently underway to demonstrate the adequacy of the RAMA Fluence Methodology for determining the fluence of the core shroud and the top guide.

RAI 121-2 **Comment:** The staff requests that the BWRVIP provide a justification of the statement in the BWRVIP-121 report, "The nature of the guidelines is applicable to BWR plants without jet pumps...". In most BWRs, the dosimeters are placed behind the jet pump which introduces spectral distortions, particularly for Fe and Ni dosimeters. If the BWRVIP report is indicating that the RAMA bias and uncertainties, based on jet pump plants, are applicable to plants without jet pumps, then the staff requests that the BWRVIP justify this statement.

Response: The intent of the statement is to indicate that the general modeling guidelines and process for evaluating the adequacy of the RAMA methodology described in Ref. 7 are valid for BWR plants with and without jet pumps. There is no intent to imply that the results obtained from evaluations performed in accordance with the methodology described in Ref. 7 are the same for BWR plants with and without jet pumps. Paragraph 4 on Page 1-1 of Ref. 7 has been revised to clarify this matter. The revised Page 1-1 is provided in Attachment 5 to this document.

RAI HC-1 **Comment:** The surveillance capsule is situated directly behind the jet pump. Given the "window" in the inelastic scattering of Fe in the 1.0 to 2.5 MeV range, what is the effect of the spectrum on the Fe, Ni, and Cu activation?

EPRI Proprietary

Response: The RAMA Fluence Methodology has the capability to accurately represent jet pumps in the transport model. As a result, the spectral effects associated with the presence of the jet pumps is implicitly included in the transport calculation. Comparative studies show that the calculated activities for Fe, Ni, and Cu are consistently predicted (Refs. 2, 3, and 9) for jet pump and non-jet pump plants. Relative to each isotope, Cu activities have shown a consistent ~5% negative bias relative to Fe and Ni. Because jet pump and non-jet pump plants show the same trend, it is suggested that the difference in the calculated Cu activities is attributable to either the Cu cross sections or unaccounted for impurities in the metal (see RAI HC-4 and RAI HC-5).

RAI HC-2

Comment: There is no mention of the estimation of the neutron spectrum in these calculations. The report states that there are 12 segments in the cycle, with different material compositions. It seems that the major differences in these segments are the decreasing concentration of U-235, the increasing concentration of Pu-239, and the increasing concentration of fission products. How do these changes affect the spectrum and how is it calculated?

Response: Each segment (or state point) represents an exposure interval of the reactor cycle. The intervals for the analysis were selected in accordance with the criteria presented in Section 5.2.1 of Ref. 7. The state point data for each state point includes fuel isotopics (i.e., the number densities for the uranium and plutonium nuclides) corresponding to the exposure of the state point. The spectrum is calculated in RAMA using a weighting based upon the contribution of the various uranium and plutonium nuclides, as described in Equation 4-25 of Ref. 1.

RAI HC-3

Comment: What were the findings/results from the sensitivity study? Are the parameter default settings optimized?

Response: The results of the sensitivity study for Hope Creek are reported in Section 4.4 of Ref. 9 and are consistent with the results observed for the other operating plants (BWR and PWR) reported in Refs. 2 and 3. All of the parameters except the mesh size and angular quadrature selection are optimized. These latter two parameters can have significant computational penalties, thus both are evaluated to provide an acceptable balance between accuracy and computational performance. The mesh size results in <3% deviation from asymptotic value and the angular quadrature selection results in <7% deviation from the asymptotic value. The parameter set used in the fluence

evaluation provides acceptable accuracy and computational performance.

RAI HC-4

Comment: Given the systematic underestimation of the Cu dosimeters, address whether an investigation shall be launched to determine if a dosimeter-specific bias exists?

Response: It is observed from the benchmarks that the underestimation of Cu activities is consistent and on the order of about 5%. It is noted in the H. B. Robinson benchmark report (Ref. 10) that impurities in the Cu metal, specifically cobalt, can account for about 2% of the difference. Predicated on this statement and the response provided for RAI HC-5, it is not clear whether the observed bias is material or cross section related. Further investigation would need to include the full compositional characterization of the Cu metal. The BWRVIP has no plans to investigate this matter.

RAI HC-5

Comment: The report states that the Cu discrepancy could be due to Co-59 impurity. The staff requests that the BWRVIP address that dosimeters supposed to be chemically and isotopically pure?

Response: The possibility of trace (on the order of <0.25 ppm) cobalt impurity in pure copper has been acknowledged by copper industry experts (Ref. 11). Due to the large thermal neutron reaction rate of cobalt-59, this level of impurity can lead to a few percent of additional cobalt-60 in the dosimeter due to the activation of cobalt-59. A correction of approximately 2% for cobalt impurity in the copper dosimetry was provided for in the H. B. Robinson Unit 2 Cycle 9 benchmark results reported in Ref. 10.

REFERENCES

1. BWRVIP-114, "BWR Vessel and Internals Project, RAMA Fluence Methodology Theory Manual," EPRI, Palo Alto, CA 2003. 1003660.

2. BWRVIP-115, "BWR Vessel and Internals Project, RAMA Fluence Methodology Benchmark Manual - Evaluation of Regulatory Guide 1.190 Benchmark Problems," EPRI, Palo Alto, CA 2003. 1008063.

3. BWRVIP-117, "BWR Vessel and Internals Project, RAMA Fluence Methodology Plant Application - Susquehanna Unit 2 Surveillance Capsule Fluence Evaluation for Cycles 1-5," EPRI, Palo Alto, CA 2003. 1008065.

4. ASTM E-263-93, "Standard Test Method for Measuring Fast-Neutron Reaction Rates by Radioactivation of Iron," ASTM Standards, Section 12, American Society for Testing and Materials, Philadelphia, PA, 1995.

5. ASTM E-523-92, "Standard Test Method for Measuring Fast-Neutron Reaction Rates by Radioactivation of Copper," ASTM Standards, Section 12, American Society for Testing and Materials, Philadelphia, PA, 1995.

6. ASTM E-264-92, "Standard Test Method for Measuring Fast-Neutron Reaction Rates by Radioactivation of Nickel," ASTM Standards, Section 12, American Society for Testing and Materials, Philadelphia, PA, 1995.

7. BWRVIP-121, "BWR Vessel and Internals Project RAMA Fluence Methodology Procedures Manual," EPRI, Palo Alto, CA 2003 1008062.

8. *Susquehanna Steam Electric Station Unit 2 Vessel Surveillance Materials Testing and Fracture Toughness Analysis*, GE Nuclear Energy, GE-NE-523-107-0893, DRF 137-0010-6, October 1993, Rev. 1.

9. "Hope Creek Flux Wire Dosimeter Activation Evaluation for Cycle 1," TransWare Enterprises Inc., TWE-PSE-001-R-001, Rev. 0, October 2003.

10. I. Remec and F. B. K. Kam, "H. B. Robinson-2 Pressure Vessel Benchmark," NUREG/CR-6453, Oak Ridge National Laboratory, ORNL/TM-13204, February 1998.

11. Personal email communication from Dr. Horace Pops of Superior Essex to Mr. William Black of the Copper Development Association, "Cobalt Impurity in Copper Wires," April 14, 2003.

EPRI Proprietary

Attachment 1

BWRVIP 114: BWR Vessel and Internals Project RAMA Fluence Methodology Theory Manual, Revised Page 7-16

EPRI Proprietary

Activation, Fluence, and Uncertainty Methods

The bias, based upon comparison of calculated to measured dosimeter results, is:

$$B_b = \frac{1}{M}\sum_{i=1}^{M}\frac{m_i - c_i}{c_i} = \frac{1}{M}\sum_{i=1}^{M}\left(\frac{m_i}{c_i} - 1\right) \qquad (7\text{-}38)$$

where m_i is the i-th measured activation value in the database and c is the i-th calculated activation value. Note that an implicit assumption in Eg. (7-38) is that the relative bias based upon comparison to measured values applies to RPV locations as well.

The elements contributing to the comparison uncertainty analysis are generally quite different for the vessel simulator benchmark evaluations as opposed to operating light water reactor dosimetry evaluations. As a result, the bias and uncertainty (standard deviation) are determined using the above methodology for two different measurement databases: (1) the vessel simulator benchmark database consisting of comparison results for the PCA and VENUS-3 benchmark problems, and (2) the operating system database consisting of dosimetry measurement data from operating light water reactor plants.

The comparison databases must be evaluated to confirm their statistical validity for use in determining the RPV "best estimate" bias. Statistical valid databases must meet three criteria: (1) the database should provide a representative sample over the range of operating states for which the fluence evaluation methodology is to be applied, (2) the uncertainty in the database comparisons should be small compared to the comparison bias, and (3) the calculation and measurement errors of the comparison ratios must be uncorrelated (i.e., no systematic bias is present in the comparisons).

The method of evaluating the extent of correlated comparisons in the databases, and the method for removing the correlated bias is described in [9]. The database comparisons are expressed in a regression model of the form:

$$\left(\frac{m}{c}\right) = \mu_{m/c} + \sum_{k=1}^{K} c_k \alpha_k \qquad (7\text{-}39)$$

where $\mu_{m/c}$ is the fitted mean of the comparisons, c_k are fit coefficients, and α_k are parameters that represent various possible correlation conditions, such as the type of detector, the location of the detector (e.g., in-vessel and behind jet pumps), the energy threshold of the detector, etc. The statistics of the fit parameters are used to determine correlated parameters. The regression model of Eq. (7-39) is used to remove the systematic bias from the measurement comparisons. The measurement comparisons are used to determine an adjusted bias, as in Eq. (7-38).

7.3.3 *Combined Uncertainty*

[[

Content Deleted
EPRI Proprietary Information

]] TS

EPRI Proprietary

Attachment 2

BWRVIP 114: BWR Vessel and Internals Project RAMA Fluence Methodology Theory Manual, Revised Page 7-17

[[

Content Deleted
EPRI Proprietary Information

]] TS

7.3.4 *Best Estimate Fluence*

The combined fluence bias and standard deviation determined from Section 7.3.3 are used to compute the best estimate neutron fluence from the calculated fluence as specified in [1] using the following methodology.

If the combined standard deviation is ≤20%, the best estimate neutron fluence is

$$\varphi = \varphi_c\left(1 + B_c\right) \tag{7-44}$$

where φ_c is the calculated neutron fluence and B_c is the combined fluence bias. If the combined standard deviation is greater than 20% but less than 30%, the best estimate neutron fluence is

$$\varphi = \varphi_c\left(1 + B_c + \frac{\sigma_c(\%) - 20}{100}\right) \tag{7-45}$$

where σ_c is the combined fluence standard deviation from Eq. (7-43).

EPRI Proprietary

Attachment 3

BWRVIP-117: RAMA Fluence Methodology Plant Application – Susquehanna Unit 2 Surveillance Capsule Evaluation, Revised Page 5-5

The combined capsule bias (and uncertainty) is the weighted sum of the analytic and comparison biases (and uncertainties) where the weighting factors are inversely proportional to the analytic and comparison variances, respectively [3]. Table 5-4 shows that the combined capsule uncertainty is determined to be 10.0% with a bias of –0.7% for both the >1.0 MeV fluence and the >0.1 MeV fluence. The combined uncertainty is less than 20 percent as recommended in Section 1.4.3 of Regulatory Guide 1.190 [6].

Table 5-4
Combined Capsule Uncertainty

Energy Range	Analytic Bias Weight Factor	Comparison Bias Weight Factor	Combined Bias %	Combined Uncertainty % (1σ)
>1.0 MeV Average	0.22	0.78	-0.7	10.0
>0.1 MeV Average	0.22	0.78	-0.7	10.0

5.4 Best Estimate Neutron Fluence and Flux

Table 5-5 provides the RAMA calculated best estimate neutron fluence and rated power flux values for the Susquehanna Unit 2 capsule for energy >1.0 MeV and for energy >0.1 MeV. Since the combined bias from Section 5.3 of this report is substantially smaller than the corresponding combined uncertainty, the computed combined bias is not statistically significant. The combined uncertainty of 10.0% is also less than 20% as specified in Regulatory Guide 1.190. Therefore, the best estimate values for flux and fluence are equivalent to the calculated values (i.e., no bias is applicable for the calculated neutron flux and fluence). The best estimate capsule neutron fluence for energy >1.0 MeV is 1.555×10^{17} n/cm^2 and for energy >0.1 MeV is 2.801×10^{17} n/cm^2. The best estimate capsule rated power neutron flux for energy >1.0 MeV is 7.930×10^{8} n/cm^2-s and for energy >0.1 MeV is 1.428×10^{9} n/cm^2-s.

Table 5-5
Best Estimate Neutron Fluence and Rated Power Flux for Susquehanna Unit 2 Capsule

Energy Range	Fluence n/cm^2	Standard Deviation n/cm^2	Rated Power Flux n/cm^2-s	Standard Deviation n/cm^2-s
>1.0 MeV Average	1.555E+17	1.555E+16	7.930E+08	7.930E+07
>0.1 MeV Average	2.801E+17	2.801E+16	1.428E+09	1.428E+08

EPRI Proprietary

Attachment 4

BWRVIP 115: BWR Vessel and Internals Project RAMA Fluence Methodology Benchmark Manual — Evaluation of Regulatory Guide 1.190 Benchmark Problems, Revised Pages 2-46 through 2-48

[[

Content Deleted
EPRI Proprietary Information

]] **TS**

2-46

[[

Content Deleted
EPRI Proprietary Information

]] **TS**

2-47

[[

Content Deleted
EPRI Proprietary Information

]] **TS**

2-48

EPRI Proprietary

Attachment 5

BWRVIP 121: BWR Vessel and Internals Project RAMA Fluence Methodology Procedures Manual, Revised Page 1-1

1 INTRODUCTION

The BWR Vessel and Internals Project (BWRVIP) has developed the RAMA Fluence Methodology (hereinafter referred to as the Methodology) for use in calculating neutron fluence in boiling water reactors (BWRs). The current version of the Methodology is applicable for calculations at the surveillance capsule location as well as on the core shroud and within the reactor vessel over the active fuel height. The Methodology is designed to meet the requirements of the U. S. Nuclear Regulatory Commission (NRC) Regulatory Guide 1.190 [1].

The Methodology includes computerized analysis tools that perform neutron fluence calculations, modeling guidelines that describe the use of the methodology, and benchmark reports that document the capability of the Methodology to accurately predict neutron fluence. The benchmark problems that have been used to demonstrate the capability of the Methodology include the analysis of specific benchmark problems identified in the NRC Regulatory Guide 1.190 and analyses of surveillance capsule measurements for commercial BWRs.

Accurate neutron fluence determinations are required for a number of reasons: 1) to determine neutron fluence in the reactor pressure vessel (RPV) and at surveillance capsule locations to address vessel embrittlement issues; 2) to determine neutron fluence in the core shroud in order to determine fracture toughness and crack growth rate for use in flaw evaluation calculations; and 3) to determine neutron fluence in other internal components above and below the active core for structural integrity assessments or to evaluate repair technologies. Fluence predictions are potentially required in other parts and locations within the reactor pressure vessel. However, the near term need for fluence calculations includes mainly the internals such as the pressure vessel, core shroud, surveillance capsule locations, and jet pumps, at elevations within the height of the active fuel.

This manual is intended to provide guidelines for the user of the Methodology to assist in ascertaining the fluence evaluation to be performed, collecting the data needed for the evaluation, building the geometry models for the reactor and components of interest, processing material data, evaluating the flux and fluence results generated by the Methodology, and performing an uncertainty analysis of the results. The discussions and examples in this manual describe the modeling and analysis process for typical BWR plants with jet pumps. However, the basic process presented in the guidelines is applicable to BWR plants without jet pumps as well.

A summary of the remaining sections of this manual is presented in the following paragraphs.

Section 2 of this manual presents an overview of the Methodology software package. The individual software components that comprise the Methodology are presented along with a brief discussion of the calculational flow and overview of the entire modeling process.

C
RECORD OF REVISIONS

BWRVIP-114-A	Information from the following documents was used in preparing the changes included in this revision of the report: 1. BWRVIP-114: BWR Vessel and Internals Project, RAMA Fluence Methodology Theory Manual, EPRI, Palo Alto, CA: 2003. 1003660. 2. Letter from Vaughn Wagner and Tom Mulford (EPRI) to all BWRVIP Committee members and recipients of BWRVIP-114, "Errata for BWRVIP-114," dated August 18,2003 (BWRVIP Correspondence File Number 2003-300). 3. Letter from Carl Terry (BWRVIP Chairman) to Meena Khanna (NRC), "Project 704 - Errata to BWRVIP-114" dated August 21, 2003 (BWRVIP Correspondence File Number 2003-301). 4. Letter from Stephanie M. Coffin (NRC) to William Eaton (BWRVIP Chairman), Request for Additional Information – Review of BWR Vessel and Internals Project Reports, BWRVIP-114, BWRVIP-115, BWRVIP-117 and BWRVIP-121 and TransWare Enterprises Inc. Report TWE-PSE-001-R-001, Revision 0 (TAC NO. MB9765) dated April 20, 2004 (BWRVIP Correspondence File Number 2004-159). 5. Letter from Carl Terry (BWRVIP Chairman) to Meena Khanna (NRC), "Project NO. 704 – BWRVIP Response to NRC Request for Additional Information on BWRVIP-114, -115, -117 and -121" dated September 29, 2004 (BWRVIP Correspondence File Number 2004-420). 6. Letter from William H. Bateman (NRC) to Bill Eaton (BWRVIP Chairman), Safety Evaluation of Proprietary EPRI Reports, "BWR Vessel and Internals Project, RAMA Fluence Methodology Manual (BWRVIP-114)," "RAMA Fluence Methodology Benchmark Manual - Evaluation of Regulatory Guide 1.190 Benchmark Problems (BWRVIP- 115)," " RAMA Fluence Methodology-Susquehanna Unit 2 Surveillance Capsule Fluence Evaluation for Cycles 1 - 5 (BWRVIP-117)," and " RAMA Fluence Methodology Procedures Manual (BWRVIP-121)," and "Hope Creek Flux Wire Dosimeter Activation Evaluation for Cycle 1 (TWE-PSE-001-R-001)" (TAC NO. MB9765) dated may 13, 2005 (BWRVIP Correspondence File Number 2005-308). Details of the revisions can be found in Table C-1.

Table C-1
Revision Details

Required Revision	Source of Requirement for Revision	Description of Revision Implementation
Add NRC Correspondence	NRC Request	NRC Safety Evaluation added behind report title page. Remainder or correspondence added as Appendices A through B.
Section 5.2, Generating the Core Reflector Region Geometry Model	BWRVIP Response to RAI 114-2	First Paragraph: Added "...to form solution regions that have both planar and cylindrical faces." to the end of the last sentence.
Section 7.3.1, Analytical Uncertainty	BWRVIP Response to RAI 114-4	Added "It should be noted that the analytical bias is typically an integral part of the observed deviation in the comparison of calculated to measured activation since the models used for fluence evaluations are the same as those used for the measurement comparisons. Thus the analytical bias is usually zero in RAMA fluence evaluations." to the end of section.
Equation 7-38	BWRVIP Response to RAI 114-3	Revised equation to add the 1/M multiplicative factor that was inadvertently omitted in original publication.
Sections 7.3.3 and 7.3.4	Reg. Guide 1.190; BWRVIP-189; BWRVIP Response to RAI 117-7 and 117-8	Replaced "Combined" with "Calculational" when referring to uncertainty and standard deviation throughout Sections 7.3.3 and 7.3.4 to be consistent with the terminology used in Reg. Guide 1.190.
Equation 7-42	BWRVIP Response to RAI 114-5	Revised equation to correct the definition of the weighting factor. This correction was issued as: Errata for "BWRVIP-114: BWR Vessel and Internals Project, RAMA Fluence Methodology Theory Manual," 1003660 May 2003.
Equations 7-41 and 7-43	BWRVIP Response to RAI 114-6	Equations 7-41 and 7-43 are revised to incorporate a weighted treatment of the individual uncertainty components as shown in Equation 7-43 of BWRVIP-114. The weight factors of Equation 7-41 (w_a, w_b and w_c) are now multiplied by their respective estimated reliabilities to obtain a weighted mean. Text relating to the equations in Sections 7.3.3 and 7.3.4 is also revised to reflect changes in weighted treatment of individual uncertainty components. *The application of the revised uncertainty treatment is documented in BWRVIP-117, page 5-5.*
Add NEI 03-08 Implementation Requirements	BWRVIP-94, Revision 1 Requirement	Implementation Requirements Added in Section 1.9.